STUDIES IN SPECKLE INTERFEROMETRY

A thesis submitted for the degree

of Doctor of Philosopy

BRIAN PICKTHORNE

The University of Aston in Birmingham

Department of Physics

December 1982.

STUDIES IN SPECKLE INTERFEROMETRY

Brian Pickthorne

Doctor of Philosophy

SUMMARY

Initial studies were undertaken concerning laser speckle photography(sometimes called single-beam speckle interferometry)to obtain information about the technique and determine methods to enable specklegrams of high contrast and definition to be produced. This required extensive studies regarding the production, recording and processing of doubly exposed specklegrams corresponding to lateral surface displacements and investigation of the generation and measurement of the interference fringes from these specklegrams. It was discovered that marked improvements in fringe contrast and definition could be achieved using the measures and novel techniques which were devised. Information and evidence regarding the photography of these fringes was also obtained.

The main studies built upon these findings and were concerned with the exploration and formulation of precise means of measuring fringes generated from doubly exposed specklegrams. Three possible techniques were identified and systems based on these were developed. One was based on the use of a self-scanning linear photodiode array, another on a computer controlled microdensitometer system with digitized readout and computerized fringe analysis, and the third on a moiré pattern technique. These techniques had not previously been explored in this connection, and valuable comparative information was also acquired.

The moiré pattern system proved to be particularly sensitive, robust and adaptable. Consequently, it was employed in conjunction with single-beam speckle photography in the study of three applied problems in different practical contexts, viz., the investigation of contaminant layer thickness between railway wheels and track; second the 'condition' monitoring of production machines; and third the analysis of vehicle structures in the automobile industry. In addition to providing important information these applied studies demonstrated the potential of an integrated system using focused speckle photography (F.S.P.) and the moiré fringe mesurement technique as a measurement, analysis and diagnostic tool.

Key words : Speckle photography: fringe analysis systems

University of Aston in Birmingham December 1982.

D E D I C A T I O N

To Laura-Jane

May you have a long, full and happy life.

ACKNOWLEDGEMENTS

I am indebted to a large number of people for their help, support, advice and encouragement.

In particular, I would like to thank Professor G.L. Rogers for his guidance and enthusiasm throughout this quite extensive research. Sincere thanks are similarly due to Mr.W.James for his keen interest and valuable advice and for stimulating discussions. My thanks must also be given to Professor T.Mulvey for his support, guidance and useful suggestions. In addition, I wish to express my gratitude to Professor S.E.Hunt for his interest and encouragement.

Grateful thanks are due to Staff of the Department of Electrical Engineering and Technical Staff of the Department of Physics. Also to Mr.A.E.Ennos of the National Physical Laboratory and Dr.M.J.Elder of S.E.R.C. (Daresbury Laboratory) for the provision of advice and facilities.

Furthermore, I must thank Staff of British Railways Board Research Department and British Leyland Technology (Cars Division) for assistance and support in certain aspects of this work.

My appreciation and thanks are due to Mrs.D.G.Hill for many things, including the patient typing of this thesis. Finally, I must thank my wife for her support and encouragement throughout this work.

LIST OF CONTENTS

LIST OF CONTENTS (Continued)

LIST OF CONTENTS (Continued)

LIST OF FIGURES

LIST OF FIGURES (Continued)

LIST OF FIGURES (Continued)

LIST OF TABLES

CHAPTER 1.

LASER SPECKLE

CHAPTER 1.

1.1. GENERAL INTRODUCTION

The phenomenon known as 'laser speckle' was initially observed over twenty years ago, but laser speckle pattern interferometry has only evolved during the last decade or so. This development has largely stemmed from the work of Leendertz[1,2], Archbold et al.[3], Burch[4], Butters and Leendertz[5], and Stetson[6] amongst others, as will be outlined.

As Ennos[7] acknowledges, speckle interferometry has certain properties which parallel those of holographic interferometry. However,with regard to the former,the basic principle is to combine optically a speckle pattern with either a second speckle pattern or a uniform reference beam of comparable intensity. Speckle interferometry is now recognized as a valuable tool and has been successfully exploited in a variety of practical contexts.

Various techniques have been devised for obtaining, recording and analysing the interference of laser speckle fields. These include the photographic methods of Leendertz,[1,2,8] Archbold et al.[9] and the electro-optical techniques of Butters and Leendertz[10].

An application of speckle interferometry, in metrology, was reported by Groh[11] more than ten years ago.Since then, as Gregory[12] observes, there have been many demonstrations of the usefulness of speckle interferometry as a means of making,for example,sensitive measurements

and examinations or monitoring of objects which do not have a specularly reflecting surface.

Nevertheless, there remain a number of problems and difficulties concerning laser speckle pattern interferometry and its uses. Certain of these were examined in the studies reported in this thesis.

1.2. AIMS AND OBJECTIVES

The research was basically concerned with the exploration and devising of techniques which would improve the qualitative and quantitative interpretation of the interference fringes produced in laser speckle pattern interferometry. In particular, it was concerned with the determination of the spatial frequency of the Young's fringes associated with, for instance, lateral surface movements or displacements. It was then intended to investigate the application of the appropriate technique devised, in conjunction with certain measures, to problems in three different applied industrial contexts that required a sensitive, adaptable and low cost measurement system.

The laser speckle pattern interference method employed to record the surface movements or displacements was the method termed 'laser speckle photography'*. This is because the method provides permanent records, in a form suitable for comparing the techniques devised and also because it satisfies other requirements (which will be indicated later).

*Although this is not truly interferometric it depends upon the optical properties of speckle - which itself results from interference. (The theory and principles of the technique are given in Chapter 2.)

As a preliminary, it was decided to investigate the factors influencing the definition and quality of the interference fringes obtained by this method so that distinct fringes could be provided for use in the main research.

1.3. LASER SPECKLE PATTERNS

Various aspects of the nature and properties of laser speckle impinge upon the research which was undertaken in laser speckle photography. For this reason, the nature, basic theory and fundamental properties of laser speckle per se will be briefly examined in the following sections of this introductory chapter. This background information will subsequently be employed and built upon in relation to the experimental investigations which were carried out.

When an object, which has a diffusely reflecting surface, is illuminated by laser light the surface appears to be covered with a fine granular structure as shown in Figure 1.3.1. The random intensity distribution, which gives the object a sparkling or twinkling appearance when the observer moves, is called a 'speckle pattern'. This effect is observed when any diffusely reflecting surface is illuminated by coherent light, such as that produced by a laser. The theoretical basis of this effect is founded upon Fourier optics.

Studies of the 'speckle' phenomenon have been made since the time of Newton in the seventeenth century. As Dainty[13] indicates, it attracted marked attention towards the latter part of the last century. For example,

Exner[14] investigated speckle produced by candle light scattered from a glass plate upon which he had breathed.

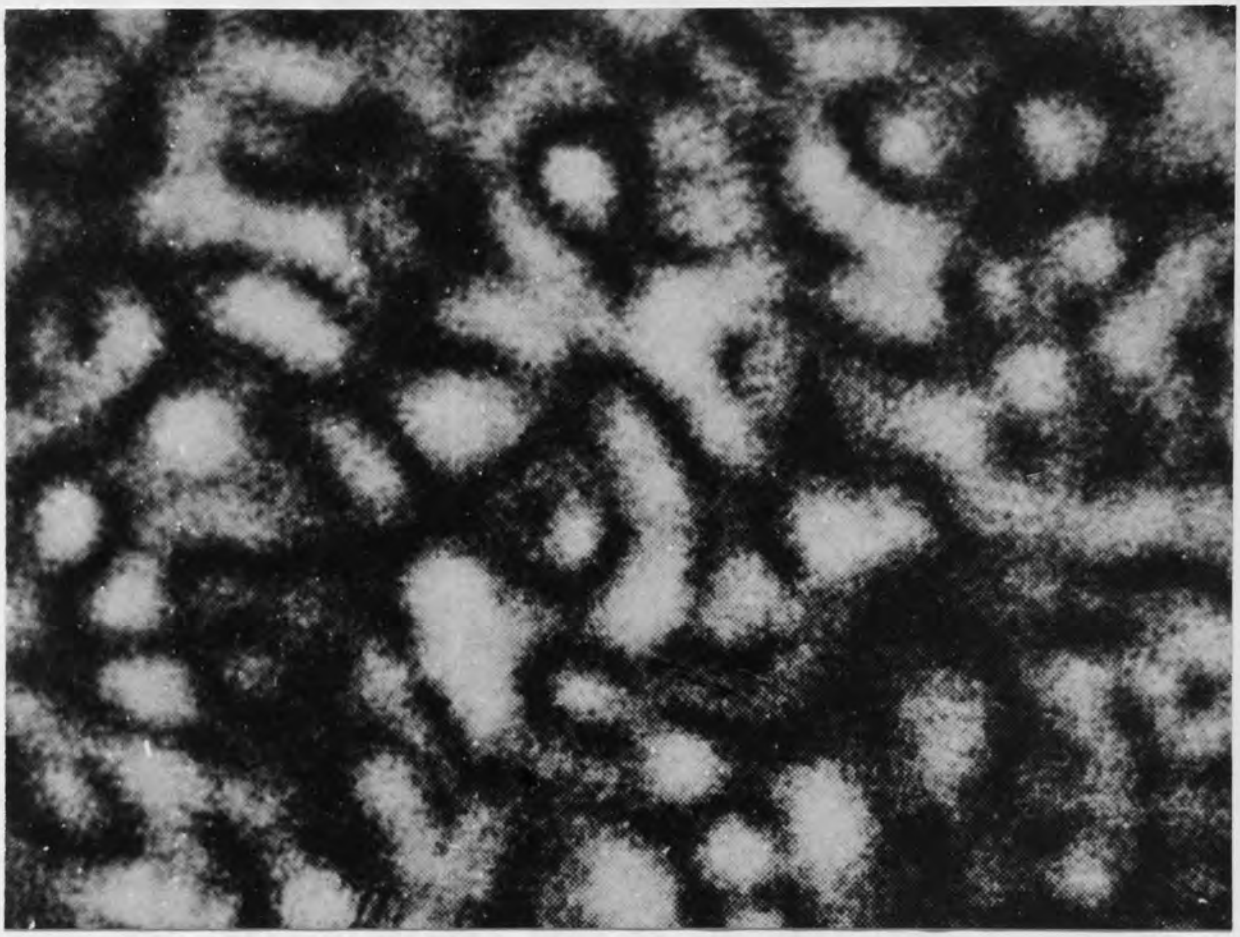

Fig.1.3.1. Laser Speckle Pattern (Enlarged)

Nevertheless, it has only been since the construction of the laser - which gives light of high spatial and temporal coherence, that interest in speckle has grown and led to the undertaking of comprehensive investigations. Initial research concerning 'laser speckle' was chiefly centred on the reduction of speckle. The reason for this, as Stetson[15] emphasizes, was because it was only regarded as unwanted background noise in connection with laser holography. Thus, it was originally considered to be of little practical use

and was only studied because it caused degradation of the quality of holographic images.

1.4. THE NATURE OF SPECKLE

The 'speckly' appearance of optically rough surfaces illuminated by coherent light is due to intermodulation of the light waves scattered from individual areas. Concerning the roughness of the surface, Ennos[16] reports that the local irregularities in depth on the object surface should be greater than one quarter of a wavelength of the light source. Tiziani[17] suggests that the coarseness of the surface ought to be at least the order of the wavelength of the illuminating light for most applications. An interesting comment regarding speckle patterns is made by Hung[18] who says of their nature :

> "The speckle pattern, caused by the random interference of light scattered from various depths on the object surface, acts as a grid naturally printed on the object surface".

1.5. BASIC THEORY OF SPECKLE PRODUCTION

Consider a non-specularly reflecting surface illuminated by coherent light. Each point on the rough surface scatters the light as a spherical wave and thus we can approximate the surface as a collection of a great number of closely packed point sources. The relative phases of these point sources are <u>random</u> because of the surface roughness. Nevertheless, they are constant with respect to time provided that the surface is stationary. The interference of the de-phased, but coherent, secondary spherical

wavefronts is responsible for the production of speckle.

In other words, the light wave reflected from any reasonably distant point on a rough surface consists of numerous coherent wavelets (each arising from a different element of the surface) and the path difference between these wavelets can differ by several wavelengths, as shown in Figure 1.5.1. The scattered waves not only have random phases but, as Tiziani[17] has shown, also random real amplitudes. It is the interference between these wavelets which results in the granular pattern of intensity. Similar effects are observed when highly coherent light propagates through a medium that has random refractive index variations.

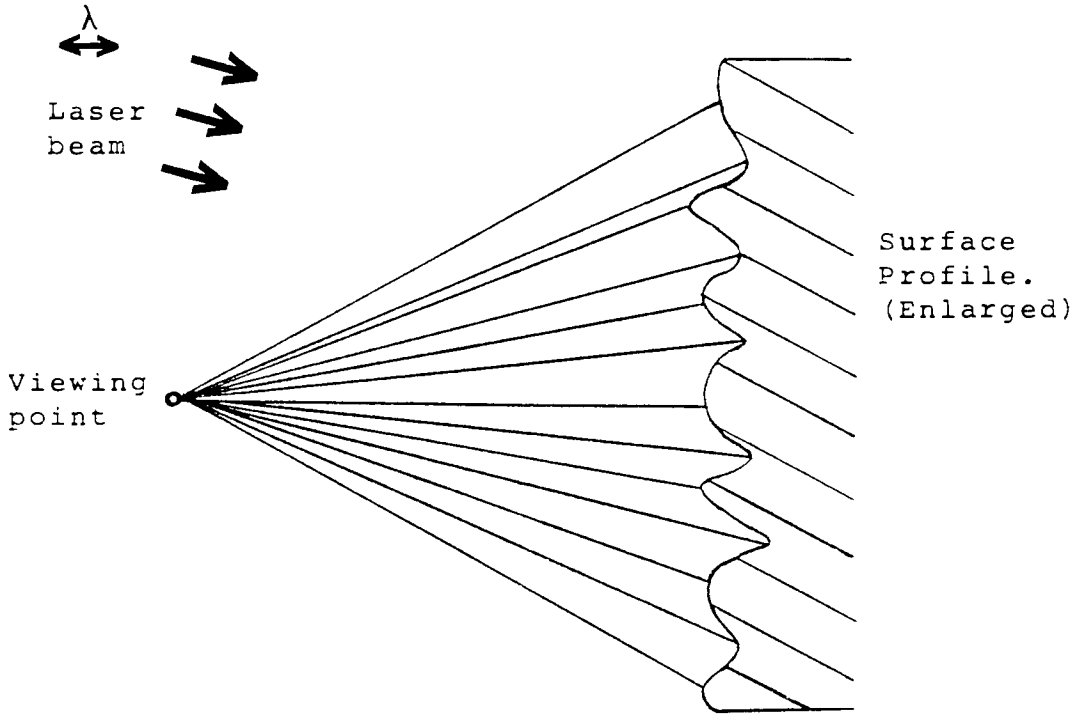

Fig.1.5.1. Propogation of a Speckle Patern in free-space.

The properties of laser light, such as long coherence length, high intensity and monochromacity have enabled these effects to be readily exploited.

When a rough surface is illuminated by coherent light, the scattered light from each object point produces an image which is dependent on the imaging system. As previously indicated it is the interference between these diffraction images which is responsible for the production of a speckle pattern. Hence, if a photographic system is employed the processed film image exhibits a speckle pattern which is dependent upon the lens aperture used to record the image.

Regarding the theory of speckle, Harvey[19] points out that each element on a surface scatters light in a complex manner to give polar patterns which are different, as indicated in Figure 1.5.2.

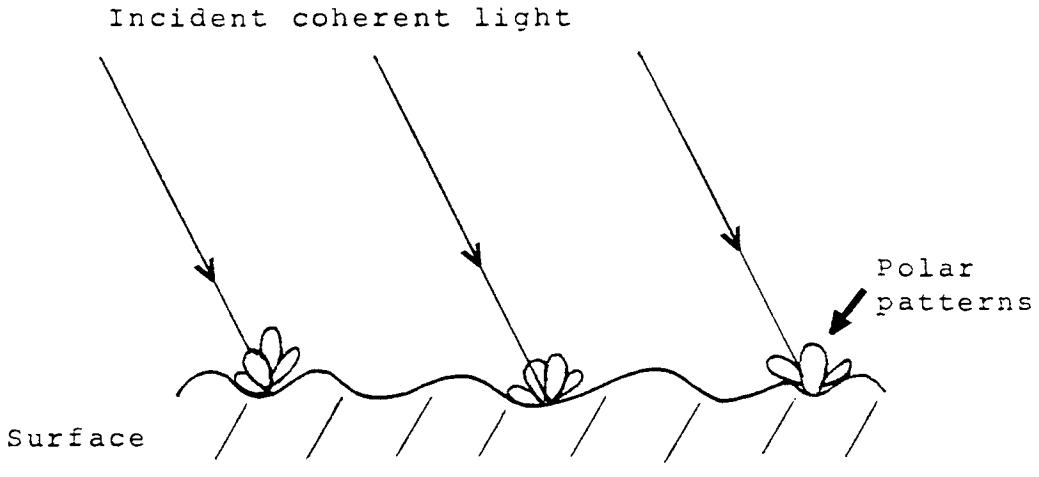

Fig.1.5.2. Random Polar Patterns.

Harvey explains that the power received at one point from a great number of randomly placed coherent sources has a probability distribution - thus causing large fluctuations in intensity in different directions. This means that the observed granular effect appears to scintillate when the observer moves. Depending upon how strong the scattering is in a given direction of observation the surface elements appear bright or dark. The granularity which is observed is due to spatial beats between the random Fourier components which are scattered from the surface.

1.6. SPECKLE IMAGES

Speckle patterns are propagated in space whenever rough surfaces are illuminated by coherent light. Thus, the formation of an image is not necessary for speckle patterns to be obtained and such a pattern may be recorded at various distances from the surface. This far-field speckle pattern is called an 'objective' speckle pattern[20]. The speckle pattern formed by imaging a coherently illuminated rough surface is known as 'subjective' speckle[21] or 'image' speckle.[22] Francon[23] suggests that, by analogy with diffraction phenomena, speckle may be regarded as being of the Fresnel type in the former case and Fraunhofer when an image is formed.

When rough, coherently illuminated surfaces are seen by eye, each point of light is imaged onto the retina. The individual point-source images are not themselves points of light because the pupil serves as

a circular aperture which diffracts the light waves which enter the eye. O'Shea et al.[24] point out that this is the reason why the individual point images are blurred and because of this they overlap with each other. In practice, the imaging system which is employed may be a photographic system or a television camera. When an optical imaging system is used it is necessary, as Goodman[25] stresses, that diffraction as well as interference effects are taken into consideration.

If an imaging system is employed (see Figure.1.6.1) it is only necessary that the diffraction limited 'amplitude' point-spread function of the system is large in comparison with the object surface variations to ensure that large numbers of de-phased coherent contributions add together at each image point.

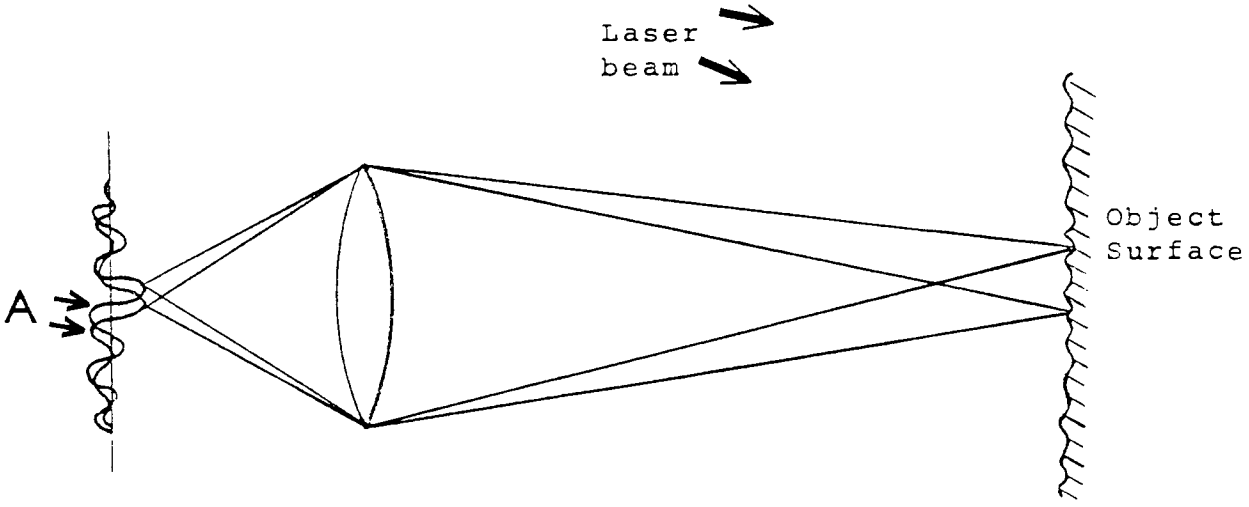

(A: de-phased amplitude spread functions)

Fig.1.6.1. Formation of speckle with an imaging system

The speckle size is correlated to the aperture of the imaging lens such that the smaller the aperture the larger the speckle. (Which is in keeping with the relationship that the diffraction pattern of a lens increases as the aperture of the lens decreases). This is because intensity variations cannot be produced inside the Airy disc diameter. Ennos[16,26] shows that the average diameter σ of 'subjective' speckles is such that :

$$\sigma \simeq \frac{0.61\lambda}{N.A.} \qquad \ldots\ldots\ldots(1.6.1)$$

(Where λ is the wavelength of the coherent illumination and N.A. is the effective numerical aperture of the lens)

If the aperture of the imaging lens is reduced in order to increase speckle size then, as Leendertz[2] points out, this is at the expense of image intensity.

When a non-specularly reflecting surface is illuminated obliquely by a coherent light source and the surface is laterally translated, as shown in Figure 1.6.2, the optical path lengths from the individual surface points to the imaging system changes. The speckle pattern also changes but, because the path length changes are co-ordinated, the speckle pattern moves 'with' the imaging system.

The property that any lateral translation of a rough surface in its mean plane does not cause the relative phases from the surface elements to vary-such that the speckle pattern in the image plane P is <u>not</u> modified, is one which led to the use of speckle patterns for surface movement and

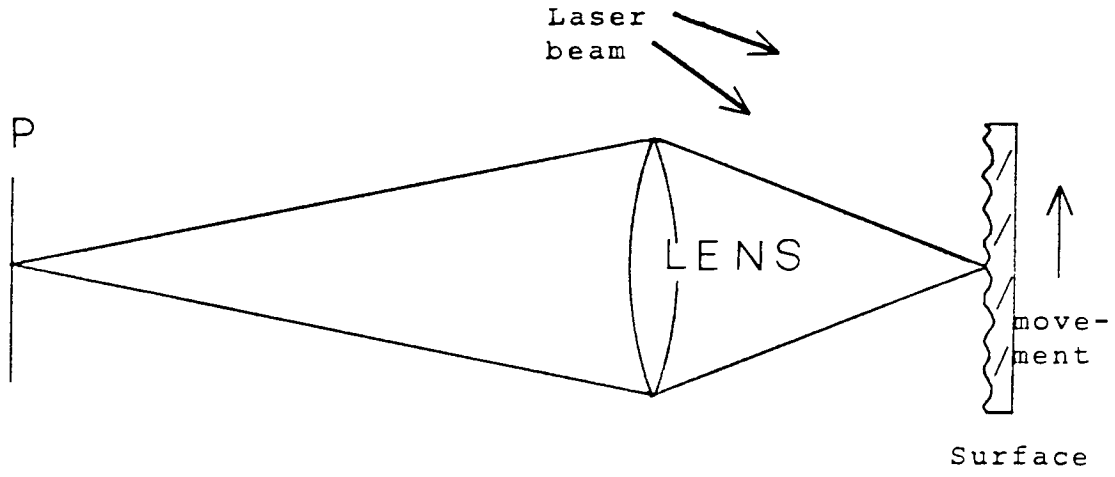

Fig.1.6.2. Lateral translation of Speckle Pattern.

displacement analysis and is particularly important in the context of the research reported in this thesis.

1.7. FACTORS INFLUENCING SPECKLE

In the case of 'objective' speckle patterns the detailed structure of individual speckles is determined by the magnitude of the illuminated object field. Speckle size is inversely proportional to the area of surface illumination. The smallest detail which can occur in the diffraction pattern is determined by the angular size of the diffracting object (as seen from the diffraction plane). As Goodman [25] has shown, the finest structure in the diffraction pattern corresponds to that which arises from

waves having the greatest mutual inclination. There are many instances regarding the uses of speckle patterns where it may be necessary to illuminate relatively large areas of the object surface. The reduction in speckle size associated with this can be influenced by factors such as the imaging lens aperture (see Equation 1.6.1) Moreover, smaller speckle size can mean that higher resolution is achieved.

It has been found that speckle size is also related to the roughness of the object surface. The spread of the diffracted light in an arbitrary plane (such as 'P' in Figure 1.7.1) is clearly greater if the surface height variations on the object surface 'S' are smaller and vice versa.

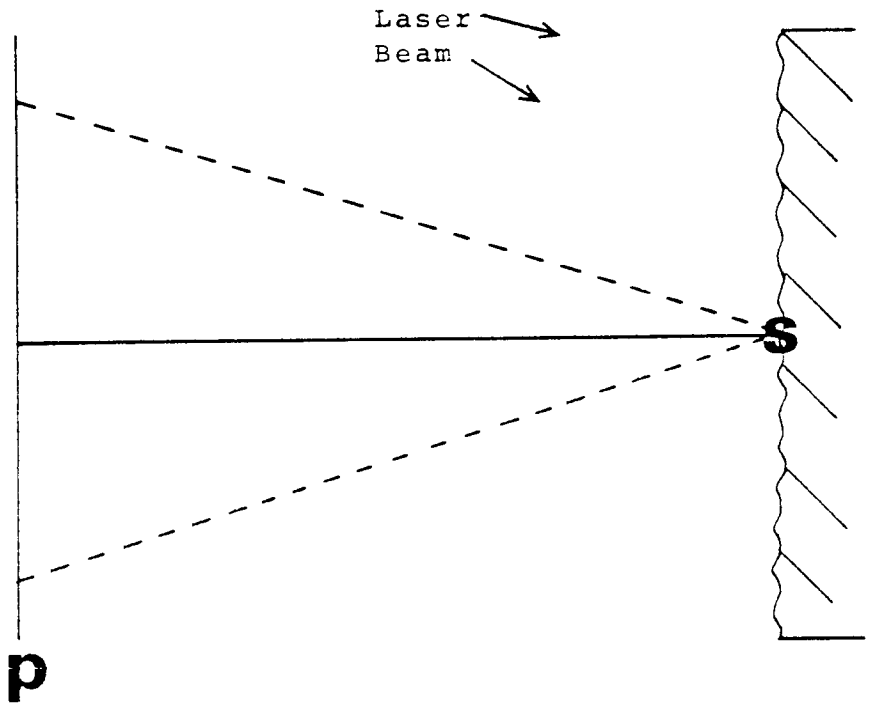

Fig.1.7.1. Effect of Surface Height Variations.

Goodman[25] has shown statistically that there is a dependence on surface roughness of speckle contrast. Furthermore, Asakura[27] has demonstrated experimentally that r.m.s. surface roughness is correlated to the contrast of speckles in the observation plane. This is such that as phase variations increase (due to the surface becoming coarser) the intensity variation at the observation plane increases. Consequently, the contrast of the speckle pattern increases. As Dainty[13] reports, the degree of spatial coherence of the illuminating source also affects speckle contrast. If only partially spatially coherent light is employed, there is a reduction in contrast.

The irradiance or brightness distribution of speckle patterns depends upon whether or not they are fully-developed patterns. Fully-developed speckle patterns are only obtained if all of the waves contributing to a particular speckle are coherent with respect to each other. In order that this latter condition is satisfied, the object surface should, therefore, not depolarise the light.

The distribution of brightness amongst the speckles of a pattern which is fully-developed follows a negative exponential relationship[25,16]. This is given by

$$P(I) = \frac{1}{I_o} \exp.\left(-\frac{I}{I_o}\right) \qquad \ldots\ldots\ldots (1.7.1)$$

$P(I)$ is the probability of an individual speckle having an irradiance between I and $I + dI$.

I_o is the mean irradiance of speckles in the pattern. A

graphical plot of this relationship (Figure 1.7.2) shows that the most probable irradiance in a speckle pattern is zero.

Fig.1.7.2. Probability density function of the brightness distribution of a single speckle field.

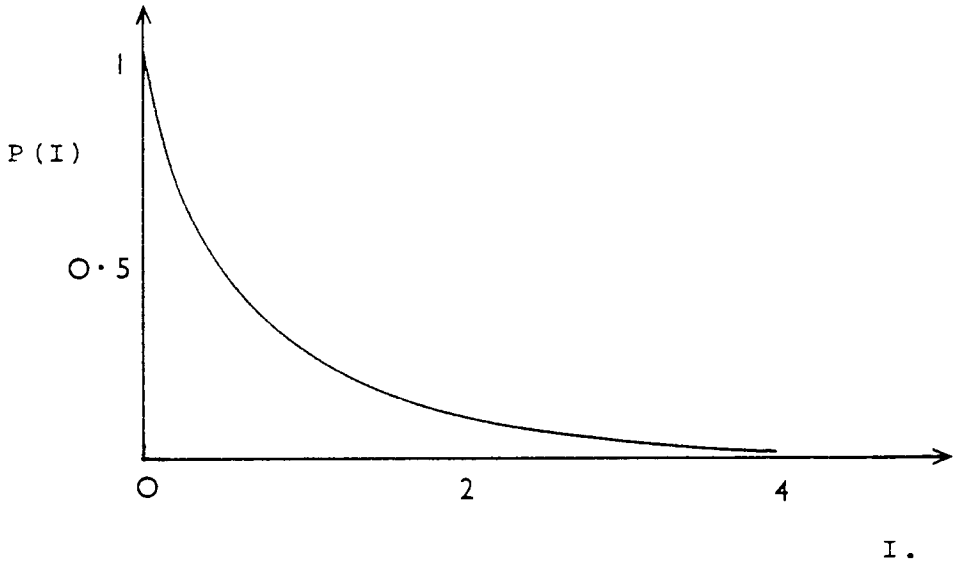

Thus, in a speckle pattern there are more 'dark' speckles than there are speckles having any other irradiance. (McKechnie[28] has verified this relationship experimentally) This property is an important distinguishing feature for fully-developed (i.e.fully coherent) speckle compared to a speckle pattern which is less fully-developed (i.e.partially coherent). It is particularly significant, as Ennos[16] observes, if the speckle pattern is recorded on nonlinear photographic film or observed visually.

A measure of the contrast of a speckle pattern is the

ratio:

$$C = \frac{\sigma_{S.D.}}{I_o} \qquad \ldots\ldots\ldots(1.7.2)$$

$\sigma_{S.D.}$ is the standard deviation of the irradiance.

I_o is the mean value of the irradiance.

For the case of the distribution given by Equation (1.7.1) the speckle contrast is unity.

1.8. SPECIAL PROPERTIES OF SPECKLE PATTERNS.

There does not appear to be any obvious relationship between the macroscopic properties of the object and the detailed structure of the speckle pattern. Nevertheless, the use of statistical methods and probability theory has proved useful in this context. For example, in the case of the incident illumination being monochromatic and linearly polarised and the object surface not depolarising the light, Goodman[25] has demonstrated that the analysis is basically equivalent to the classical problem of a two-dimensional random walk. It is assumed that the amplitude and phase of each component are statistically independent and are also independent of the amplitudes and phases of all other components. In addition, it is assumed that the phases are uniformly distributed over all values between $+\pi$ and $-\pi$ (in other words, that the surface roughness is greater than the wavelength of the light source).* The

---

*These are all assumptions which generally apply to the investigations undertaken.

probability distribution for the resultant amplitude at any point in such a case has been shown by Goodman to be Gaussian. Thus the resultant intensity distribution follows a negative exponential law. (see Equation 1.7.1.) Tanner[29] has confirmed that the intensity variation follows a Rayleigh distribution.

It has been shown by Goldfischer[30] that a speckle pattern contains all spatial frequencies up to the highest which our observing system can resolve. Moreover, concerning the spatial frequency distribution of interference 'fringes' which contribute to speckle patterns, it has been found, as Vest[31] points out, that the distribution of irradiance over fringe frequency is linear.

Finally, although the effects associated with the use of polychromatic light sources and wavelength change do not concern us here, it must be acknowledged that these do have effects on speckle patterns (see,for example,Francon[23]). Similarly, there are effects due to the employment of partially coherent light which must not be overlooked (see Parry[32]) and which have actually been applied and developed. All these and certain other factors, which will subsequently be identified, will be taken into account in respect of the experimental investigations that are described later.

1.9. SUMMARY.

The speckle effect, as Wykes[33] points out, occurs

because the amplitude of the scattered light at a given point is the sum of a large number of coherent components scattered from different parts of the surface. If the surface is sufficiently rough these components have random phases and the addition of these components gives rise to a random intensity and a random amplitude. Various aspects of the nature and theory of laser speckle have been discussed and factors influencing the size, brightness and contrast of speckle patterns have been analysed,since these are particularly relevant to the studies which were undertaken.

In conclusion it is worth noting the suggestion of Butters and Leendertz[34], that a speckle pattern may be regarded as a 2 dimensional coded record of a general 3 dimensional object. Furthermore, as Francon[23] suggests :

> "The development of speckle technique in the past few years has been such that there is little doubt that a new chapter in optics has been opened".

These and certain other points will be expanded in the following chapter prior to the preliminary experimental investigations described in Chapter 3. The initial investigations were intended to examine and explore various facets which would then be employed in the investigations.

CHAPTER 2.

SPECKLE PHOTOGRAPHY

CHAPTER 2.

2.1. INTRODUCTION

Techniques employing laser speckle patterns can be separated into two broad categories, namely, speckle interferometry and direct laser speckle photography. However, as Ennos[16] observes, the latter category does not involve the use of reference beams. The distinction between the two groups is not always clear since both involve interference and both involve photography - or an appropriate alternative means of visualisation. Nevertheless, Stetson[15] has suggested a simple but fairly satisfactory means of distinguishing between the two. If there are regions in the two images where the speckle patterns of each are well correlated then he proposes that the process be classified as "speckle photography" (see, for example, early references to techniques in this grouping [9,36,37,38,39,40]. On the other hand, if the fringes form as the consequence of fluctuations in the correlation of the speckle patterns between the two images (whether there is translation or not between the correlated regions of the speckle patterns) then Stetson suggests that the process is classified as "speckle interferometry". (See, for example, early references to techniques in this grouping [1,2,3,4,35,38]. The former category is the one which is of primary concern in respect of the work that will be described here.

Speckle photography can itself be separated into

several categories(e.g. single-beam illumination[9,18,37,40,41] and dual illumination beam[9,36]) and sub-categories regarding different modes or areas of application for the various techniques. These categories include focused speckle photography[37], defocused speckle photography[42,43], incremental speckle photography[44] and double speckle camera systems[45]. The investigations which will shortly be detailed were fundamentally based upon a form of single beam illumination, focused speckle photography.

2.2. THE PHOTOGRAPHY OF LASER SPECKLE PATTERNS

To facilitate the explanation of the special measures and techniques which were adopted in the experimental work, brief consideration will be given to the theory and principles concerning the basic photography of speckle patterns. There are three main factors which require to be taken into account in this context. These are the camera lens aperture ratio, the film type (and exposure) and the processing of the film.

In Section 1.6 it was shown that the size of individual speckles in the image plane is related to the effective numerical aperture of the lens: (see Equation 1.6.1) When a camera is used it is more convenient to relate the speckle size to the aperture ratio of the lens. The magnification (or demagnification) of the image must also be taken into account - assuming that the lens actually images the diffusely reflecting surface. Equation 1.6.1 concerning the speckle size σ is then rewritten as :

$$\sigma \triangleq 1.2\ M\lambda F \qquad \ldots.(2.2.1)$$

'M' is the image magnification and 'F' is the aperture ratio of the lens ('f' number).

A conventional 35mm single lens reflex (S.L.R.) camera, with the lens set at a moderately high aperture, is generally found satisfactory for speckle photography. Ennos[7] suggests that the quality of the photographic lens used is relatively unimportant. Nevertheless, Archbold and Ennos[37] have noted cases where lens aberrations (particularly distortion), play a limiting role. Moreover, Stetson[46] has reported that the effects of lens aberrations not only include loss of speckle correlations and subsequent halo fringes but also distortion of halo fringes (which can result in false information about object motion if the photography is undertaken in the context of surface displacement studies). However, if a reasonable quality lens is employed and it is not used far off axis then Stetson acknowledges that the effects are considerably reduced.

Regarding the film used to record speckle patterns, Archbold et al.[9] have demonstrated that fine grain, high contrast emulsions are more suitable than relatively coarse grain, low contrast emulsions. Although fine grain emulsions require longer exposures, they consider that the higher density and resolution of such emulsions is more significant in terms of the results obtained. Stetson[15]

points out the need for film used for speckle photography to have a high modulation transfer function (M.T.F.) because of the wide range of spatial frequencies in a speckle pattern.

Film 'speed' varies inversely with resolution and since fairly high resolution photographic emulsions are generally considered to be particularly suitable for speckle photography this means that relatively long exposures may be necessary. Tiziani[17] has indicated that the exposure used should be one which gives an overall intensity transmittance for the processed film of about 50% (see Figure 2.2.1). As exposure ε is equal to the product of the incident irradiance distribution $I(x,y)$ and the duration of the exposure this means that $\varepsilon(x,y) = I(x,y)t$.

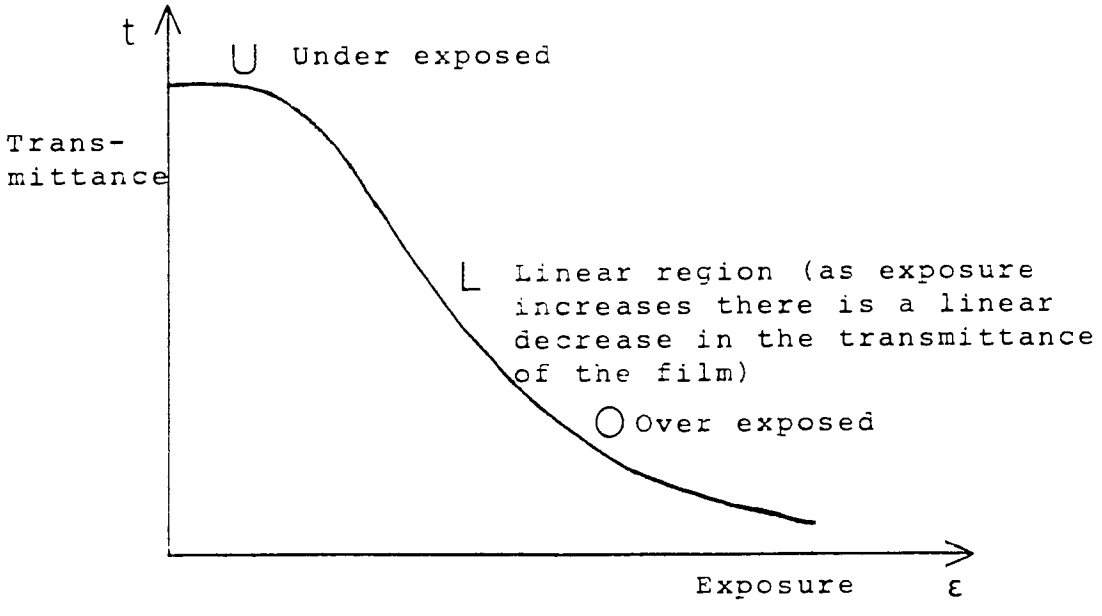

Fig.2.2.1. Amplitude transmittance versus exposure for a negative after development.

It is emphasized by Vest[31] that speckle photographs should be exposed and developed in such a way that high contrast is achieved so that good diffraction efficiency is achieved. He stresses that care must be taken in developing speckle photographs so that the photographic negative (transparency) or 'specklegram' is a complete and true record. Manufacturers of emulsions for use in this field also endorse the need for careful processing of the exposed film (e.g. Agfa-Gevaert[47]).

All the aforementioned factors and conditions were taken into account as were the effects of emulsion thickness, illumination levels, focusing, surface finish, bleaching of the processed film and further factors which could influence the quality of the processed latent image. (See Section 2.7).

2.3. DOUBLE EXPOSURE SPECKLE PHOTOGRAPHY

The single illumination beam, double-exposure technique for laser speckle photography was initially demonstrated by Archbold et al.[9]. This technique does not rely on the non-linearity of the recording medium and only requires that the object is illuminated by a divergent, coherent beam 'B', from any angle, as shown in Figure 2.3.1.

The speckle pattern produced by the object is imaged by a camera, such as an S.L.R. 35 mm camera, located in the image plane. Continuous wave (C.W.) low power lasers

are generally employed as illumination sources. For example, Helium-Neon, Argon, Krypton and also free-running pulsed ruby lasers can be used. Temporal coherence and environmental stability requirements are not so rigid as they are for conventional holography.

Double-exposure photographs are taken (on fine grain film) before and after the specimen surface has been laterally displaced. The two recorded speckle patterns are locally identical,but displaced by an amount and in a direction which is related to the movement of the corresponding surface element. Surface movement in any direction orthogonal to the line of sight may be analysed.

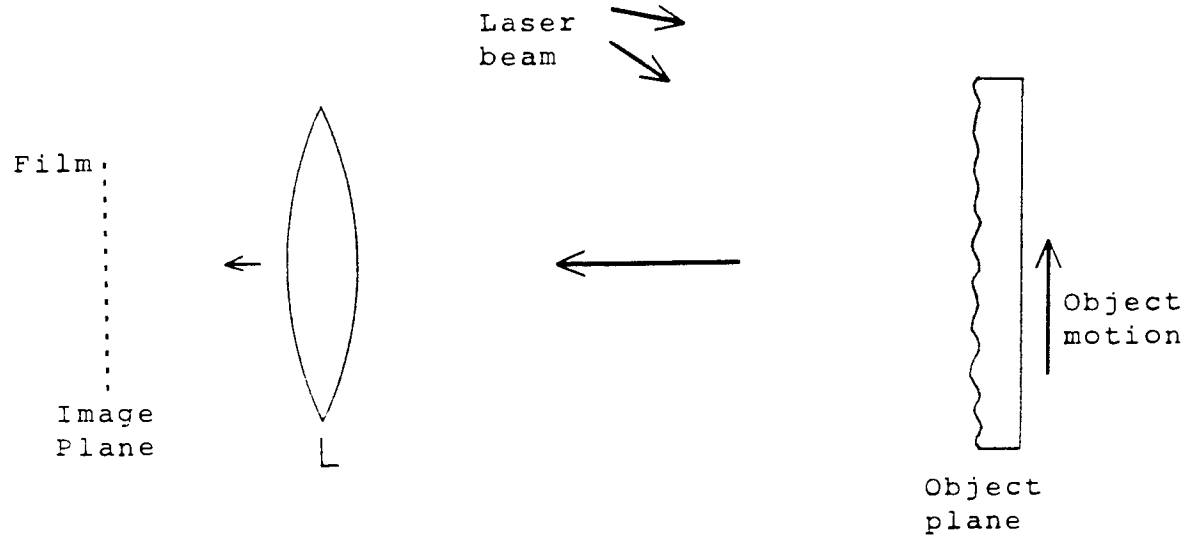

Fig.2.3.1. Recording Lateral Displacement.

Ennos[7] has explained that, because the speckle field intensity distribution is independent of the phase of the illuminating source and is only slowly affected by a change in its direction, the laser does not need to be rigidly mounted with respect to the object. However, it is important to minimise any undesired movement between the camera 'L' and the object. This is because such movement could cause false information to be recorded by the speckle-gram . It could also mask the surface movement which is under investigation. If the correlation of the speckles is maintained between the two exposures the speckles behave like a moiré grid that is attached to the object surface. However, unlike a moiré grid, a speckle pattern is aperiodic and so normal means of observing moiré interference cannot be employed.

Analysis of the double-exposed specklegram is basically undertaken by directing a narrow beam of light onto its surface as indicated in Figure 2.4.1 (see later). The grain structure on the film spreads the beam out by diffraction and the diffraction halo which is produced is modulated by interference fringes. It is the spatial frequency of these fringes which enables a quantitative measure to be made of the local displacement which has taken place on the object surface. The normal to the fringe direction indicates the direction of the displacement.

Hung[18] and others[7,37] have shown that this technique does not require the special vibration isolation

which is generally demanded in dual-beam speckle interferometry. Neither does the interpretation of the interference fringes depend upon the direction of illumination. This means that a diverging illumination beam can be employed, and, as Hung indicates, restrictions on object size are therefore reduced.

With regard to speckle interferometry systems the output information is obtained by distinguishing between parts of the field where the field is correlated and where it is not. However, this pre-supposes that the displacement of individual speckles in the image plane does not exceed their diameter. If the translation is greater than the speckle diameter then the lateral displacement of a localised area can be measured by positional correlation of the pattern at that point, without using a reference beam, by the technique of double-exposure laser speckle photography.

2.4. BASIC THEORY OF DOUBLE EXPOSURE TECHNIQUE

If a single exposure specklegram is illuminated normally by a convergent beam of coherent monochromatic light, it diffracts the beam into a cone of well-defined angle. When this is projected onto an opaque screen it forms a circular halo of light surrounding the unscattered beam. The intensity distribution of the diffracted light decreases radially as the square of the auto-correlation function of the lens aperture. This diffracted light is

called the auto-correlation halo. It can be shown that, for an imaging system, the angular radius of this halo corresponds to the maximum spatial frequency recorded and it extends over approximately twice the angle of the cone of light which generated the speckle pattern. Archbold et al.[9] have indicated that the angular radius of this diffraction halo is roughly equal to the numerical aperture of the recording lens.

When two speckle patterns are recorded on the same film (double exposure) and if between the exposures the object surface was laterally displaced by an amount 'd_1' (the recorded speckles will displace by a corresponding amount 'd') then <u>two</u> diffracted cones are generated. They interfere together forming equispaced parallel fringes modulating the auto-correlation halo.

These cosinusoidal fringes can be imaged on a screen placed in the Fourier plane, as shown in Figure 2.4.1. Ennos[16] has shown that the intensity 'I' of the recorded lightis related to the image displacement d as follows :

$$I \propto |F|^2 \cos^2 (kvd/2) \qquad \ldots.(2.4.1)$$

$|F|^2$ represents the diffraction halo due to the speckle pattern. The $\cos^2$ term represents its modulation (interference fringes) : $k = 2\pi/\lambda$ and v is an angular coordinate.

If the displacement is less than one speckle diameter the interference fringes will fall outside the diffraction halo and so will not be detected .

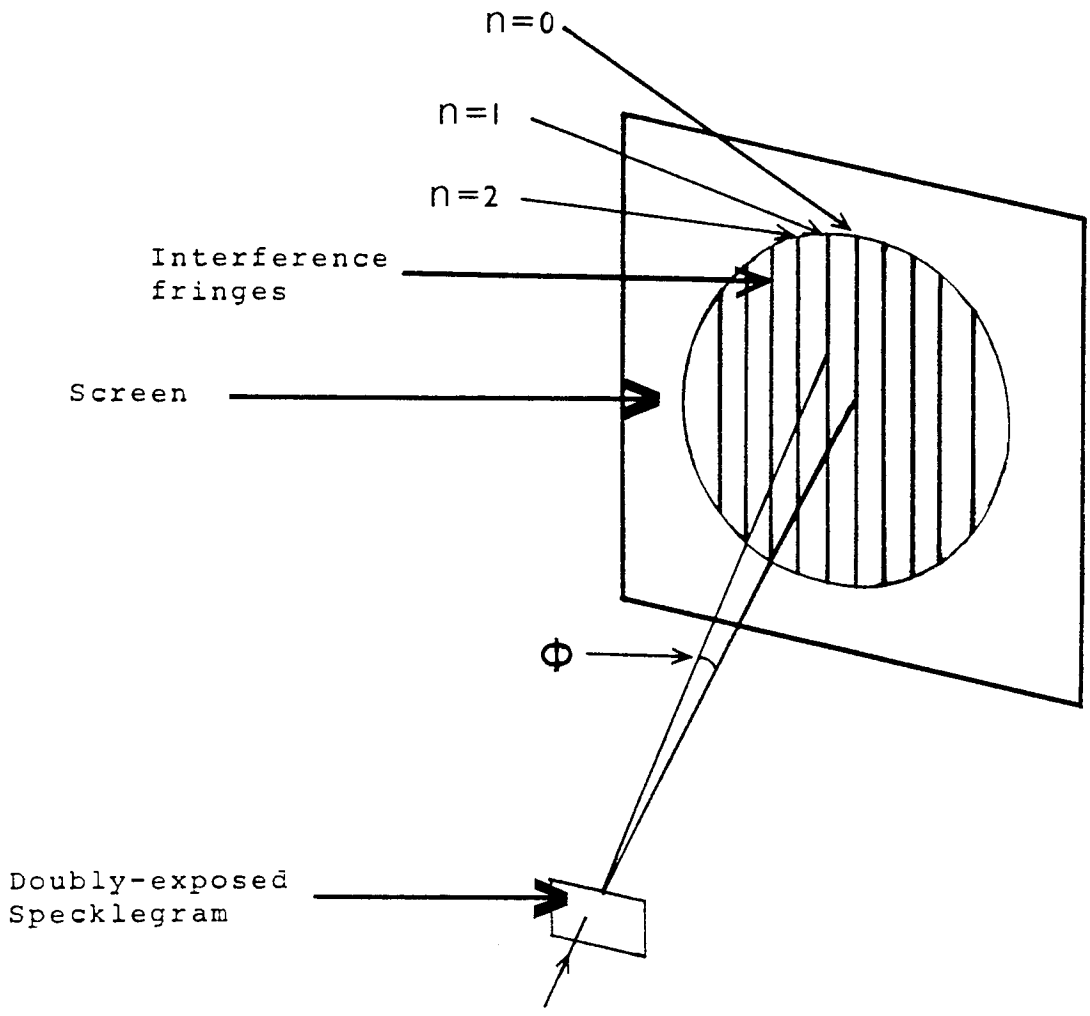

Fig.2.4.1. Production of Young's fringes

The angular distribution of the fringes is given by:

$$d \sin \phi = n\lambda \qquad \text{.....(2.4.2)}$$

where n is the order number of the fringe and λ is the wavelength of the illuminating beam.

[The interference fringes actually arise from a dark speckle which has moved between the two exposures due to movement of the object surface. It thus creates a pair of transmitting areas on the specklegram that act as the two point sources of light do in Young's experiment.]

2.5. MEASUREMENT OF LATERAL MOTION

Single-beam illumination double-exposure laser speckle photography can be used to measure the lateral displacement of specimens[9,18,37,48]. If the magnitude 'd' of the image displacement is greater than the speckle size 'σ', the processed double exposure film will contain a pair of identical speckle patterns which are separated by a distance dM. (where M is the lateral magnification of the imaging lens used for the recording). The lateral displacement of each point of the recorded image may be evaluated from the Young's fringe pattern as follows:

From above, the lateral displacement vector d_l of the specimen is related to this fringe pattern according to the equation $d_l = \frac{d}{M}$

Hence, from equation 2.4.2,

$$d_l = \frac{n\lambda}{M\sin\phi} \qquad \text{.....(2.5.1)}$$

It has been reported[16] that small displacements in the line of sight direction do not affect the measurement of lateral motion. Moreover, the sensitivity of displacement measurement can be varied considerably by changing the magnification. For a recording lens aperture ratio F the speckle size σ is given by Equation 2.2.1. The corresponding speckle size on the object will be given by:

$$\sigma_o = 1.2\ M\lambda F \qquad \text{.....(2.5.2)}$$

(For HeNe laser $\lambda = 633$nm)

Thus, for example, if unit magnification is employed

and the lens aperture ratio is f/4 then, using Equation 2.5.2 it can be seen that lateral movements greater than 3μm can be measured. However, if the same aperture ratio is used but a 10 times demagnification is employed this means that movements greater than 30μm are measurable. The upper limit of measurable displacement is dictated by the resolution of the Young's fringes which can be achieved (since their spacing is inversely proportional to the displacement). Experimental data reported in the literature[37] on speckle photography (not just the single-beam method) indicates that surface motions which produce speckle translations in the range 15 - 200μm (in the film plane) may be measured. The lower limit is about five times the size of the speckles formed with an f/4 lens and in the case of the upper limit the corresponding object surface translation is about ten per cent of the entrance pupil diameter of a 35mm camera lens, at the above aperture ratio.

2.6. MEASUREMENT OF TILT

It is possible to employ double exposure speckle photography to measure out of plane rotation or 'tilt' of specimens[12, 37]. For instance, Tiziani[49] has shown that, by modifying the recording system outlined earlier, small object tilts can be analysed. In this situation, the recording film is not used in the image plane but in the back focal plane of the lens (see Figure 2.6.1). One exposure is taken before the object tilts and one after it has tilted by an amount 't'.

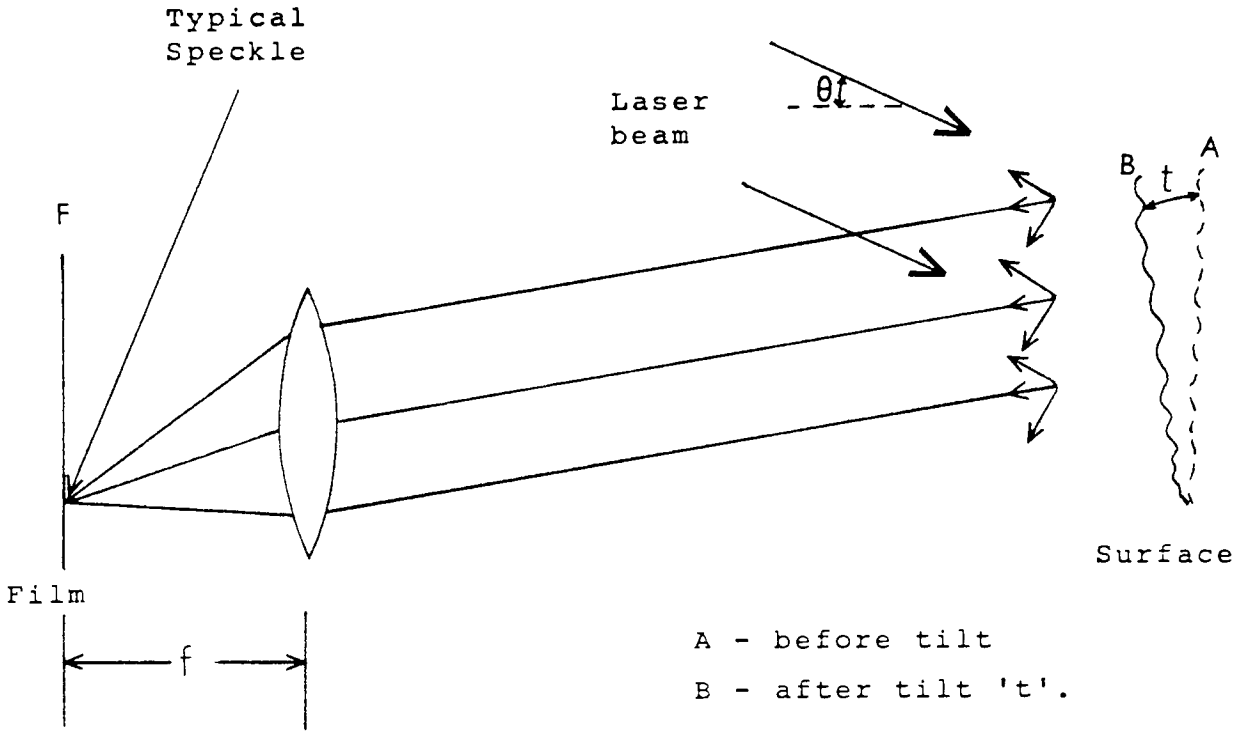

Fig. 2.6.1. Measurement of Surface Tilt

As shown, the speckle pattern is recorded in the Fourier transform plane F (Fraunhofer diffraction plane). Although there is basically no difference, it is usual to refer to the Fourier transform plane when the speckles of the object are recorded in the back focal plane of the lens and to the Fraunhofer plane when the interference fringes are displayed.

When the object tilts, the speckle pattern in the Fourier plane translates. Every ray which contributes to the formation of a single speckle leaves the object surface at a different location but they all travel in almost the same direction. The effect of the object tilting is to cause a systematic change of relative phase amongst these

rays. For angles of incidence and viewing which are close to the normal, the surface thus acts like a mirror to the speckle pattern which rotates as if reflected by the tilted object surface.

The double exposure recording is carried out with the camera de-focused by a known amount (by focusing on a plane at a predetermined distance before or behind the surface to be tilted). It has been found[18,37] that the more de-focusing which is employed the greater the area of the surface over which the tilt is averaged. If the angle θ (Figure 2.6.1) is small and the aperture of the lens is not too large (see below) then the translation d_t of the speckle in the Fourier plane is:

$$d_t = f(1 + \cos\theta)t \qquad \ldots\ldots\ldots(2.6.1)$$

(f = focal length of imaging lens)

Archbold and Ennos[37] have confirmed that the tolerance on the tilt angle is inversely proportional to the camera aperture ratio and to the amount of demagnification. An aperture of f/4 and a demagnification of x7 is found to enable a tilt of 15 mrad to be measured.

Interference fringes are produced when the double exposure specklegram is illuminated by a converging beam and these can be related, as will be demonstrated, to the magnitude of the object tilt. It has been shown by Gregory[12] that it is possible to record and measure tilt independently of lateral motion by regarding the object surface as a mirror and focusing on the plane

behind the object which contains the 'mirror' image of the laser source. For this to be readily achieved, the illumination direction needs to be close to the line of sight of the recording system.

2.7. ANALYSIS OF DOUBLY-EXPOSED SPECKLEGRAMS

Data reduction techniques for processed double-exposure specklegrams have been devised for a variety of forms or applications of laser speckle photography. In general, these techniques are related to particular methods or uses of speckle photography - such as lateral displacement measurement, tilt measurement, surface microstructure analysis, vibration analysis, creep measurement and strain examination. A number of investigators (for example[9,16,21,36,37,42,44,45,48,49,50,51,52]) have suggested methods and explored applications of speckle photography for which a number of techniques for the analysis of specklegrams have correspondingly been described. These techniques have chiefly involved illuminating the specklegram with coherent monochromatic light (mainly using low power C.W.lasers - but special white light speckle techniques have also been devised) and it is upon a coherent technique that the studies which will be detailed later were based. Fundamentally, they were concerned with the devising of means which would enable detailed analysis of specklegrams of object surfaces that had undergone lateral displacement to be carried out with sensitivity and reliability. (This principal objective was approached in such a way that three

different methods were devised and the most appropriate of these was then employed in connection with specific applied problems).

Local in-plane translations can be determined from double exposed specklegrams by measuring the separation (see Section 2.5) of each speckle pair using a travelling microscope. This method is often inconvenient and poses practical problems in some cases (such as when the processed specklegram corresponds to very small displacements). However, using simple coherent optical processing of the specklegram the displacement can be displayed in the form of a Young's interference fringe pattern that can be measured and the result used to calculate the magnitude of the displacement.

One method of coherent optical processing which may be used employs a spatial filtering (Fourier filtering) system - such as that devised by Archbold and Ennos[37] or by Duffy [53]. Alternatively, the specklegram can be examined one region at a time by illuminating it with a narrow beam, such as an unexpanded C.W. laser beam, as suggested by Archbold et al.[9] (see Section 2.4 for basic theory of this technique). It is this latter method which was chosen as the means of producing the Young's fringes for analysis and spatial frequency determination. This is because the method is best suited to the type of technique envisaged for spatial frequency measurement and also because the point by point record of the spacing and direction of the fringes, which the method enables to be

readily built up, is a valuable feature with regard to the applied research that was subsequently to be undertaken.

Production of Interference fringes:

The basic arrangement to produce the interference fringes on an opaque screen is shown in Figure 2.7.1.

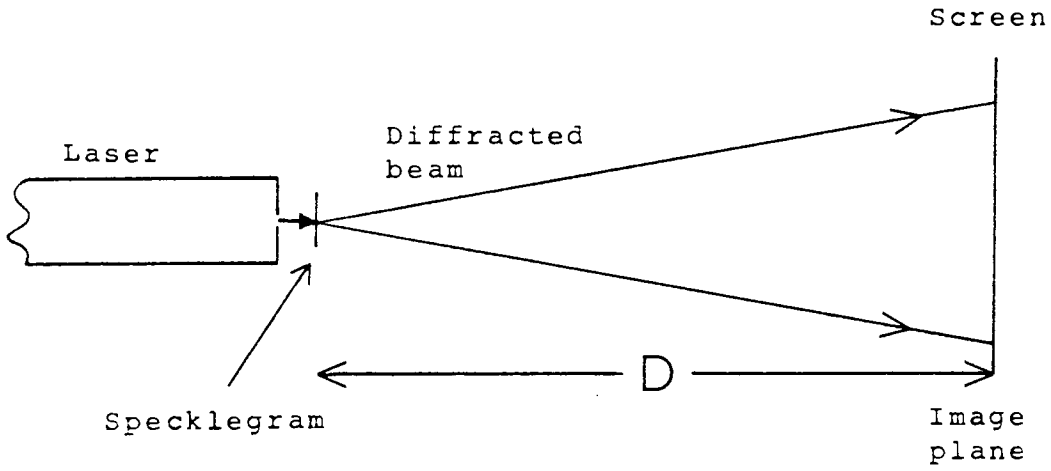

Fig.2.7.1. Production of Interference Fringes

The distance 'D' between the specklegram and the screen and the spatial frequency 'x' of the interference fringes are both measured. For an image magnification M the lateral object displacement d_l can be found (see Equation 2.5.1) from the relationship:

$$d_l = \frac{\lambda D}{xM} \qquad \text{.....(2.7.1)}$$

Ennos[7] suggests that it is possible to achieve an accuracy of at least 0.1μm using this method. For a camera aperture ratio of f/4 and image speckle size σ =3μm

then a film resolution of at least 300 lines per mm would be required.* Since, for a fringe pattern to be discernible amongst the speckle, as was indicated earlier, the fringe spacing must be approximately 5 times larger than the speckle size σ; then from the equation below we have, for a specimen of diameter 'l' which is displaced laterally by an amount d_l:

$$5\left(1.22\,\frac{\lambda M}{l}\right) = \frac{\lambda M}{d_l}$$

$$\text{or } 'l' = 6d_l \qquad \ldots\ldots\ldots\ldots (2.7.2)$$

Thus, for lateral displacement of an object (which is not also undergoing tilt, deformation or rotation) the maximum measurable displacement is theoretically one sixth of the lateral dimension 'l' and is not dependent on the magnification employed. However, lens aberrations will lead to a fall in contrast of the transform fringes corresponding to large lateral displacements and so this will limit the theoretical maximum value.

A double-exposure specklegram relating to surface tilt can be measured by illuminating it with a converging spherical wave formed by a lens (focal length 'f_s') which forms a speckle pattern on a screen located in the Fourier plane that is modulated by cosinusoidal fringes. The spacing 'x' of these fringes (shown in Figure 2.7.2 is found by:

$$x = \frac{\lambda f_s}{d_t} \qquad \ldots\ldots\ldots\ldots (2.7.3)$$

---

*Holographic films (35mm) with resolving powers of 5000 lines/mm are readily available.

Hence, the tilt 't' of the object (from Equation 2.6.1) is found from :

$$t = \frac{\lambda f_s}{f(1+\cos\theta)x} \qquad \ldots\ldots\ldots\ldots (2.7.4)$$

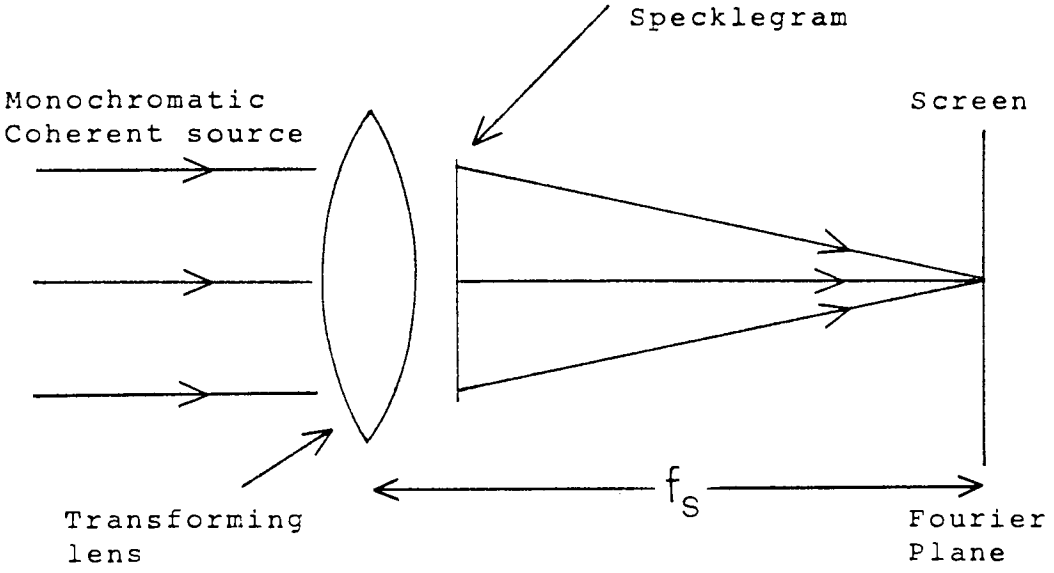

Fig.2.7.2. Specklegram interrogated with use of transforming lens.

Superimposed movements of an object surface, where one movement is a lateral displacement and the other is a tilt perpendicular to it, can be recorded in different planes so that the two can be easily separated for analysis. This is carried out by recording the lateral displacements in the image plane and the tilt in the Fourier transform plane. The two movements can then be separately measured using the techniques for in-plane

and tilt measurement previously described. In the investigations reported in the following chapters in-plane or lateral displacements alone were measured.

2.8. LIMITATIONS OF SPECKLE PHOTOGRAPHY

Since the detection of correlation between speckle patterns produced by the object surface at different times is the underlying requirement in speckle photography, it is important for the intensity distribution of the speckles to remain unchanged- unless it is affected by changes in those parameters which are being measured. This means that other factors that could alter the speckle correlation may impose limitations on the applications and conditions for which double exposure speckle photography may be employed. However, as Archbold et al.[52] have shown, effects such as those due to aberrations of the imaging lens can be minimised or their influence accounted for.

High speckle correlation is also required in order that good interference fringe contrast is obtained from the specklegram. Francon[54] has reported that a change in wavelength of the object illumination beam between exposures can produce a significant decorrelation of speckle patterns with consequent loss of fringe visibility.

The object surface should not change microscopically while it is being measured because a change will cause de-correlation of the speckle patterns. This means that mechanical wear, fracture, oxidation of the object surface

and similar effects occurring during recording will give rise to a reduction in fringe contrast. Furthermore, as Archbold and Ennos[37] have shown, the nature of the scattering surface itself can influence speckle correlation if the object is tilted. The reason for this is that substances such as paints and some organic materials do not scatter the illuminating beam two-dimensionally, as do surfaces such as abraded metal, but three-dimensionally (i.e. the light partially penitrates the surface and is scattered three dimensionally within the material). Thus, if the surface undergoes a small tilt the path changes which result from this will randomly vary from point to point. This means that the tolerance on the allowable degree of tilt is somewhat reduced.

For lateral displacement and tilt analysis, the lower limit is dictated by the size of individual speckles - which is related to the lens aperture, as was shown. The movement is required to be greater than the speckle size in the particular direction. However, Vikram and Vedham[55] have measured subspeckle-size lateral displacements using a modified form of single-beam speckle photography. Tiziani[17] reports that for high speckle correlation an accuracy of $\sigma/50$ can be achieved with a speckle size σ of only 1μm (in the appropriate plane).

Motion of the object surface towards or away from the camera has little effect in double exposure speckle photography if the axial movement is small. If it is not small, then, as a result of the change in image magnification produced by the motion, the recorded speckle

patterns will be displaced radially as found by Archbold and Ennos[37]. Large axial movements can also bring about a de-correlation of the speckle patterns (because the speckle goes out of focus as the axial displacement gets bigger). As the image becomes progessively de-focused the intensity distribution of the speckle can change. It will only remain approximately the same if the change in focus between the two exposures lies within the Rayleigh limit. For a change in focus Δ_f this means that

$$\Delta_f \leq \pm 2M^2F^2\lambda \qquad \ldots\ldots\ldots\ldots\ldots\ldots (2.8.1)$$

This limit on the change of focus thus imposes a limit in the line of sight movement (towards or away from the camera) which can be tolerated - particularly if a high aperture (small F value) is employed. Larger axial movements can be tolerated if demagnification of the object is employed. However, demagnification causes a reduction in sensitivity (because the speckle displacement in the image is similarly demagnified). As Ennos[16] has pointed out, for unit magnification the uncertainty of measuring the speckle displacement is approximately $\lambda/3$ and progressive demagnification produces a proportional reduction in sensitivity. When an object surface is tilted, a point is reached when the speckles have moved right across the imaging lens - resulting in decorrelation. The limitation on the amount of surface tilt which can be measured by speckle photography is also dependent on the recording camera aperture and degree of image

magnification (if large apertures and high magnifications are used the limit is raised). In practice the effect of lens aberrations would obviously further lower this limit.

There are other limitations concerning the application of double-exposure speckle photography which must be taken into account. A tilt introduced between exposures produces a shift in the speckle pattern in the entrance pupil of the image forming system. However, lateral object displacement produces a phase shift in the entrance pupil and a lateral shift of the speckle pattern in the image. In speckle photography only intensities are recorded and so tilts do not affect the sensitivity of in-plane object motion measurement. For small movements, in-plane displacements do not impair the accuracy of tilt measurements. Nevertheless, it is found that the contrast of the interference fringes is reduced because of some decorrelations which it causes in the speckle pattern.

2.9 SUMMARY

The theory and principles of laser speckle photography have been outlined and particular emphasis given to the double-exposure, single-beam illumination single aperture technique. In addition, the applications of the technique with particular regard to surface lateral displacement and tilt measurement, have been examined along with means of analysing the double exposed specklegrams. The latter was chiefly concerned with the means of obtaining good definition and contrast interference fringes

since the experimental investigations of this research project are directly related to the precise measurement of these fringes.

A number of limitations and potential problems associated with speckle photography and its uses have been analysed. Some limitations, such as the influence of laser spatial coherence on speckle brightness, are not particularly significant because of improvements in lasers and optical devices. Moreover, speckle photography has a number of advantages, in terms of range of measurement, degree of mechanical stability required and so on, compared to other speckle techniques. In addition, it must be noted that certain devices and methods such as strain gauges, dial gauges and similar devices give either overall information or information only on limited regions. They often do not enable small changes across a surface to be identified against an overall surface movement and those which do may be of limited sensitivity or range.* It is for situations where these various properties are required that speckle photography is particularly suited and also because expensive or complex equipment is not essential.

Various conclusions have been drawn regarding the

---

*These methods are ones which generally require contact with the specimen (and may not give permanent records of the movement).

possibilities and limitations of single-beam double exposure speckle photography. Certain of these were examined and explored in the preliminary investigations (see Chapter 3) as a background to the studies concerning the formulation of means by which the spatial frequency of the resulting interference fringes could be determined with good accuracy and reliability. These fringes are frequently of a rather indistinct nature and this has led to various restrictions or requirements with respect to the uses of speckle photography. It was therefore intended to attempt to devise means for determining the fringe spatial frequencies that would be both sensitive and versatile. In conjunction with the use of speckle photography,detailed investigations of certain applied metrology problems were subsequently carried out (in industrial and technical research settings). This meant that the applicability and adaptability of the spatial frequency analysis technique that was devised could then be assessed more fully.

CHAPTER 3.

PRELIMINARY INVESTIGATIONS

CHAPTER 3.

3.1. INTRODUCTION.

A number of preliminary experimental investigations of the single illumination beam technique of speckle photography were undertaken. After which various initial experiments concerning the measurement of the spatial frequency of the interference fringes produced by this technique were carried out. Briefly, these preliminary investigations were concerned with :

(a) Exploration of the various aspects of the technique and examination of the factors influencing the overall quality of the specklegrams(and resulting interference fringes).

(b) Investigation of measures to improve both the definition and contrast of the interference fringes produced from double exposure specklegrams.

(c) Initial studies and assessment of methods of measuring the spatial frequency of the interference fringes with good accuracy.

N.B. These preliminary investigations were quite broadly based because of the number of different factors involved. However, the findings and general experience of potential difficulties which these studies provided was such that it more than justified the experimental work involved. This also enabled high quality specklegrams to be

produced for examination in the three main studies of techniques for sensitive spatial frequency measurement and analysis of the interference fringes.

3.2. FACTORS INFLUENCING SPECKLEGRAM CONTRAST AND DEFINITION.

The various aspects of the single illumination beam and aperture, double-exposure method of speckle photography were investigated along with factors influencing the overall quality of specklegrams (including those factors indicated in the previous chapter which can affect the definition and contrast of the interference fringes produced by the specklegram). There was some overlap in the various experimental studies because account had to be taken of the interaction of the different variables involved. The main variables investigated were :

1. Object illumination (i.e. laser illumination).
2. Object surface finish and material.
3. Camera position, aperture ratio and focusing.
4. Film type (emulsion) and exposure.
5. Film processing and treatment.

These studies were carried out in the context of in-plane object displacements (see later details of methods) and the chief criteria used in assessing the influence of different factors was the contrast, definition and 'noise level' of the resulting interference fringes. Each of the above five variables was examined in turn with the

other variables fixed (at nominal values). To limit the extent of variation only two different power helium-neon lasers, two different 'quality' S.L.R. cameras and two different object materials (mild steel and aluminium) were employed. However, in every case, each of the two was sufficiently different from the other to give a reasonable variation. Two different devices for producing lateral displacements were also employed. One simply enabled object displacements in the general vertical plane to be provided (at various angles - see Figures 3.2.2 and 3.2.3). The other device was designed to enable small horizontal displacements to be made with high accuracy (the displacement was measured with a sensitive dial gauge, as shown in Figures 3.3.1 and 3.3.2.)

To minimize vibration the experiments were conducted on a special bench which consisted of a heavy concrete base with a 460mm thick layer of expanded polystyrene on top of this and a further 250mm thick concrete layer above. The bench had a heavy-gauge steel top and the displacement apparatus, camera and other equipment were rigidly held to this by large magnetic clamps. A heavy-duty optical bench was used to hold the laser and beam expansion components. The camera was operated by a remote cable-release fitted with a locking screw and the laser beam was cut-off between double exposures by a remote cable-operated shutter. Photographic recording was carried out in darkness and a hand-held safelight was used to enable fine adjustments to be made to the displacement apparatus between exposures.

Special facilities were provided to ensure that the experimental environment had low atmospheric dust levels.

1. Object (surface) illumination.

The same object surface 'S' (lightly abraded aluminium) was illuminated, as shown in Figure 3.2.1, by each laser in turn. One laser had an output power of 1mW and the other 8mW (checked by a laser power monitor). Both emitted linearly polarised light of wavelength 633nm. In each case the lasers were given 30 minutes 'warm-up' time before they were used. The stability of the laser output beams was monitored (every 2 minutes over a 30 minute period) by viewing the beam pattern after it passed through a Fabry-Perot etalon. It was found that both beams were satisfactorily stable during the periods of use.

For the experimental work each beam was carefully 'expanded' using a system consisting of three elements. These were, a negative lens'L' to cause weak divergence of the laser beam from a virtual source, a short focal length lens 'M' (microscope objective) to bring the beam to a real focus and a pinhole 'P' placed at the focal point of the microscope objective.* Alignment of the pinhole with the objective was undertaken using a device suggested by Rogers[56]. (Basically, the pinhole cuts off the transverse modes of the laser and passes only the axial mode. The intensity across the beam then corresponds quite

---

*Several objectives were tried (a X10 was found generally suitable).

closely to a Gaussian distribution).

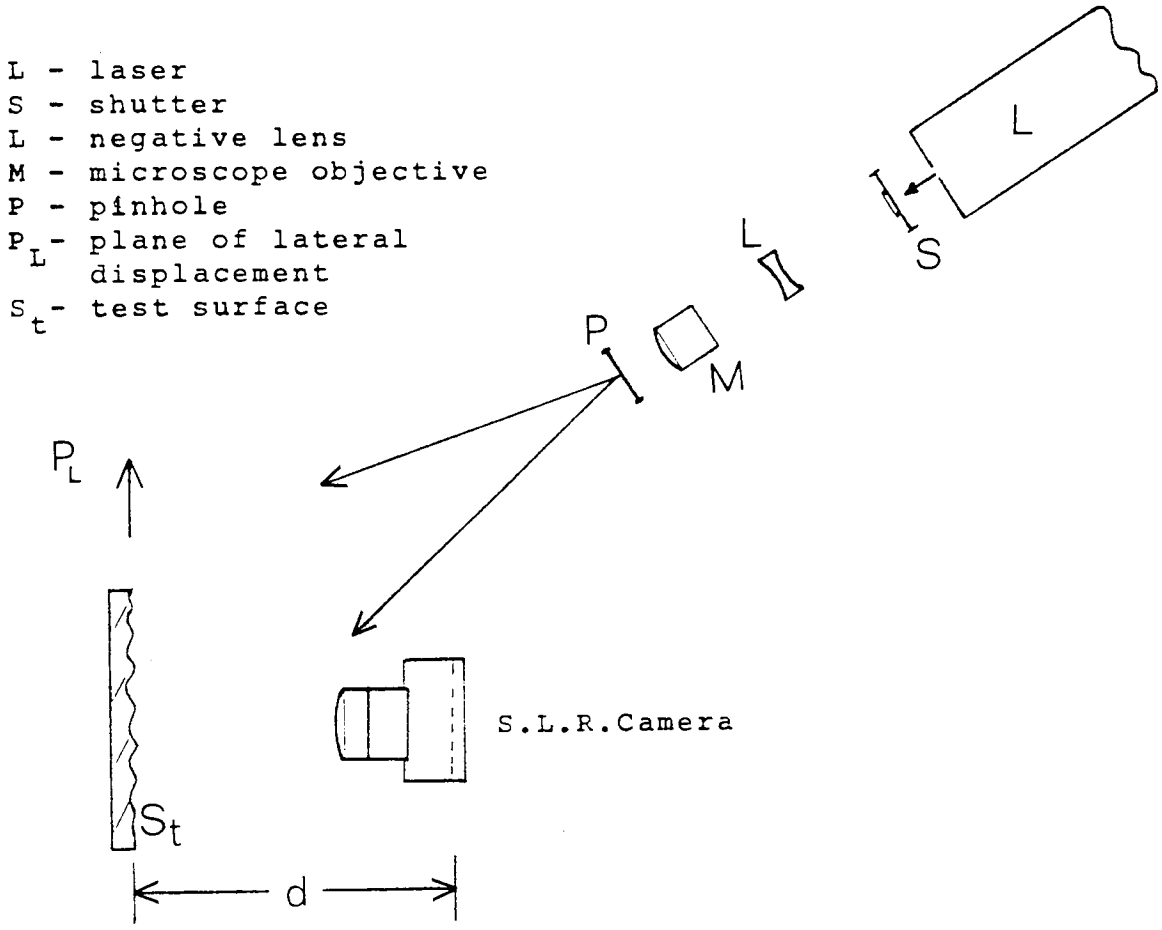

Fig.3.2.1. Basic System for Recording Specklegrams.

Initially, each laser beam was expanded and then after checking the uniformity (using a screen) the beam was projected onto the test surface. The latter was rigidly mounted in a double-plate hinge arrangement which was fitted with adjusting screws that had a fine thread. The arrangement, shown in Figure 3.2.2, was designed to enable the test surface to be given small displacements in the vertical plane in the range 0.05mm to 0.25mm.

(Chosen because this would allow the demagnification ratio M to be kept constant).

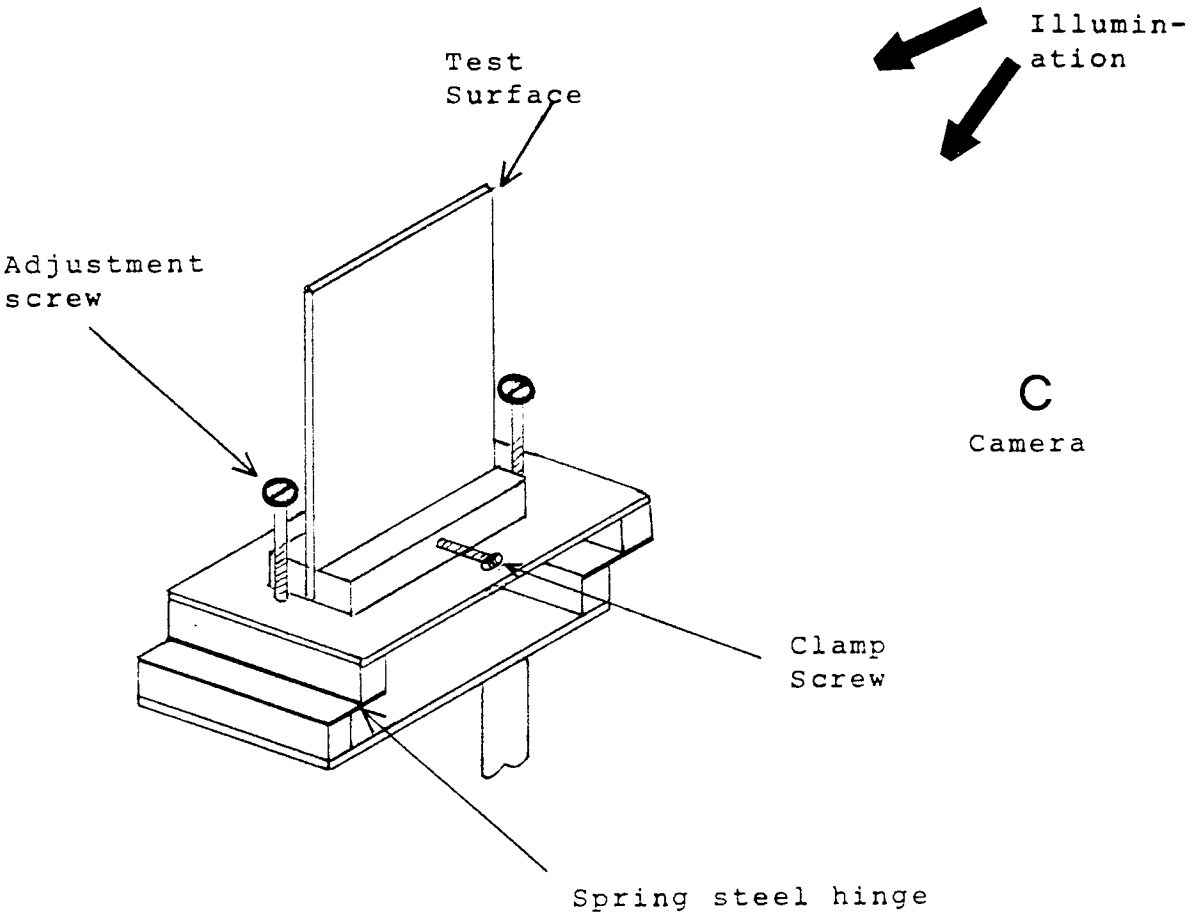

Fig.3.2.2. Part of Surface Displacement System

A series of double exposure specklegrams were recorded (as will later be described) for the surface displaced by different amounts and illuminated at different angles of normal incidence. The angles were increased from 15^{o} to 75^{o} with respect to the normal with the surface, in steps of 5^{o}. Care was taken to ensure that the surface was fully illuminated in each case. Specklegrams were obtained using each laser in turn. These were then examined

and the interference fringes produced from them were also studied (see details). For those angles which were found to yield the best results, in terms of interference fringe contrast and definition, a further series of experiments was undertaken in which the illumination distance (from pinhole to test surface) was varied in 50mm steps from 200mm to 1000mm. This was carried out to provide information concerning the effect of distance between the beam expansion system and the object surface, in terms of laser output power and illumination angle. Similarly, the effect of using a poorly expanded beam, which provided a non-uniform field of illumination, was investigated (and specklegrams recorded as before). This information was subsequently taken into account in the further investigations.

In these experiments and the surface finish studies, the same type of recording film (Agfa-Gevaert 10E75), camera aperture (f/4), object demagnification (x2), exposure (2 x 20 seconds) and film processing was employed. They were chosen as being fairly typical (as indicated in the literature outlined in the previous chapter) and because they would provide a good basis for comparison. In later investigations, the influence of these variables (with regard to the production of interference fringes from specklegrams) was examined.

The specklegrams obtained in these experiments were briefly examined with a densitometer so that the respective contrast levels could be assessed. Then representative

samples of the specklegrams were illuminated by an unexpanded laser beam and interference fringes subsequently obtained on a screen (as described in Section 2.7). Initially these fringes were examined visually to obtain an assessment of respective 'noise' levels and fringe clarity. Later the rear of the ground glass screen (onto which the fringes were imaged) was slowly scanned with a phototransistor (2N986)* which was mounted inside a short narrow tube (to reduce the detection of light randomly scattered from the screen). The output from the transistor was then displayed on an oscilloscope for analysis of relative intensity and 'noise' levels. Several areas of each specklegram were examined by illuminating them with the laser beam and obtaining interference fringes. All the variables involved were kept constant so that the respective results could be more reliably compared.

2. Object surface finish.

As indicated earlier, two widely used materials (aluminium and mild steel) were examined. For each of these, two common surface finishes were employed (lightly abraded and coarse ground) and, as a further study, rolled aluminium plate coated with matt white paint was used. In each experiment, the test surfaces (40mm x 50mm) were given the same lateral displacement of 0.15mm and all other variables were kept the same (using values identified in the previous studies as producing the most satisfactory results - in

---

*Preliminary investigations concerning this had previously been undertaken.

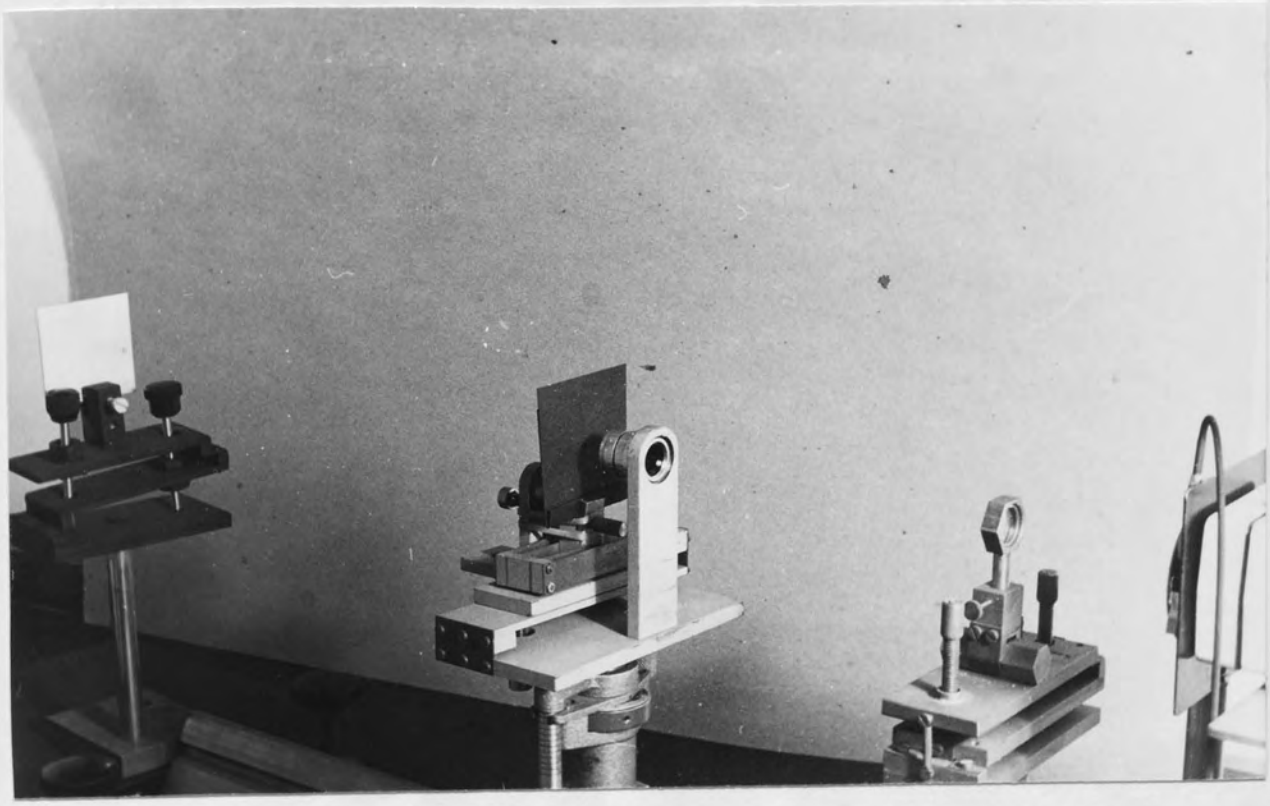

Fig.3.2.3. Experimental System used for initial surface displacement studies.

terms of interference fringe quality.) The only exceptions were that the surfaces were illuminated at what had been found from the previous investigation to be the most desirable angle of incidence and also the least desirable. Moreover, so that the effect of different illumination levels could be assessed, the experiments were carried out with a 1mW output power laser and later with an 8mW output power laser. Figure 3.2.3 shows a typical experiment (the white painted surface is the specimen being studied).

Quantitative information concerning the surface finish of the specimens was obtained by carrying out an analysis of each surface using a 'stylus' type profilometer. The following traces(Figures 3.2.4 and 3.2.5)show typical surface profiles for lightly abraded aluminium and coarse ground steel respectively. Table 1 gives the 'Ra' value(mean value of surface finish* in microns) for each of the samples employed. All values given were taken across the surface (in the same direction as the surfaces had been displaced between the double exposure photography) this was 'with the lay' (i.e. the direction of the predominant surface pattern).

The white matt paint employed was a cellulose type and two coats were applied (aerosol spray) after which the specimen was left for 48 hours to dry. In addition, a coarse finished (Ra=3.85) aluminium sample, which had large (random) surface profile variations, was briefly

*See Appendix 1 for details.

See Table 1

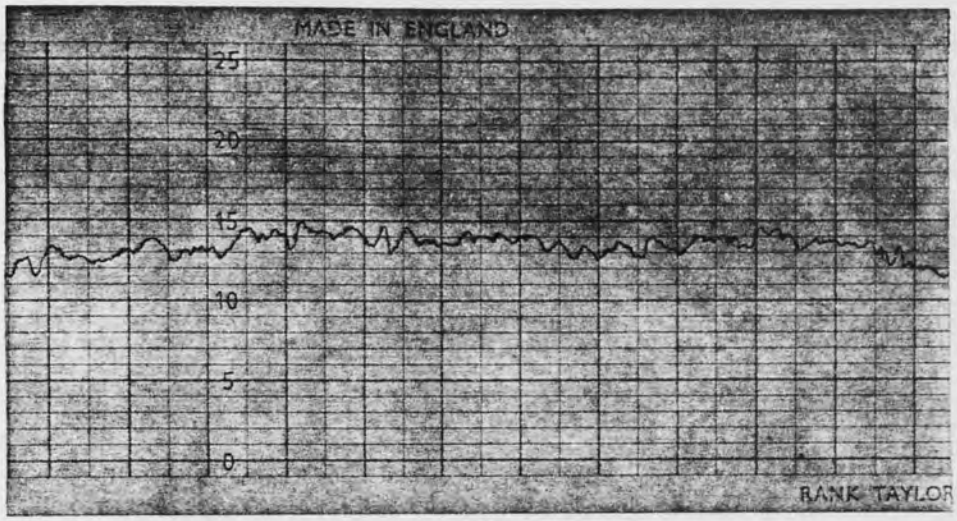

Fig.3.2.4. Surface profile trace: lightly abraded aluminium.

See Table 1

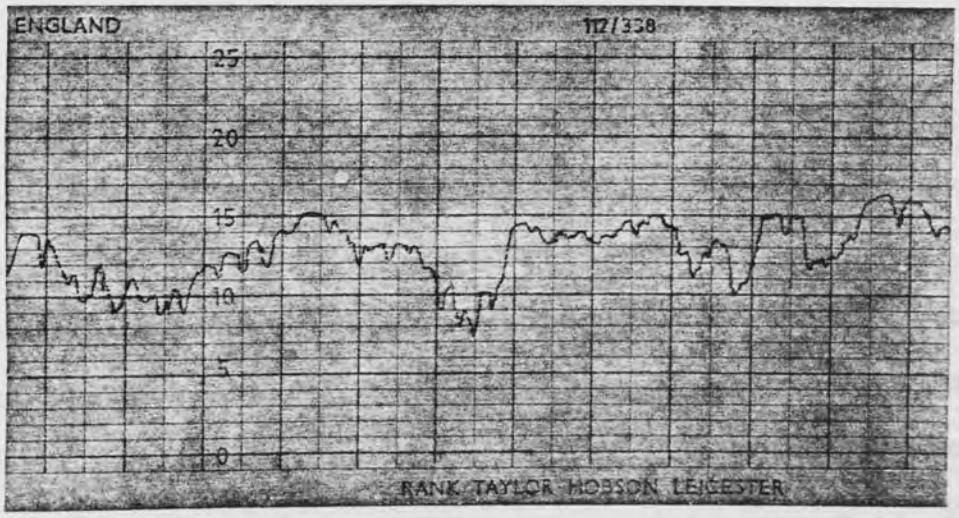

Fig.3.2.5. Surface profile trace: coarse ground steel.

studied to discover if such variations produced significant effects on the definition of interference fringes obtained from doubly-exposed specklegrams of such surfaces.

Surface Finish and Material	Ra value
Coarse ground steel	3.20
Coarse ground aluminium	3.60
Lightly abraded steel	0.60
Lightly abraded aluminium	0.70
White painted aluminium	1.40

TABLE 1. Surface Finish Values

3. Camera position, aperture ratio and focussing.

Each of the two cameras which were used in these investigations were 35mm S.L.R. cameras. One was fitted with a 58mm, 6 element, F2 lens and had a higher quality lens system. The other camera had a 55mm, 4 element, F2.2 lens system.

All the experimental studies were undertaken using the same extension tubes* fitted to the cameras. (The same photographic emulsion and processing was employed as had been used in the preceding investigations). The specimen surface employed was the lightly abraded aluminium surface (since this would enable a critical comparison to be made of the camera's imaging of the speckle

*The effect of these on the camera aperture was accounted for : See Appendix 2.

pattern). Studies were carried out using each of the lasers in turn and the surface was illuminated at the angle of incidence which had previously been found to be the most satisfactory. Only this angle was used because in this series of experiments one of the variables was the camera to object surface angle. Two illumination distances (pin-hole to surface) were used in these experiments. These were 250mm and 500mm respectively.

In an initial series of experiments, concerning the effect of camera to surface angle, a demagnification of x2 was used (as in the other studies). Starting with the lens of the camera parallel to the object surface, a range of angles (in 5° steps) with respect to the normal to the surface was used, up to a maximum of 15°. Double exposure specklegrams were recorded in each case, with the surface displaced laterally by the same amount (0.15mm) and the same procedure repeated with the illumination provided by the higher power laser. The entire experiment was then undertaken using the second S.L.R. camera. Finally, an examination of the specklegrams and the interference fringes obtained from them was made, as before.

A second series of experiments was carried out along the same lines as the initial studies, but this time a range of different object demagnification values was employed. These varied from x1 (in steps of x1) to a demagnification of x8 and in a further experiment using a separate lens system (200mm f/2.9 lens) a magnification

of x2 was used. The double exposure specklegrams were recorded using each laser in turn and each camera (parallel to the test surface).

Finally, with the other variables kept constant as before and with a demagnification of x2 a series of experiments using different camera aperture ratios (f/2 to f/16) was undertaken. As with other experiments in this section, results were obtained for each of the two cameras and lasers.

In addition, to explore the influence of the effect of focusing 'errors', a set of experiments was carried out with each camera set at f/4 and with a x2 demagnification factor (all other variables fixed at optimum values). Three sets of experiments were undertaken and only 'approximate' defocus amounts were used (these were 'well focused' 'slightly blurred' and 'quite blurred'). In the latter 2 cases, the camera was focused 15% and about 35% beyond the object surface focus, respectively.

4. Film type and exposure.

For the previous experiments the film used was Agfa-Gevaert 10E75, since this has been reported by some investgators[26,37] as having produced satisfactory specklegrams. To explore the possibility that other types of emulsion could help to produce interference fringes of higher contrast and definition three other types of emulsion were examined.

The 35mm films which were used in these investigations were :

1. Agfa-Gevaert : 10E75.
2. Agfa-Gevaert : 8E75.
3. Kodak: SO-253.
4. Ilford: Pan F.

Apart from the last type of emulsion all the others are holographic emulsions, with maximum sensitivity to illuminating wavelengths in the range of approximately 600-700nm (i.e. they are specially formulated emulsions for use with lasers such as helium-neon lasers). The Pan F film is a much faster film than the other three but is relatively coarse-grained and of a much lower resolving power than the others - as will be discussed in relation to the results obtained for the various emulsions.

A series of exposure trials was undertaken for each of the films to determine the optimum exposure time for a given object surface and camera aperture ratio. The surface roughness/exposure trials for each film were carried out using the surface finishes having Ra = 0.6 and Ra = 3.85 respectively. These represented the two extremes of surface finish studied. Aperture ratios used for each of these tests were f/2, f/4 and f/8; because f/4 had been found to be the aperture to yield the highest quality interference fringes in the previous series of experiments, it was thought useful to try a somewhat larger and a smaller aperture ratio for comparison. For Pan F an aperture ratio of f/16 was also employed. All other variables were fixed at values which had been identified as optimum

values in the previous studies. Exposure times employed (using the S.L.R. camera with the higher quality lens system) were: 1, 2,4, 8, 16, 32, 64 and finally 128 seconds. These values represent each exposure of the double exposure employed to record lateral displacement.

If the film stretched or expanded between exposures, this could cause spurious results (i.e. interference fringes produced from the double exposed specklegram would not be representative of the object surface movement alone). Care was thus taken to ensure that film tension was low in the cassette and that when the film was loaded into the camera it moved freely without pulling, when the film advance lever was operated. The film was stored in a refrigerator and was allowed to reach room temperature two hours before use. To test for possible stretching of the film a series of alternate single and double exposure photographs was taken of an object surface which had two reference lines on it. These lines were a known distance apart and their spacing was compared using a travelling microscope, on the single and double exposed photographs.

5. Film processing and treatment.

As reported in the previous chapter (Section 3.2) the processing of specklegrams can significantly influence the contrast and quality of interference fringes produced from them. Experimental investigations were undertaken using various photographic developers including Neofin 'Blue', Kodak D8 and Kodak D19 high contrast developer - which had

been employed in all the previous experimental studies (using optimum development times recommended by the manufacturers). All the films (Agfa-Gevaert 8E75, 10E75, Kodak SO-253 and Ilford Pan F) were developed immediately following exposure, with the developer made up to the appropriate strength at the specified temperature for processing. The double exposure specklegrams (recorded under the optimum conditions which had been discovered in the preceding experiments) were developed for times ranging from two minutes to ten minutes (in intervals of one minute) and, additionally, a development of fifteen minutes was employed for each batch. Continuous agitation was employed and processing was carried out in developing dishes (in total darkness) according to the processing scheme summarized in Appendix 3.

Having determined particular processing measures for each type of emulsion which produced specklegrams yielding interference fringes of the best definition and contrast, the effect of bleaching the specklegrams was investigated. This was carried out, after washing the negatives for forty five minutes in de-ionised water to prevent the formation of unwanted precipitate, using a mercury salt and washing with a dilute ammonia solution. A chromium salt could have been employed but it was noted that this would give lower contrast.

All three holographic films had residual sensitizing dye after processing. The Kodak SO-253 had a quite high level (this has a blue colour which could markedly absorb

the red laser light used to produce interference fringes from the specklegrams). This residual dye was largely removed by washing the specklegram in a methanol (methyl alcohol) solution[57].

NB. In subsequent investigations, in which Agfa-Gevaert 10E75 film was used, a safelight was employed in the dark-room. This was an Ilford 603 filter which, as reported by Rogers[58], does not produce fogging of this film. (A hand-held version was used in making adjustments during recording of specklegrams, as mentioned earlier).

3.3. DISPLACEMENT MEASUREMENT.

In order to assess quantitatively the sensitivity of double exposure speckle photography in relation to lateral displacement measurement, and exploit the information concerning the production of high quality specklegrams from the previously described studies, a special device to produce small lateral (horizontal) displacements was utilized. This was a form of parallel spring-plate arrangement as shown in Figure 3.3.1, fitted with a micrometer adjustment system. The test surface (seen on the left, in front of the micrometer adjustment) could be displaced by a known amount - which was measured by a sensitive dial gauge (this could be read to 0.005mm). Rather than working to the limits of the system, which could have introduced errors, actual object surface displacements were only taken to two decimal places (e.g. 0.15mm). Moreover, the range

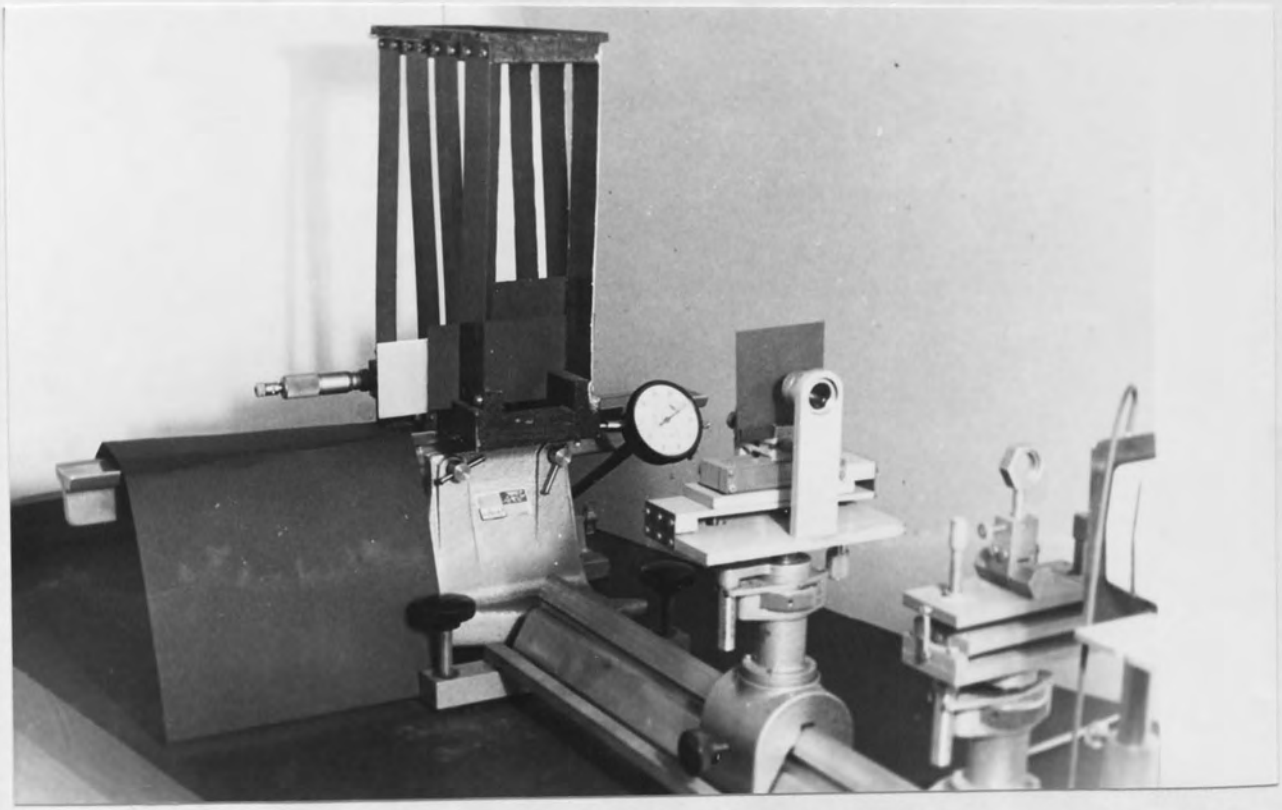

Fig.3.3.1. Horizontal displacement system.

of displacements that was employed was kept within the limits outlined in Section 2.7, so that the sensitivity was not reduced.

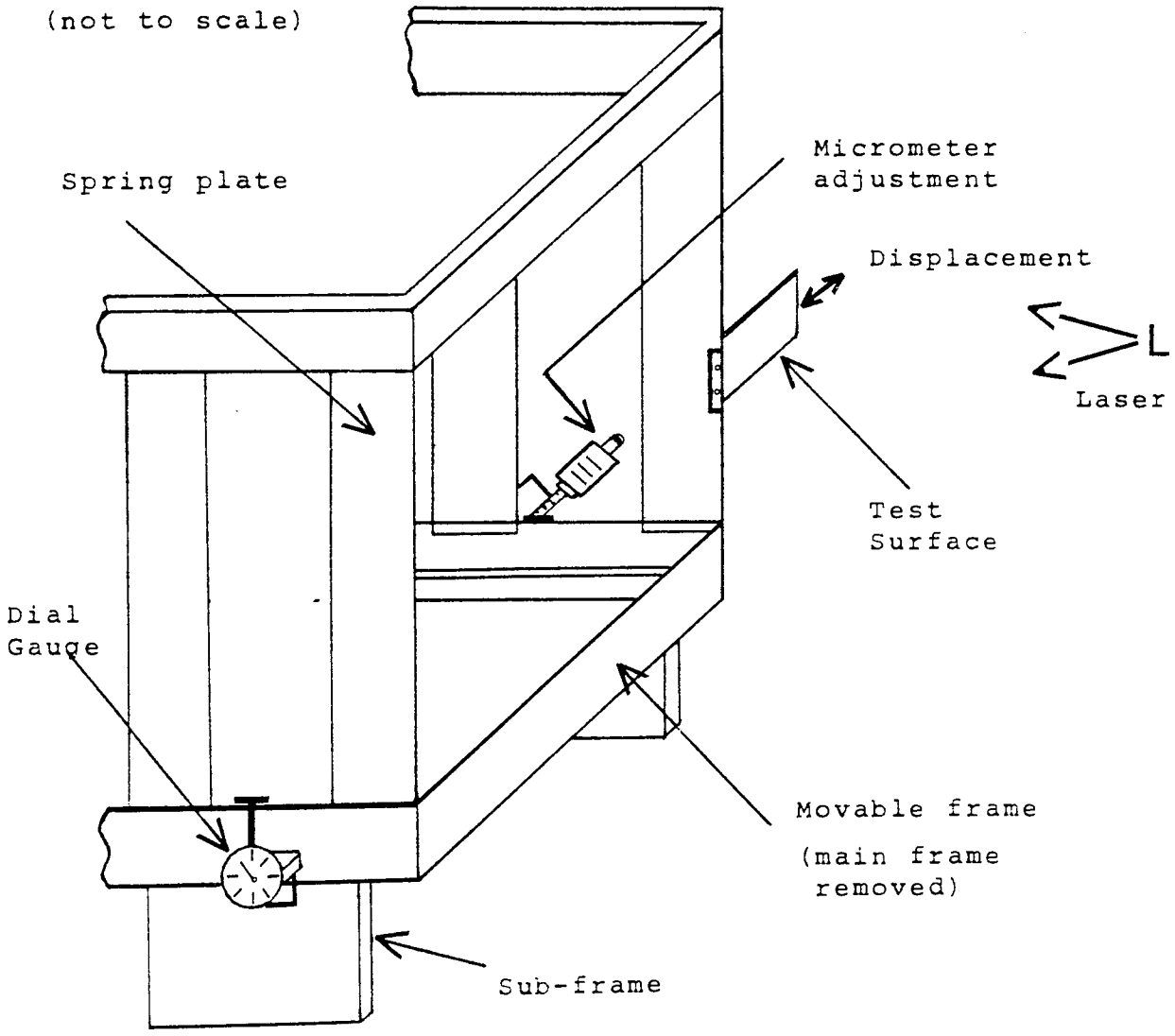

Fig.3.3.2. Simplified Diagram of Horizontal Displacement System.

The apparatus shown simplified in Figure 3.3.2 was rigidly clamped to a base unit which was, in turn, fixed to the steel topped, anti-vibration bench, by magnetic

clamps. This displacement system was designed to enable lateral displacements to be given to the test surface without any tilt or other movement of the surface.

As in previous experiments the photographic recording was carried out in total darkness (although the micrometer adjustment and dial gauge were briefly illuminated bya small hand-held safelight - between the double exposures). Lateral (horizontal) displacements, ranging between 0.05mm and 0.25mm were recorded using values, settings and so on that were discovered as being the most appropriate in the previous studies. The resulting double exposure specklegrams, corresponding to lateral surface displacements that had been recorded on the dial gauge, were carefully processed for use in the next stage of the preliminary investigations and in the main experimental studies.

3.4. INTERFERENCE FRINGE PRODUCTION AND MEASUREMENT.

The fundamental means of analysing double exposure specklegrams was described in Section 2.7 (See Figure 2.7.1) and this was used as a basis for the investigation of measures to improve the production and definition of the interference fringes from specklegrams. In the first series of experiments, the influence of the illumination area of the specklegram was explored using different diameter laser beams to interrogate the specklegram. Beam diameters of approximately 0.75mm, 1mm and 2mm were employed

(using a convex lens) and observations were carried out using an 8mW and a 1mW output power laser for comparison. A series of identical location points (based on a 5mm 'grid' type format) on each specklegram was interrogated in each case.

Following this investigation the effect of the throw 'D' of the projected fringes was examined using different distances (changed by 50mm each time) ranging from 100mm to 1000mm between specklegram and screen. Fringe definition and contrast was examined at each distance 'D' (which was measured to ±1mm) for double exposure specklegrams corresponding to the range of displacement values employed in the investigations detailed in Section 3.3. Various screens were also employed in an attempt to improve the overall contrast and definition of the fringes. Observation of the fringes from the rear of a semi-transparent (diffuse) screen was found to be convenient for fringe analysis and measurement. A variety of materials, including ground glass, white tracing paper (70 gramme),'fogged' Kodak 'Kodalith' film, and acetate diffusing sheet was employed. These were mounted in a rigid holder fitted onto an optical bench and aligned parallel to the specklegram. A 'stop' was used to remove the central undiffracted beam.

Several techniques for measuring the spatial frequency of the interference fringes were explored. The first method involved counting groups of 'bright' fringes

(e.g. 10 fringes) using a cursor and then measuring the group width using vernier callipers. In the previous work the spacing had been measured by holding a fine steel rule along a reference line and reading off the spacing but this required rather more skill and proved to be somewhat inaccurate. (When a check was undertaken using a grid of known spacing). Secondly, a fairly low magnification travelling microscope was used. This was aligned with the edge of a bright fringe and the scale read before traversing 10 fringes, when the scale was again read. Finally, measurements were made using 'grids' of known spatial frequency and adjusting the 'throw' of the projected fringes to match the grid. Several grids and masks were made and tried for this purpose (including a 'fan' type grid which did not require the throw to be changed - since it could be moved to match the fringes). Measurements were made away from the edges of the fringe pattern (where the contrast and definition of the fringes was lowest.)

3.5. PHOTOGRAPHY OF FRINGES.

A number of attempts was made to photograph the interference fringes produced by double exposure speckle-grams* and measure the fringe spacing from the photographs. The camera used was a 35mm S.L.R. type (fitted with a 58mm focal length lens and extension tubes) and it was mounted

---

*This was also undertaken to obtain information concerning the photography of these interference fringes. (There is little literature in this sphere.)

on a stand fitted onto the optical bench behind the screen on which the fringes were imaged. Photographs were taken using apertures ranging from f/2 to f/4 and exposures from 1/125 of a second to 1/30 of a second. Films used for the recording were Ilford HP5, Kodak 2485 (high speed recording film) and Ilford Pan F. Processing trials, using Ilford ID-11 and Phenisol, were carried out as was an investigation of enlarging and printing the photographs (using various grades of bromide paper). Different types of photographic developer were also tested in these trials (including Kodak PQ Universal and Phenisol).

A reference bar, drawn on the screen, was photographed below the fringes so that the magnification could later be determined. Fringe spacing measurements were taken from the photographs using a graduated perspex scale, which was placed over the fringes.

Photography of the fringe patterns produced by different specklegrams was also carried out using the 'reflected' rather than 'transmitted' pattern. This was achieved by using an opaque white screen (painted with retroreflective paint) and mounting the camera on the same side of the screen as the laser.

In addition, the effect of non-coherently blurring the image obtained from the photographic negative of the fringes was examined as a means of reducing the effects of noise

(on the final printed phtographs of the fringe patterns). The technique which was employed for this purpose involved the use of a convex cylindrical lens (2 and 3 dioptre lenses were tried) placed close to the 150mm lens of a photographic enlarger which was projecting the fringes from the negatives onto photographic paper. (See typical photograph of the effect of this - Figure 3.10.1).

3.6. USE OF LENSES TO IMPROVE FRINGE DEFINITION.

In this series of experiments lenses were used in an attempt to improve the definition and contrast of the interference fringes produced from double exposure speckle-grams. The lenses were :

(i) Acrylic Fresnel screens (two back to back).

(ii) Glass cylindrical lens (convex).

(iii) Liquid (paraffin) cylindrical lens (convex).

The Fresnel screens were used in place of the normal screen and the fringes were imaged directly upon these so that they improved the relative contrast.

Cylindrical lenses have the property of integrating light in a particular plane (rather than in two planes- as does a convex lens). This property was employed in imaging the fringes* onto the screen, as shown in Figure 3.6.1. The interference fringes were recorded photograph-ically in each case using the camera aperture, film type,

*The effect of the lens on the 'throw' was taken into account.

exposure, processing (including print making) which had been found, in the preceding experiments, to produce the most satisfactory results.

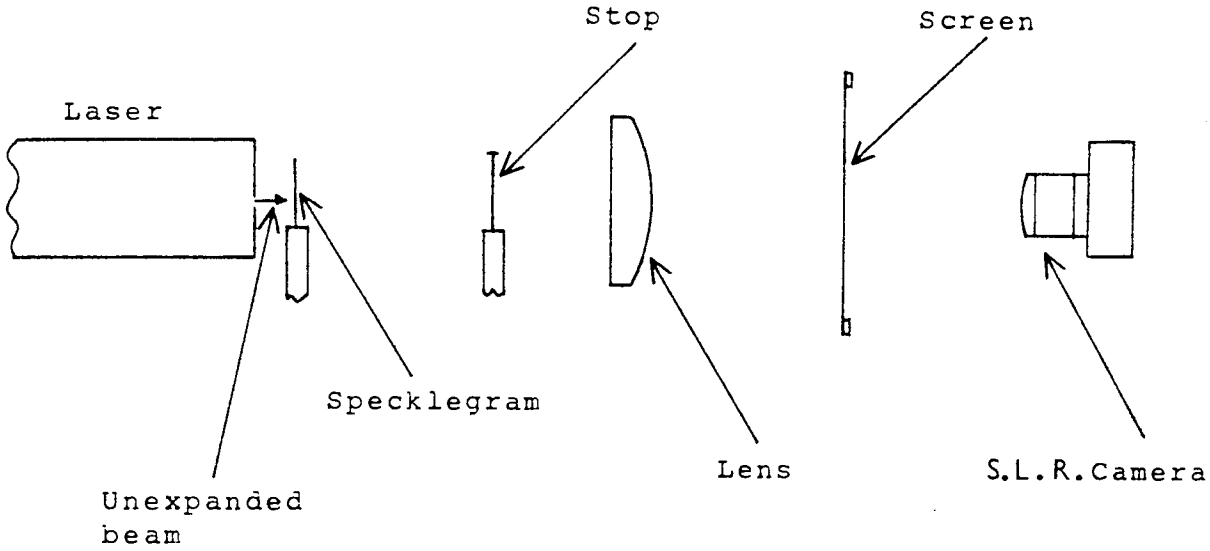

Fig.3.6.1. Lens system used for improving fringe definition.

3.7. SPECKLEGRAM VIBRATION (DISPLACEMENT).

To reduce the effects of extraneous speckles on the definition and general clarity of the interference fringes the specklegrams were displaced vertically in front of an unexpanded laser beam. As shown in Figure 3.7.1 this was achieved by fitting the specklegrams into a rigid frame* which was mounted on a heavy-duty electromagnetic

*Fitted with side supports to prevent torsional oscillations (which had been observed when conducting initial trials).

vibrator that provided vertical displacement. A signal generator was used to drive the vibrator at the different frequencies which were employed in these experiments (ranging from 20Hz to 1kHz). In order to more fully assess the integrating effect of displacing the speckle-gram, a series of different displacement amplitudes was also employed at each frequency. The amplitudes employed were 1mm to 5mm (in 1mm increments) about the mean position — measured by a dial gauge.

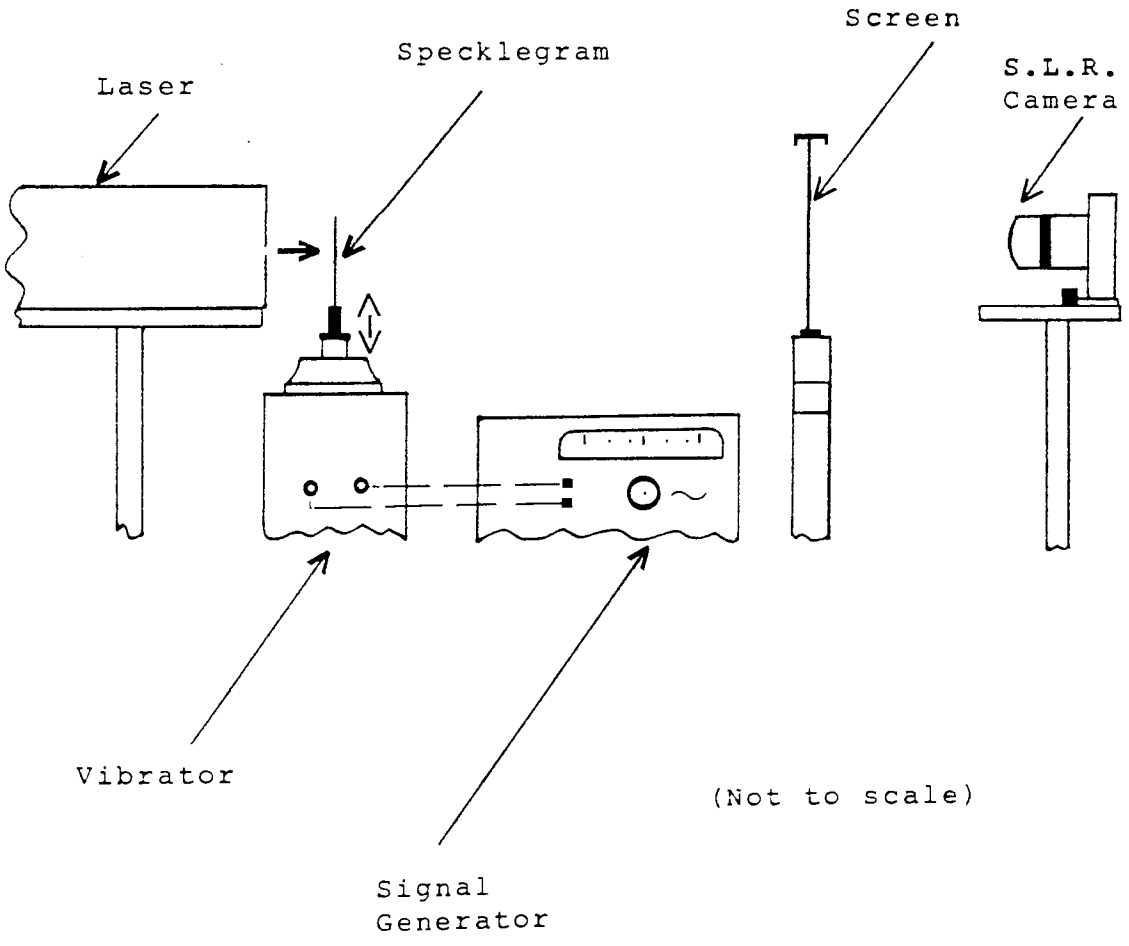

Fig.3.7.1. System for Vibrating Specklegrams and Recording Fringes.

Constancy of displacement frequency was checked using a calibrated stroboscope and found to be ±5Hz, overall. The interference fringes produced on the semi-transparent screen were photographed and various trials with different films, camera apertures, exposures and developments, were undertaken (see typical results - Figures 3.10.5 and 3.10.6.) Further investigations were carried out with the specklegram displaced, as previously, but illuminated by an expanded laser beam and imaged, via a diffractometer system, onto the recording film in the camera. In a final series of experiments, the camera lens system was removed from the camera body and displaced (parallel to the film plane) at low frequencies (between 10 and 25Hz) which were different to the frequencies at which the specklegram was being displaced. Again the fringe patterns obtained from double-exposure specklegrams, corresponding to different object surface displacements,were photographed and prints made - from which measurements of spatial frequency were taken.

3.8. RESULTS CONCERNING THE RECORDING AND TREATMENT OF DOUBLY-EXPOSED SPECKLEGRAMS.

As indicated earlier, a large number of experiments and trials were undertaken in these preliminary studies. Consequently, only the main findings and significant results or observations will be presented.

1. Object (surface) illumination.

It was generally found that the 8mW output power laser allowed greater freedom of choice of angles of incidence and laser to surface distances than the 1mW laser. Nevetheless, for both lasers, relatively small angles of incidence, with respect to the object surface, were found to produce specklegrams (for a given film, camera aperture and so on) that yielded interference fringes of higher contrast than corresponding speckle - grams for larger angles of incidence (>60^{o} in particular).

Similarly, relatively small laser beam expansion to object surface distances were found to be preferable, in terms of producing specklegrams that, in turn, produced higher contrast and more distinct interference fringes than those obtained for larger illumination distances (especially in the case of the lower power laser). It was noted that the uniformity of the beam expansion and the required area of illumination* must be taken into account in relation to determining optimum illumination distances.(A distance of 250mm from the pinhole to the object surface was found to be particularly satisfactory for the test surfaces used but in later work 500mm had to be employed to illuminate the larger surfaces examined.) In addition, the proximity of the recording camera may

*It must not be overlooked that intensity across the beam varies approximately as a Gaussian distribution.

impose restrictions on the closeness and position of the laser beam expansion apparatus to the object surface.

The uniformity of the beam expansion was found to influence significantly the uniformity and overall contrast of the doubly exposed specklegrams. This was especially noticable for the 1mW output power laser - when a poorly expanded beam was employed. However, some improvement was found possible by adjusting the exposure and processing times to compensate for areas of low contrast (but this meant that other areas were somewhat over-exposed).

2. Object surface finish.

The relative influence of the five basic surface finishes that were studied was assessed in terms of both the measured specklegram contrast and the contrast of the interference fringes produced from the specklegram. Table 2 lists the surface finishes in terms of the best overall respective contrast and fringe contrast results. Account was also taken of the overall fringe definition and this was included in determining the position, on a scale of 1 to 5, of each surface.(The lower number is the best and the higher worst).

The significance of the results summarised in Table 2 will be discussed in Section 3.11. However, it should be pointed out that when the surfaces were illuminated by a 1mW laser the resulting specklegram contrast for the lightly abraded steel and aluminium surfaces was markedly

Surface finish (See also Table 1)	Overall contrast/ fringe definition
Coarse ground steel	2
Coarse ground aluminium	1
Lightly abraded steel	5
Lightly abraded aluminium	4
Matt white painted	3

TABLE 2. Fringe Contrast/definition for different surface finishes.

poorer than when an 8mW laser was employed. As will also be discussed, it was found that the contrast was influenced by the angle of the incident illumination on the surfaces. Moreover, the results obtained for the special surface, which had large non-uniform variations in surface roughness, indicate that this not only causes significant differences in contrast over the specklegram but also relatively high noise levels for the interference fringes obtained from the specklegram.

3. Camera position, aperture ratio and focusing.

A small angle of the camera lens θ, with respect to the normal with the object surface, did not produce a significant effect on specklegram contrast (or on the contrast of the interference fringes obtained from the doubly-exposed specklegrams). However, at values of θ

equal to 10^{o} and more, variations in contrast across specklegrams were noticable. The other effect which was observed was that since the camera lens was not parallel with the object surface, the distance d_1, was not equal to d_2 (See Figure 3.8.1). This not only influenced the uniformity of focusing but meant that the image demagnification varied across the surface.

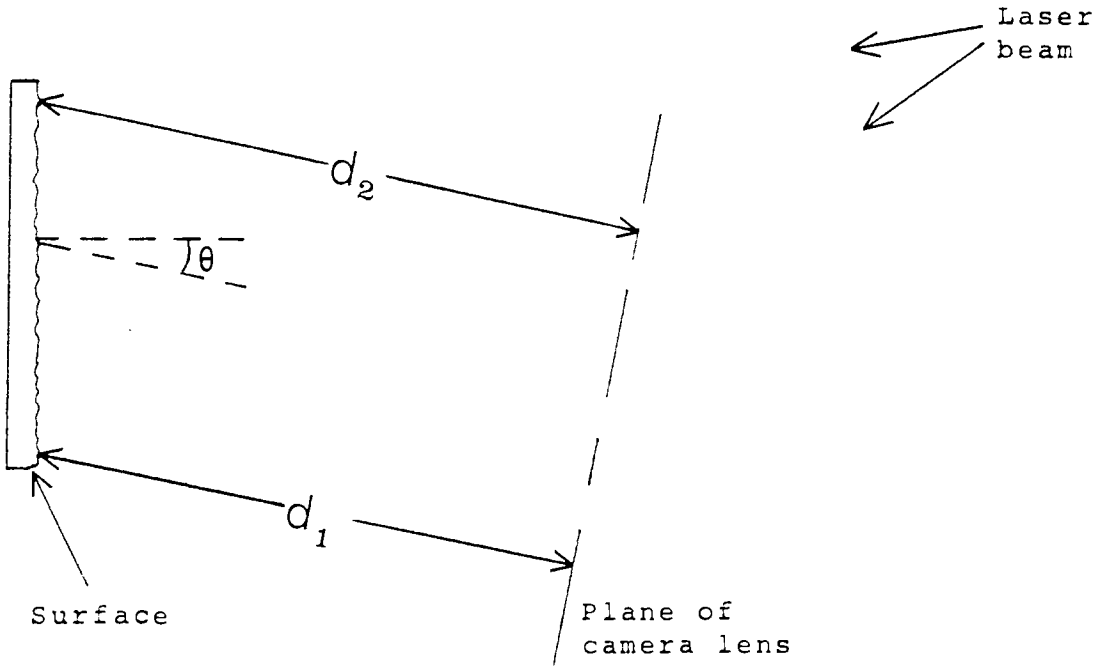

Fig. 3.8.1. Relation between camera angle and distance to surface.

It was found that variations in camera to object surface distance (to produce different image demagnifications) influenced the contrast and definition of the interference fringes produced from doubly-exposed specklegrams (for a given surface displacement). An optimization was identified in terms of the decrease in the signal to noise ratio (which can be thought of as the

ratio of fringe spacing to speckle size[9]) which accompanied an increase in demagnification (and the loss of sensitivity). A compromise was found (for the particular surface, film and so on employed in this study) to be gained by using demagnification values of x2 or x3. Nevertheless, as will be later discussed, account must also be taken of the fact that higher demagnification ratios enable object displacements of greater magnitude to be measured.

The results obtained for the experiments concerning the effect of the camera aperture ratio were such that an aperture ratio of f/4 was found to be a convenient overall compromise in accounting for :

i) depth of focus

ii) size of speckle

iii) image demagnification

iv) surface displacement magnitude

These experiments were undertaken with Agfa-Gevaert 10E75 film but other types of emulsion were examined in later experiments, as will shortly be outlined. However, the same trend was found, in terms of the limiting factors of the depth of focus and surface displacement along with speckle size (which is larger for smaller apertures) and demagnification (which decreases the speckle displacement in the image). The aperture also governs the exposure time and the effect of this was explored in a further series of experiments that is summarised later. Nevertheless, it should be noted that it was found to be

advantageous to use a fairly large aperture so that the exposure time of the relatively 'slow' 10E75 emulsion could be reduced. Accounting for this further reinforces the conclusion regarding the use of an aperture ratio of f/4. However, an aperture ratio of f/16 (which increases the resolution of the speckles), could be more suitable, as will be described, for faster and lower resolution emulsions.

The effect of a 'moderate' degree of defocus (i.e. <15% out of focus) of the recording camera was not found to be significant either in terms of the contrast or the definition of the interference fringes subsequently generated from the doubly-exposed specklegrams. Some loss of definition and contrast was observed in the case of the somewhat larger degree of defocus ($\triangleq$35%) which was also studied. Little difference in the specklegrams or resulting interference fringes was identified for corresponding object surface displacements recorded by the two S.L.R. cameras. It was noted that fringe contrast and definition reduced slightly more rapidly (when these were produced by interrogating the edges of specklegrams) recorded by the 4 element F2.2 camera lens compared to those recorded by the 6 element F2 camera lens. (This loss of contrast and definition is considered to be attributable to lens aberration effects and is in keeping with the findings of Stetson[45] and Roblin et al.[59]).

4. Film type and exposure.

The photographic emulsion that was found to provide specklegrams from which interference fringes could be generated that were of the highest overall definition (and had the best relative contrast) was Agfa-Gevaert 10E 75. This emulsion was found to be the most 'adaptable' (in terms of treatment, tolerance and general use) of all the emulsions that were employed in these studies. Although this emulsion has a rather higher sensitivity than Agfa-Gevaert 8E 75 emulsion, the latter has a higher resolving power (5000 lines/mm compared to approximately 3000 lines/mm - according to the manufacturers). Of the three 'holographic' emulsions which were examined, the 'fastest' (i.e. most sensitive) was Kodak SO-253. However, this emulsion displayed the most marked reciprocity and, for a given surface illumination, gave the lowest contrast specklegrams of the three. (Some improvement in contrast was brought about by special measures that are described in the following section)

Specklegrams recorded on Ilford Pan F emulsion yielded interference fringes which had lower contrast than corresponding ones obtained from the other emulsions. Moreover, it was noted that this was effectively made even lower because of quite high 'noise' levels.(See Section 3.11.) An aperture ratio of f/16 employed with this quite fast but low resolution emulsion produced the best specklegrams (in terms of generating interference

fringes that were the most distinct). Nevertheless, these specklegrams were generally inferior compared to those produced from the other emulsions using the same exposure.

In the case of the holographic emulsions, an aperture ratio of f/4 was identified as being the most suitable. Using this aperture ratio, it was found that for the Agfa-Gevaert 10E 75 emulsion exposures of about 16 seconds (x2: because double-exposure) produced distinct fringes for both the lightly abraded and the coarse finished surfaces. The Kodak SO-253 emulsion and Agfa-Gevaert 8 E 75 were found to require slightly shorter and slightly longer exposures respectively, in order to provide well-defined fringes under the same conditions. For all of the emulsions it was observed that when the two exposure times (of the double exposure) were equal the contrast of the interference fringes generated from the specklegrams was greatest.

Regarding the possible stretching of the films, during the double exposure interval, no evidence of any significant stretching was discovered for any of the films. This is attributed, in part at least, to the precautions taken in order to minimise this possibility.

5. Film Processing and treatment.

It was discovered that processing the doubly-exposed

films with 'Kodak D19' developer produced higher contrast (and definition) specklegrams than the other developers which were employed in this investigation. It provided more latitude for processing than Kodak D.8 and processing times using this developer proved to be controllable yet fairly flexible (although a much longer processing time was required compared to that for Neofin Blue). A development time of 4 - 5 minutes proved to be suitable for all the emulsions that were examined but the Kodak SO - 253 could be developed for up to 8 minutes (to enhance the contrast) without too much increase in the 'noise' level.

The contrast of the latter film was further improved (which meant that the interference fringes generated from the double-exposure specklegram were also of increased contrast) by removing the residual sensitizing dye. This was achieved by putting the developed film into a bath containing a 75% methanol solution for about 3 minutes.

Although bleaching of the processed, doubly-exposed film (specklegrams) produced an improvement in the intensity of the interference fringes generated from them it was generally found to be a fairly small improvement. This only proved to be worthwhile when the specklegrams were over-exposed or had been processed for too long - so that they had a very high photographic density. More will be said concerning bleaching in Section 3.11.

3.9. RESULTS OF DISPLACEMENT MEASUREMENTS.

Horizontal displacement measurements were calculated from the result of the interference fringe spacing values (obtained from specklegrams as described in Section 3.3.) The horizontal in-plane displacement 'd_1' was calculated in each case (using a form of Equation 2.7.1*) and compared with the recorded displacement of the object surface- which was read on the sensitive dial gauge. Initially, the spacing of the interference fringes was determined by direct measurement of groups of 10 bright fringes using special vernier callipers, as outlined in Section 3.4.

Typical results obtained were :

fringe spacing $x = 0.0055m$
film-screen distance $D = 0.50m$
M(image demagnification) $= 2.6$
illuminating wavelength $\lambda = 0.633 \times 10^{-6}m$.

$$\therefore d_1 = \frac{0.633 \times 10^{-6} \times 0.5 \times 2.6}{0.0055}$$

Thus surface displacement = $149.62 \times 10^{-6}m \pm E$

or $0.1496mm \pm E$

(This was for a displacement set on the dial gauge, using the micrometer adjustment, of 0.15mm)

The expected error E was calculated using the quadratic relation : $E^2 = 2a^2 + b^2 + 2c^2 d^2$. Contd.

*In these experiments the image was demagnified not magnified.

(where a, b, c and d correspond to the maximum errors in the four variables.) For the typical results overleaf E is equal to±4.8% and this is, of course, a maximum expected error.

3.10. SUMMARY OF FINDINGS CONCERNING THE GENERATION AND MEASUREMENT OF THE INTERFERENCE FRINGES.

The interference fringes produced by interrogating a doubly-exposed specklegram with an 8mW output power laser were of higher contrast than those produced with a 1mW output laser. (Contrast also depends upon the particular specklegram.) An interrogating beam diameter of 1mm proved to be suitable for most specklegrams (in terms of generating interference fringes of highest contrast and clarity) and this was found to apply to both lasers. In addition, it was observed that interrogating the specklegrams with a beam diameter of <0.75mm generally resulted in higher relative 'noise' levels for the interference fringes. This is also in keeping with the observations of Adams and Griffiths[44] that for beams of diameter rather less than 1mm edge diffraction becomes a problem.

Acetate diffusing sheet was found to be the screen material that yielded fringes (on transmission) of superior clarity and contrast. However, this was only marginally better than any of the other materials which, apart from the ground glass plate, were of roughly the

same thickness. (The latter had the advantage of being rigid.)

The projection distances between specklegram and screen were relatively large (e.g. 250mm) and it was possible to measure these, on the optical bench, to ±1mm overall. This means that, except in the case of projection distances of small magnitude, errors in this context are negligible.

It was not found to be satisfactory to use a low-magnification travelling microscope to measure the interference fringe spacing. This was mainly because the 'edges' of fringes were difficult to discern, when viewed through the microscope, owing to the magnification of speckle 'noise' and the limited field of view. The employment of 'grids' of known spatial frequency to enable the fringe spacing to be determined by 'matching' was simple in practice but also lacked sensitivity because of the problem of discerning the edges of the fringes. Nevertheless, it was more sensitive than the simple direct measurement technique using vernier callipers. Preliminary findings regarding the use of a photo-transistor to scan and measure the fringes indicated that further exploration in this context should be carried out (See Chapter 4).

The photographing of the interference fringes provided a small improvement in the definition and contrast of the fringes. Moreover, by blurring the

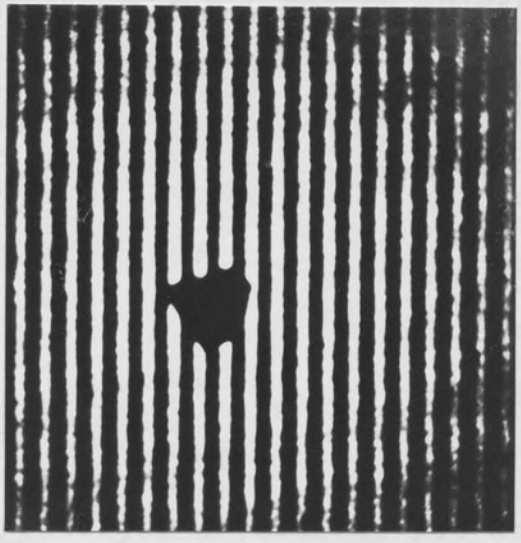

Fig.3.10.1. Fringe photograph after non-coherent blurring

photographic image non-coherently, prior to printing on bromide paper, the effect of speckle 'noise' was further reduced slightly (See Figure 3.10.1) and so fringe clarity was enhanced.

As mentioned earlier, little information is available concerning the photography of interference fringes in this context. However, it was found that relatively fast emulsions (such as Ilford HP5) used at a camera aperture ratio of f/4 (or f/5.6) and exposed (typically) for 1/60th of a second were generally convenient and provided superior photographs. Developing with Phenisol (1:4 dilution at 21°C) printing on No.3 bromide paper, using a 150mm enlarger objective, set at f/5.6, proved to be particularly suitable in most cases.

Minor additional improvements in the contrast and clarity of the interference fringes were obtained by replacing the simple screen with Fresnel screens (lenses). However, the use of a cylindrical lens, in conjunction with the simple screen (shown earlier in Figure 3.7.1), provided a more significant improvement in fringe contrast and definition. Figure 3.10.2 shows the effect of employing a glass cylindrical lens and Figure 3.10.3 indicates the added improvement on fringe visibility obtained by using a liquid cylindrical lens. In each case, the fringe spacing was measured directly from the photographs, as explained, but care was taken to avoid making measurements at the extreme ends where the

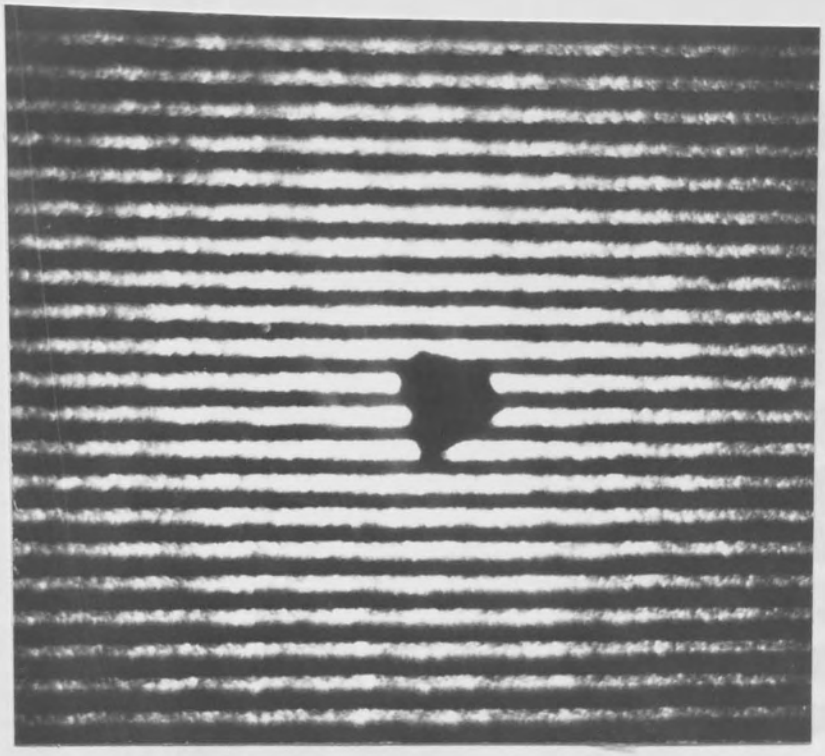

Fig.3.10.2. Fringe photograph using glass cylindrical lens

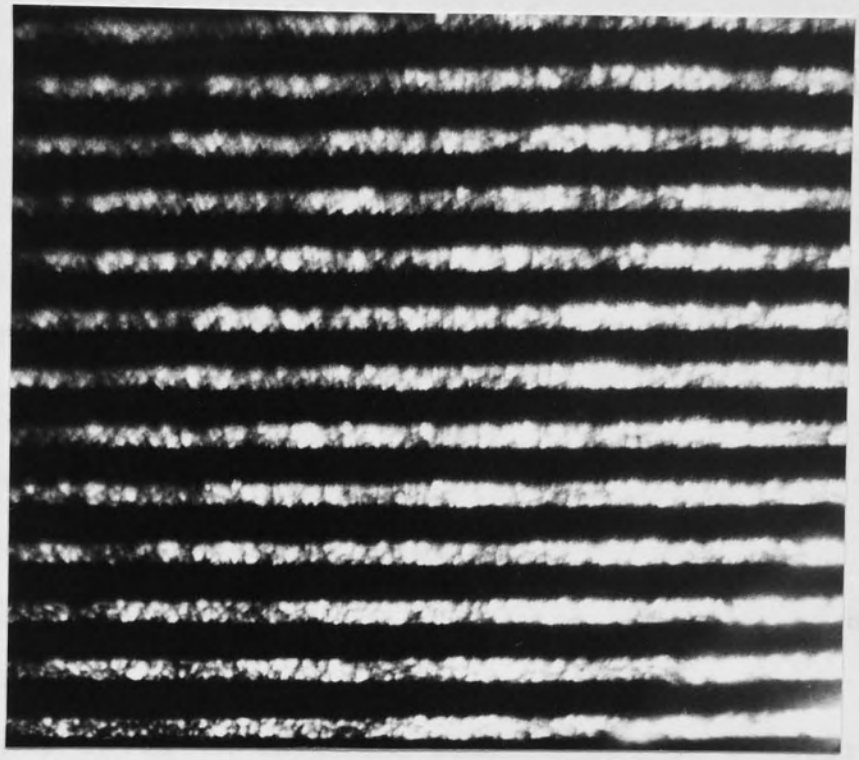

Fig.3.10.3. Fringe photograph after using liquid (paraffin) cylindrical lens

fringes could be slightly distorted by the lens.

The vibration (displacement) of specklegrams, which was described in Section 3.7, was found to be marginally superior to the use of cylindrical lenses with regard to reducing the effects of speckle 'noise' on fringe definition. A displacement frequency of 100 Hz (with an amplitude of 2mm) was identified as being particularly effective for doubly-exposed specklegrams recorded at an aperture ratio of f/4 (using Agfa-Gevaert 10E75 film) corresponding to object lateral displacements between 0.05 and 0.25mm (at a demagnification of x2 or x3). Generating the interference fringes from these specklegrams using an expanded laser beam, in a diffractometer system, and then photographing the projected fringe patterns produced the best overall improvement in the fringe definition. The actual final results obtained were also influenced by the photography of the fringes (See Figures 3.10.4 and 3.10.5)

Typical results obtained using Ilford HP5 film, exposed for 1/30 second at f/4 and developed in Phenisol (1:4 dilution) for 5 minutes at 21^{o}C, are shown in Figure 3.10.4. As can be seen in Figure 3.10.5, it is possible to obtain photographs which provide clearer fringes if a slower film (Ilford Pan F) is employed. Exposures of 2 (or 3) seconds with a camera aperture of f4 and processing this film with ID11 developer (full strength) for 7 minutes at 21^{o}C were found to be generally

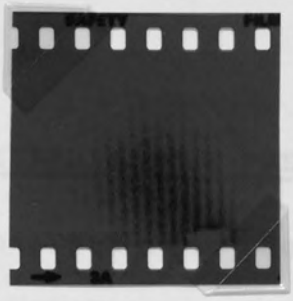

Fig.3.10.4. Fringes obtained from displacement of specklegram (recorded on HP5 film)

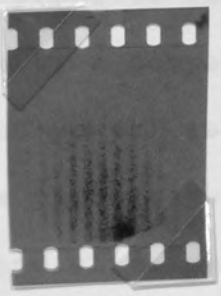

Fig.3.10.5. Fringes obtained from displacement of specklegram (recorded on Pan F film)

most suitable. Further comments on these and the results of other experiments will be presented in the following section.

3.11. CONCLUSIONS REGARDING THE PRELIMINARY STUDIES.

The evidence obtained from the experiments concerning single beam illumination speckle photography suggests that low angles of incidence, with respect to the object surface, are desirable since doubly-exposed specklegrams recorded under these conditions yield interference fringes of higher respective contrast. The latter is also influenced by the degree of beam expansion (a large area has a lower intensity of illumination than a small area) and the uniformity of the expansion - variations in intensity produces variations in contrast. While illumination using a comparatively high power laser (e.g. 8mW output power) is not considered to be essential for speckle photography, it enables exposure times to be shorter and gives more latitude in terms of areas and angles of illumination which may be used without significant loss of intensity.

It was reported that, for specklegrams recorded under the same double-exposure conditions, higher contrast photographs were obtained for objects having coarser surface finishes (higher R_a values). This finding endorses the results obtained by Asakura[27] outlined in Section 1.7. However, as Francon[23] observes, it is

not only the depth of the surface imperfections but also their uniformity of distribution (i.e. spatial frequency) which needs to be considered. This was borne out by the results obtained for the surface which had large random imperfections, as described in Section 3.8. In the case of the surface which had been painted (matt white) it is probable that the illuminating laser beam partially penetrated the surface and, as Ennos[7] suggests, was multiply-scattered causing depolarisation, such that a fully-developed speckle pattern was not obtained. This could explain the fact that fringes generated from double-exposure specklegrams obtained from this surface were of relatively lower contrast than could perhaps be expected for a surface of this roughness. If further research was undertaken in this context the use of a polarising filter, fitted to the recording camera, could be examined as a means of achieving improvements in the subsequent fringe contrast.

With regard to the aperture ratio of the recording camera, it was reported earlier that an aperture of f/4 was found to be particularly suitable for use with fine-grain emulsions. A large aperture decreases the speckle size and thus limits the minimum displacement that can be measured. If a smaller aperture is used the speckle size is increased and this decreases the sensitivity. However, the effect of the latter can be partly off-set if the degree of demagnification employed is not large (although

this then limits the maximum displacement which may be measured and so a compromise may be necessary).

There were some reductions in interference fringe contrast and definition detected which were attributed, as explained earlier, to lens aberration effects. It is noteworthy that Archbold et al.[52] have described speckle decorrelation effects which are considered to be due to certain lens aberrations and, as they suggest, this can reduce the accuracy of lateral displacement measurement by speckle photography.

A fine-grained emulsion is considered to be desirable for recording speckle patterns in order that the speckles are resolved. Moreover, wider camera apertures may be employed with such emulsions (this also helps to compensate for their lack of speed). It was observed that the coarse-grained emulsion which was studied produced a higher level of background 'noise' than the holographic emulsions. This could be due to the fact that the larger grains would scatter the light more. The fine-grained Agfa-Gevaert 10E75 emulsion has an average grain size of 0.09μm and the silver halide crystals in this emulsion are of a fairly uniform and small size distribution. Malin[60] points out that a narrow size distribution yields higher contrast and resolution. This is particularly important with respect to speckle photography because high contrast (of the specklegram) gives good diffraction efficiency (for fringe generation).

However,as Archbold et al.[9] have reported, contrast does not increase with increase in the photographic density of the specklegram to the extent predicted theoretically.

As discussed in Section 2.2 an exposure time which gives an overall intensity transmittance of 50% is desirable for double-exposed specklegrams to yield high contrast fringes. Francon[23] has indicated that when multiple exposures are employed in recording speckle patterns, equal exposure times are preferable and this was found to be so with regard to the experimental results obtained in these preliminary studies. While, theoretically, each exposure (of the double exposure) is half of the total required exposure in a given situation, it was found in practice to be somewhat more than half. This finding, concerning Agfa-Gevaert 10E75 emulsion, endorses the observations of Tiziani[17].

The developer Kodak D19, which was reported earlier as producing high contrast negatives and providing good processing flexibility, was found to deteriorate markedly (so it was stored in airtight containers and used at full-strength). Thorough washing of the exposed film (before and after development) and careful drying (no heat or blown air) was observed to minimise 'random' scattering effects when the processed film was interrogated with a laser beam. Bleaching of the film tans the gelatin and can improve the interference fringe brightness and uniformity (because localised variations of

density on the specklegram are converted to phase variations). Moreover, as Stetson[15] points out, by bleaching the specklegram and converting metallic silver to a silver halide, the processed image becomes more even in tone. Thus, in cases such as where an object surface has large variations in reflectivity (which result in variations in exposure over the specklegram surface) bleaching of the specklegram can be advantageous.

The results obtained in the displacement measurement studies using single illumination beam speckle photography were all within the calculated expected error (<±5%) as indicated in Section 3.9. These compare favourably with corresponding results obtained by Luxmore et al.[61] under similar conditions. A major factor, in terms of improving the overall sensitivity of measurement, is increasing the accuracy of the interference fringe spacing measurement. (This was the chief concern in the main studies, which will shortly be described). As explained, it was found that some improvement in this respect was facilitated by the use of cylindrical lenses and photography of the fringes (which reduced the effects of background 'noise' on the visibility of the fringes). Interrogating the specklegram with an expanded laser beam in a diffractometer arrangement, with the specklegram being displaced in front of the beam, was also found to be helpful in reducing the effect of speckle noise. However, this is only considered to be advantageous when noise

levels are high and fringe contrast is poor.

These preliminary studies not only provided valuable information, experience and evidence which was profitably exploited in the main studies but also helped to reveal possibilities which were subsequently explored.

Factors which could help to improve the recording, processing and analysis of specklegrams were identified in these studies and these were all accounted for in obtaining and recording specklegrams for use in the main investigations concerning interference fringe measurement.

CHAPTER 4

LINEAR ARRAY FRINGE MEASUREMENT SYSTEM

CHAPTER 4.

4.1. INTRODUCTION.

As indicated in the previous chapter (3.2) a brief investigation concerning the scanning and measurement of the interference fringes obtained from doubly-exposed specklegrams was undertaken using a simple solid state opto-electronic device (phototransistor system). The preliminary findings suggested that the use of a solid state opto-electronic system should be explored further. In order to obtain high resolution, it was decided to employ a solid state linear array instead of a photo-transistor. The characteristics of silicon photodiode arrays, as described by Fry[62] were considered to be well suited for such an application. Moreover, as Bartlam[63] points out, such devices are simple, rugged and relatively low-cost. Various types of solid state arrays are currently available which could be employed in this context. As Noble [64] observes, the major types are photodiode devices, charge injection devices (C.I.D.) and charge coupled devices (C.C.D.). As will later be explained, a linear photodiode array device was employed in this investigation.

At the time this research was undertaken, there was no work found to be reported in the literature regarding the use of linear photodiode arrays in this sphere (Maddux et al.[65] had reported the use of a large photodetector,

which was used in conjunction with mechanical scanning of the interference fringes.) Some work had been undertaken by investigators such as Ineichen et al.[66,67] who employed a hybrid optical and electronic system, but the only reported system in which a linear photodiode array was employed for fringe measurement was that devised by Kaufmann et al.[68] which was published some time after this investigation was carried out.

4.2. BASIC THEORY AND PRINCIPLES OF LINEAR ARRAYS.

The photo-electric effect, which is basically the excitation of electrons by photons, is the fundamental process on which the operation of a solid state photodiode depends. Nevertheless, as Fry[62] observes, the overall mechanism of photocurrent production is quite complex.

i) Solid state photodiodes.

Basically, in a semiconductor such as silicon, the electrons occupy energy states which are divided into two 'energy bands'. These are the 'valence' band and the 'conduction' band (higher energy) and there are no allowed energy states between these. Only the conduction band electrons are mobile and able to contribute to conduction. Electrons are thermally 'excited' into the conduction band at room temperatures and leave gaps in the valence band termed 'holes' which are positively charged and may also contribute to conduction.

Excitation of electrons from the valence band to the conduction band is called 'electron-hole' pair production and can be brought about by the absorption of a photon. The photon must have energy equal to or greater than 'Eg' the 'energy gap' between the valance and conduction bands (for silicon 'Eg' = 1.1eV) if it is to excite an electron across to the conduction band.

Solid state photodiodes consist of a layer of 'P type' (positive) semiconductor material and an adjoining layer of 'N type (negative - excess electrons) semiconductor material. If the polarity of the electrical connections to the photodiode are such that the P-N junction is 'reverse biased' (see Figure 4.2.1) then the electron-hole pairs that are produced will separate and accelerate across the junction, thus constituting a current. The 'mobile' charge carriers (i.e. electrons or holes) generated near the diode junction must diffuse to it in order to be accelerated across and contribute to this current.

Thermal and photon excitations produce this current in the case of a photodiode. The constituents being termed, respectively, 'dark' (leakage) current 'I_D' and 'photo current' ('light' current) 'I_L', as indicated in Figure 4.2.1. Photocurrent is proportional to the number of photons having sufficient energy (such that this energy is $\geq$ 'Eg') that are incident on the surface in unit time.

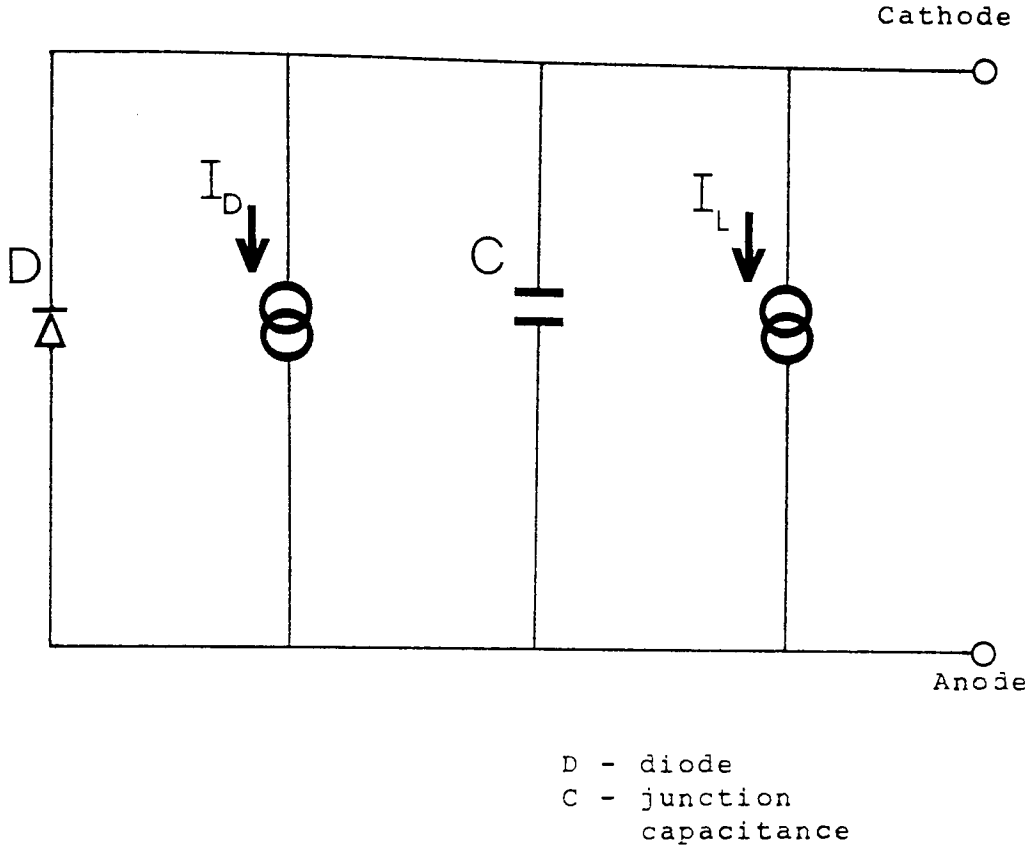

Fig.4.2.1 Silicon photodiode Equivalent Circuit.

ii) Linear solid state arrays.

Two main types of photosensors are available in the form of 'linear arrays'. These are photodiode arrays and the more recently introduced charge coupled devices (C.C.D's). There is a hybrid form of these two called a charge coupled photodiode array (C.C.P.D.) that is also now available.

iii) Linear self-scanned photodiode arrays.

A linear self-scanned photodiode array consists of a narrow photosensitive strip which has rectangular photodiodes arranged along it as indicated in Figure 4.2.2.

A metal oxide semi-conductor (M.O.S.) switch

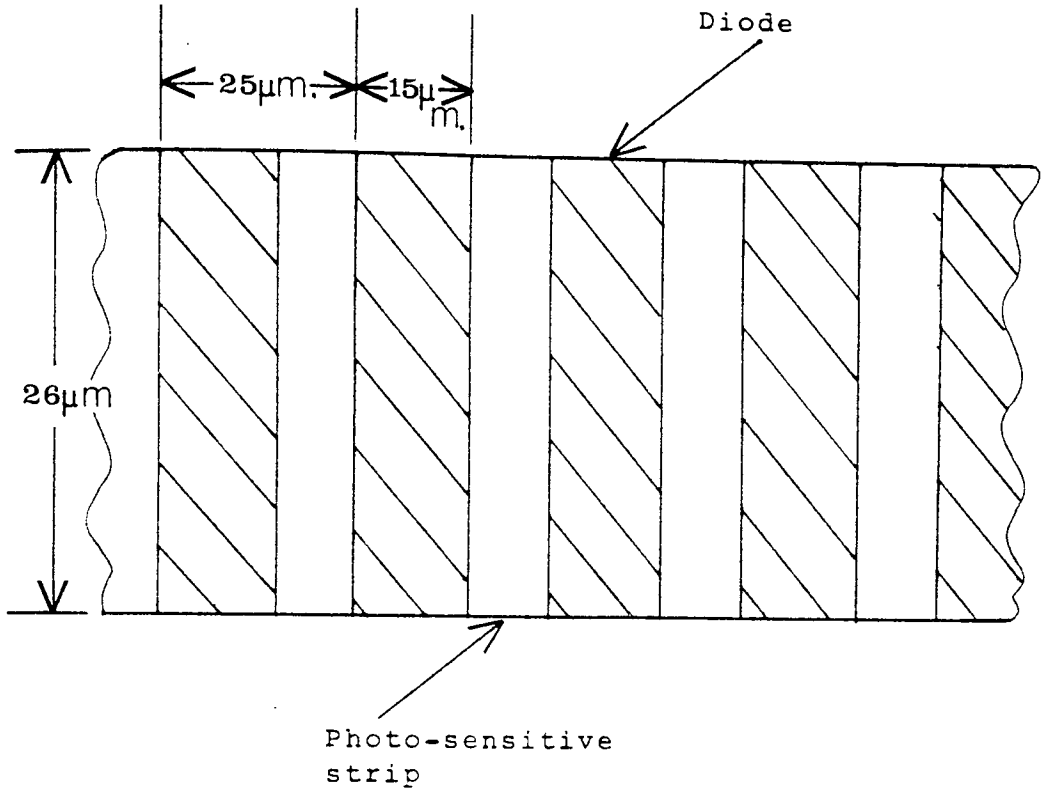

Fig.4.2.2. Section of a Linear Photodiode Array

(This is a 'Reticon' RL2569 array which was used in the investigation and the parameters shown are those of this array).

connects each photodiode to a common video output line. An internal shift register operates these switches and causes the information from each diode to pass, serially, to the 'common' line. For each scan of the linear array, the light energy incident on each diode since the preceding scan, is measured. Basically, this is done by 'topping-up' the charge on the capitance 'C' associated with each of the diodes and measuring the 'top up' which is required. A simplified circuit, showing part of a typical linear array system, is shown in

Figure 4.2.3. Charge is removed between each topping-up by a photocurrent at a rate which is in proportion to the amount of light (radiant flux) on the photodiode. Hence, the output gives the amount of light (integrated with respect to time) or the radiant flux on each photodiode between scans.

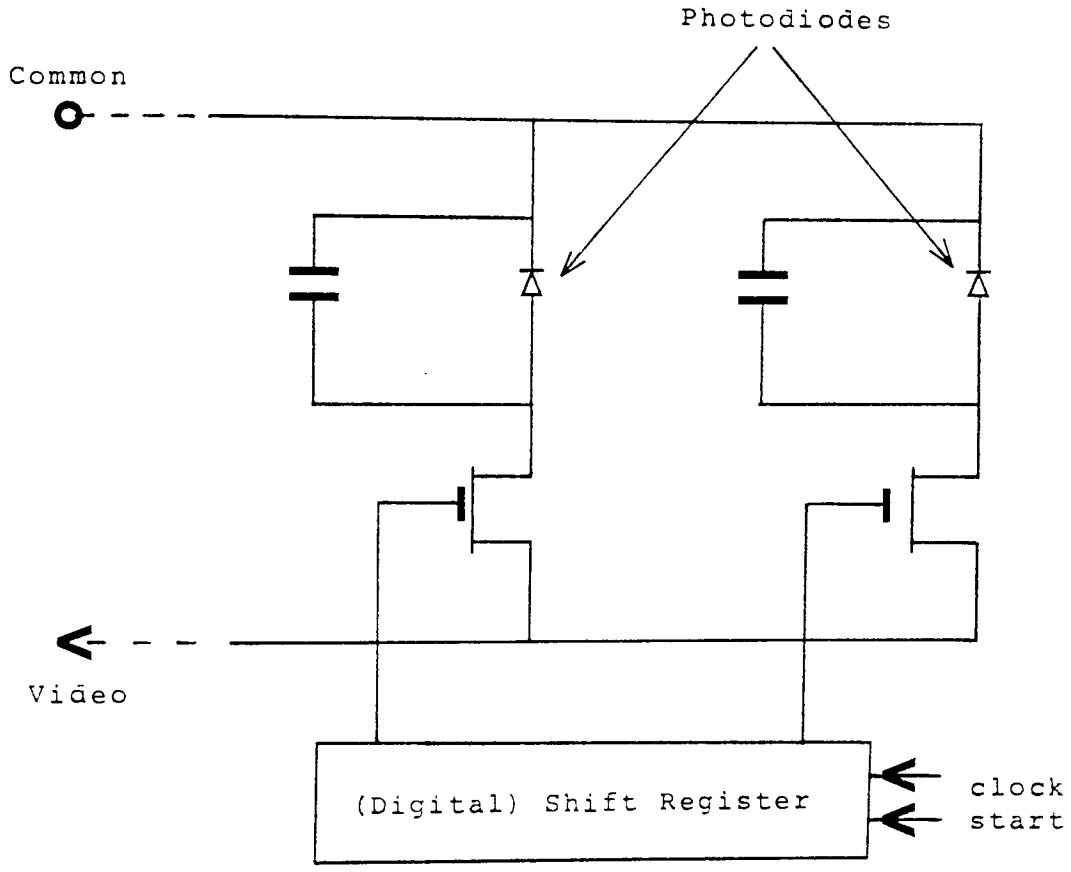

Fig.4.2.3. Simplified Circuit Diagram of Part of Array Circuit.

4.3. LINEAR ARRAY PARAMETERS AND PROPERTIES.

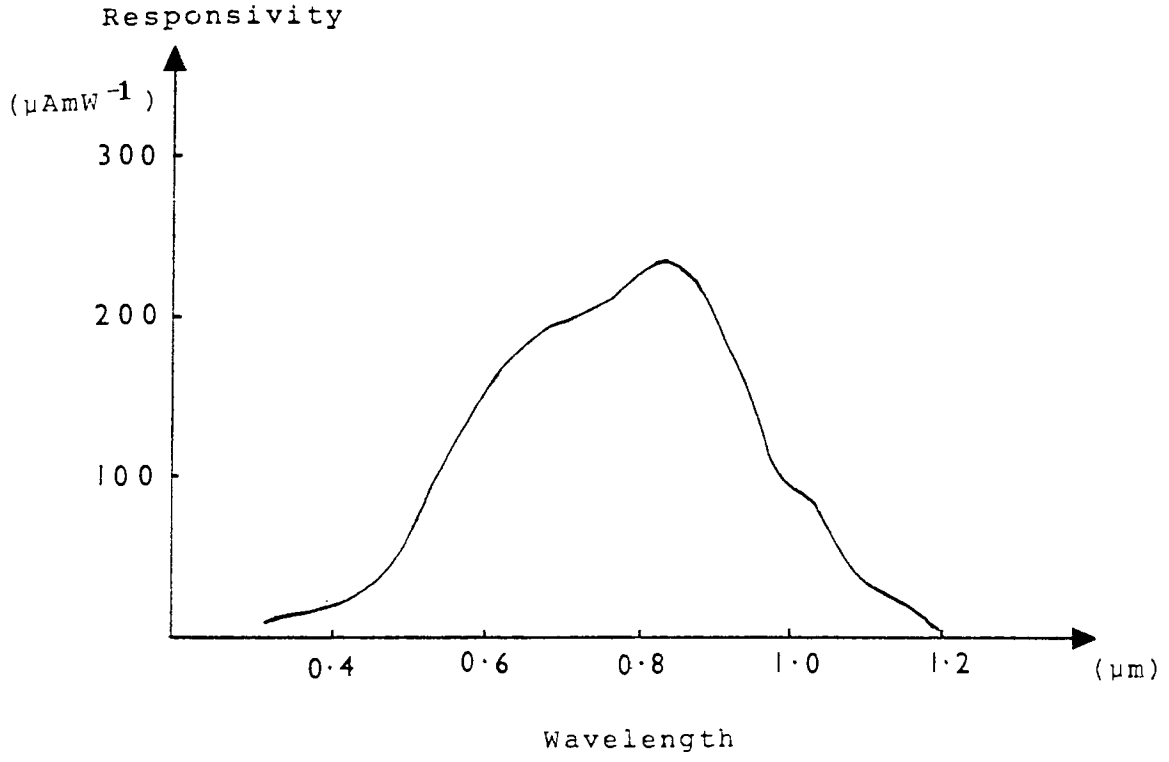

Fig.4.3.1. Silicon Diode Spectral Response.

As can be seen from reference to Figure 4.3.1. the typical spectral response of a silicon diode is satisfactory with regard to the light emitted from a helium-neon laser (wavelength 0.633μm).

The sensitivity of photosensors may be expressed in terms of the quantity of charge produced per irradiation. However, the responsivity of a photosensor depends upon the spectral distribution of the source.

This can be related to the quantum efficiency (η) of the photosensor which basically defines the ratio of the charges produced (in the junction) to the number of photons which are incident:

$$\eta = \frac{\text{number of electrons produced}}{\text{number of incident photons}} \quad ..(4.3.1)$$

The particular linear array which was employed in this investigation has relatively high responsitivity, as indicated in Figure 4.3.2.

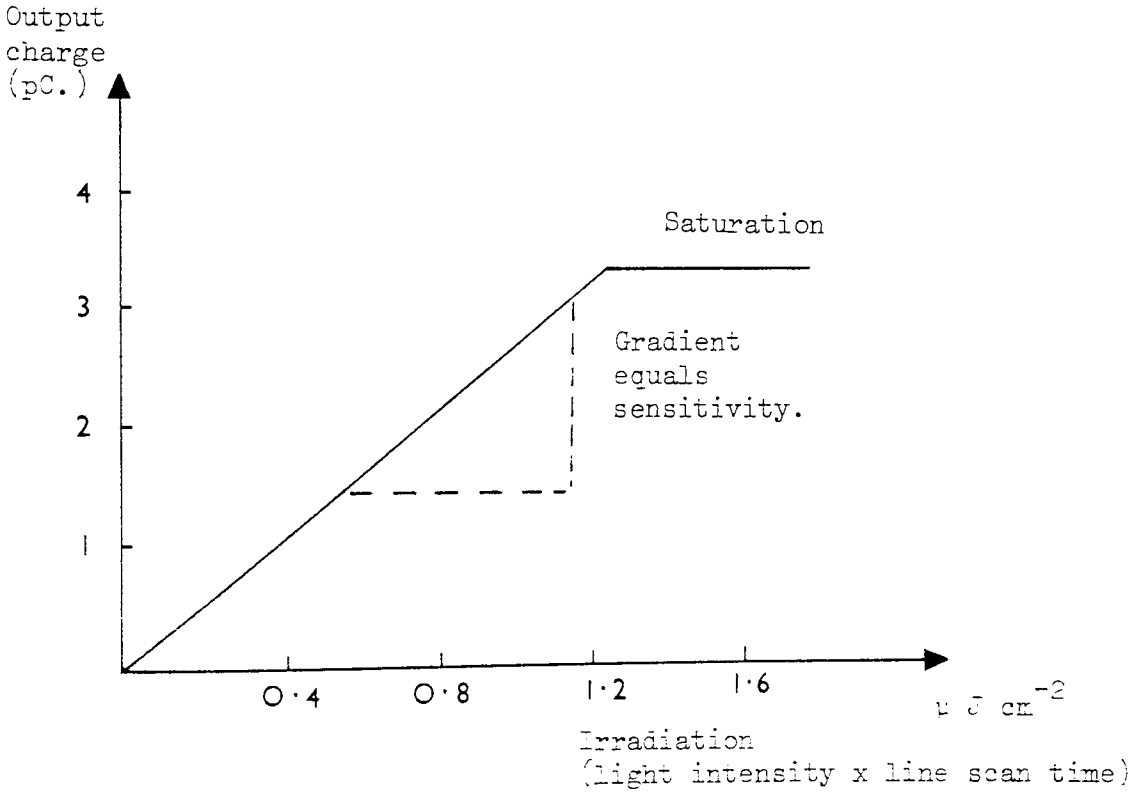

Fig.4.3.2. Signal Charge per Cell as a Function of Irradiation

Uniformity of response along the length of a photodiode is a function of wavelength. For the visible

wavelengths the response of the particular array used in this research was reasonably uniform*. Again this property is desirable with regard to the intended application of the linear photodiode array with laser illumination.

The charge output of each photodiode in a linear array can be varied (see Figure 4.3.2.shown previously) by changing the light intensity or changing the 'line scan' time (i.e.changing the integration time - which is controlled by the switching system). Integration time 't_L' is the time interval between successive scan pulses. This has a minimum value which is the product of the number of photodiodes and the time required to sample and recharge each photodiode. Typically , this is one 'clock period' of an external single-phase clock. An increase in integration time can be achieved by adding a blank period between the end of one scan pulse and the start of the next.

Account must be taken of the fact that some photons may be incident on the regions between successive photodiodes. As a result, there may be photocharges produced in these regions (which can constitute a significant portion of the photosensitive area of the array) and these will tend to arrive at the nearest possible photodiode. However, some may diffuse the other way, producing

---

*According to the manufacturer's data[69].

a response along the array length.

Another important factor to be taken into consideration regarding linear array parameters is 'crosstalk'. This is the response of one photodiode to light falling on an adjacent photodiode. Crosstalk is due to charge carriers diffusing to the wrong photodiode. The deeper in the substrate the charge carrier is produced the further it has to diffuse and the more chance there is of it arriving at the wrong photodiode. Consequently, crosstalk increases with increasing wavelength of the incident light. It also increases as the distance between adjacent photodiodes is decreased. (For the array which was employed these factors were accounted for.)

4.4. DETAILS OF THE ARRAY AND SYSTEM EMPLOYED.

The self-scanning linear photodiode array that was used in the investigation was a 'Reticon' (G series) type RL256G. This array offers adequate resolution and speed at relatively low cost. There are 256 photodiodes in this array (the dimensions are shown in Figure 4.2.2 which was given earlier.) The array is a monolithic self-scanning linear photodiode array and each photodiode has an associated storage capacitor on which to integrate photocurrent (and a multiplex switch is provided for periodic read-out via an integrated shift register scanning circuit).

The shift register clock driver is also integrated -so that only a single phase T.T.L. clock is required for scanning. Associated with the photodiodes is a row of 'dummy' diodes which are read out differentially with the photodiodes to allow cancellation of multiplex switching transients (and to provide a clean video signal with a minimum of external circuitry). As shown in Figure 4.4.1 the system basically consists of two main circuit boards. These are the 'motherboard' (M) which contains most of the circuitry and the small 'array board' (A).

Fig.4.4.1. Array and Mother Boards.

The 'array board' is basically made up of the linear photodiode array and the few components that must be closely linked to it. To provide freedom of movement the 'mother

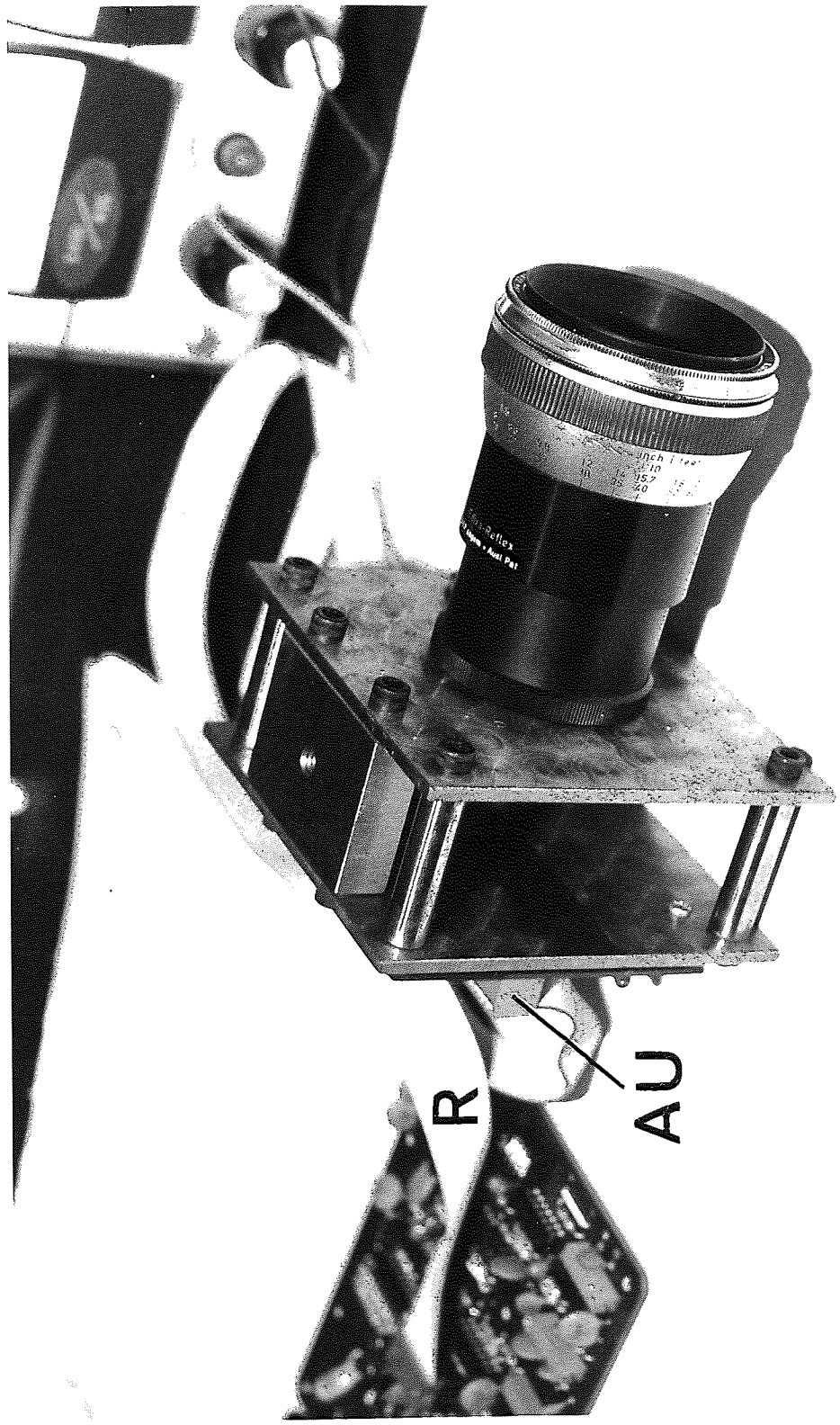

Fig.4.4.2. System constructed to house linear array unit

board' and 'array board' were interconnected via a ribbon cable 'R' as indicated in Figure 4.4.2 (the 'array board' is mounted at the back of the array unit 'AU').

The aperture length of the array used was 6.4mm and the array was protected by a ground and polished optical window. Two separate power supplies (+5V and -8V) to the array are required and these were provided by stabilised power supplies which are shown on Figure 4.5.1 (as will later be indicated.) The 'array board' employed was a Reticon 'RC104' and the'mother board' used was a Reticon RC100B.(See Appendix 4 for the details of these).

4.5. METHOD

The basic experimental system which was used in this research concerning measurement of the fringes generated from doubly-exposed specklegrams is shown in Figure 4.5.1. A special frame held the array (mounted on the 'array board') and this had a 40mm photographic lens mounted on the front. The latter was only employed for setting up, alignment and checking (using a low intensity light source). Care was taken to ensure that the laser beam was not directed onto the array and, to protect the array from damage by the undiffracted laser beam, a small stop was used.

After undertaking a number of preliminary experiments, it was decided to mount the array unit on a rigid tripod,

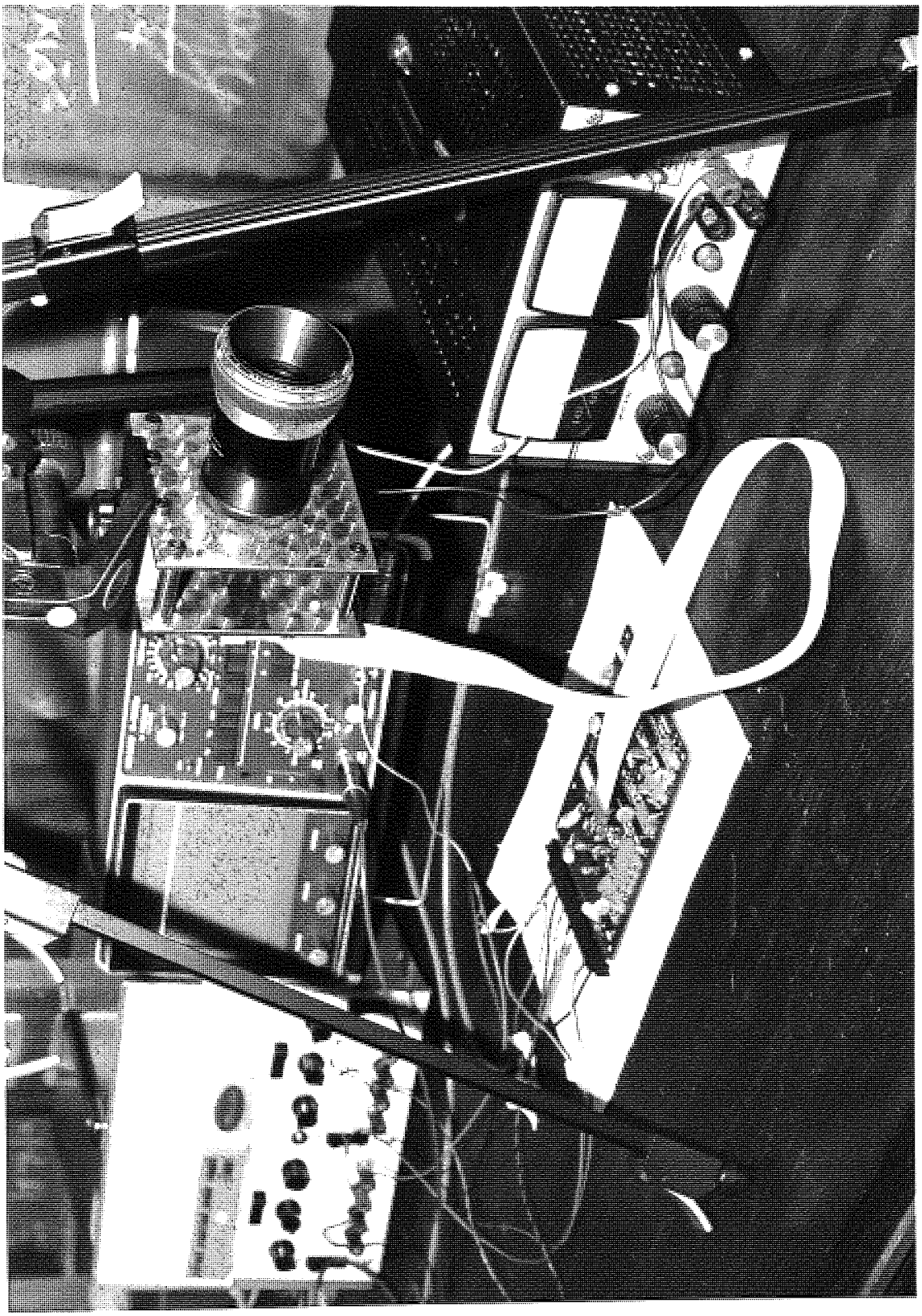

Fig.4.5.1. Linear array: experimental system

as can be seen in Figure 4.5.1. This enabled height adjustments of the array to be made. It also meant that the array could be raised, so that the interference fringes could be checked and adjusted (using a small screen) then lowered back into position.

A cylindrical lens 'C' was used (see Figure 4.5.2) to compress the diffracted cone of light leaving the specklegram onto the array such that the 'noise' associated with each interference fringe is reduced (by the integrating action of the lens). In order to provide a basis for reference and comparison the specklegrams examined were the same ones that had been obtained and analysed in the displacement measurement study described in the previous chapter (Sections 3.3 snd 3.9). A 1mW output power laser was employed (unexpanded beam diameter 1mm) to illuminate the specklegrams (which were mounted in the special adjustable holder, as in the preliminary studies). In a final series of experiments a laser of 8mW output power, but of the same beam diameter, was used to interrogate the same specklegrams so that the influence of different illumination levels could be assessed.

Precautions were taken to prevent extraneous light reaching the array by keeping the background illumination level relatively low and fitting shields around the array unit (in Figure 4.4.2 and 4.5.1. the shields are removed). The orientation of the fringe pattern and the projection

M - Mother board
A - Array
AU -Array unit

S - specklegram (in holder)
C - cylindrical lens
(short focal length)

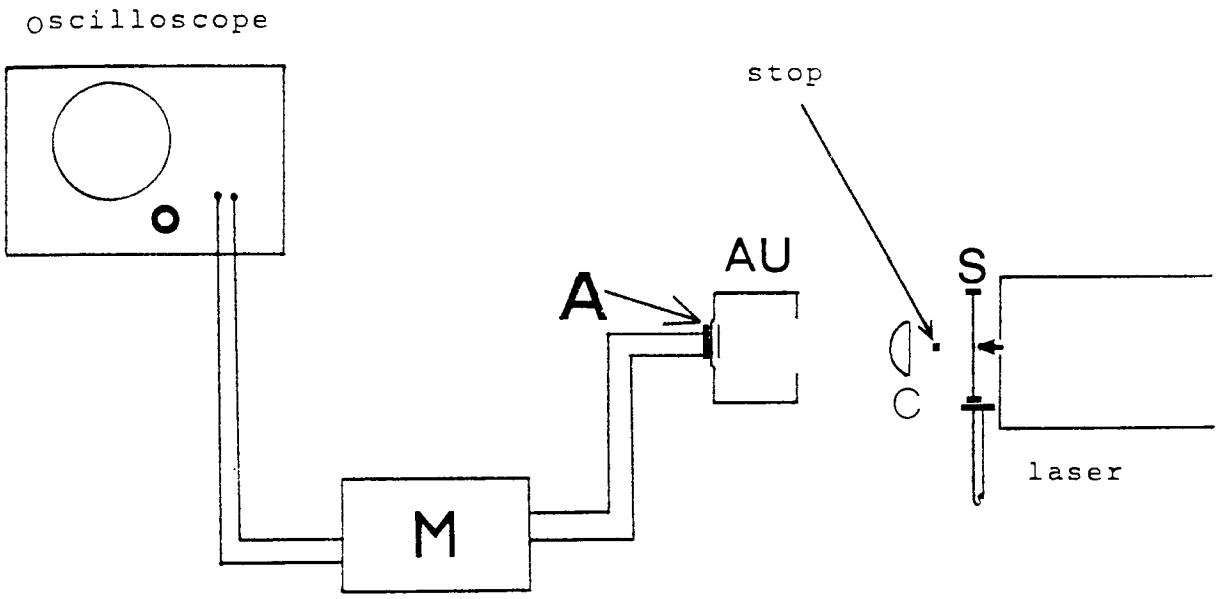

Fig.4.5.2. Experimental System Using Linear Array

distance from the specklegram to the array was carefully adjusted for each specklegram so that the projected fringes aligned with the photodiodes on the array. Further adjustments were made, using the cylindrical lens, to ensure that the fringes projected onto the array were uniformly spaced and not distorted (over the length of the array). Having set this up, the specklegrams were then interrogated, in turn, and a series of corresponding areas on each specklegram was examined.

The output from the array system was displayed on an

oscilloscope for analysis (the video waveform output is an electrical analogue of the irradiation of the linear array). Adjustments were made to the oscilloscope so that a large, stable waveform was displayed for measurements to be taken from (a calibration check was also made before each set of readings were taken). The distances between a number of successive wave crest centres (which corresponded to 'bright fringes') was recorded, since this is proportional to the fringe spacing. Readings of the oscilloscope settings were recorded in each case, in order that the fringe spacings could be calculated. By carrying out a point by point analysis of each specklegram in this way the mean fringe spacing was then determined from the results in each case.

Regarding the array processing circuit, the main parameters that were adjusted were the clock frequency and the time interval between the start of successive scans. Initially, a clock frequency of 500KHz was employed - this is generated on the 'mother board'. However, due to problems of 'noise' in the output waveform (as will later be explained) the clock frequency was later changed by modifying the'mother board' circuit. The 'mother board' also periodically generates a pulse which starts the array scanning. It is the interval between these pulses that is the integration time 't_L' (as outlined in Section 4.3) and this is a

fixed number of 'clock'periods (which were pre-set on the 'mother board').

An integration time of 0.5ms. was used in the preliminary experiments, but this was subsequently increased, in stages, to a maximum of 35ms. This was achieved by reducing the clock frequency and was done, as will be described, in order to increase the sensitivity of the photodiode array system.

The possibility of digitizing the output from the array (using an analogue to digital converter) was finally briefly investigated. A digitized output was obtained and this was presented to a microprocessor (an Intel'8085') so that the feasibility of analysing the digitized interference fringe data could be examined.

4.6. RESULTS OF THE INVESTIGATION.

The mean fringe spacing value for each specklegram which was measured using the linear array system was used to calculate the object surface displacement corresponding to that specklegram (using the equation described in 3.9). These specklegrams, which corresponded to surface displacements in the range 0.05mm to 0.25mm, were the same ones that had been obtained and analysed in the preliminary experiments outlined in Chapter 3. This provided a basis for comparison for this technique of fringe measurement.

The calculated results obtained by this method, with the system operating at a clock frequency of 500kHz, were all close to a maximum error of ±5% (compared to the object surface displacement recorded by the sensitive dial gauge). Problems were experienced (at this clock frequency) in measuring the video waveform displayed on the oscilloscope, because the waveform profiles were distorted (due to 'noise' effects).

There are three main factors* which influenced the 'noise' levels (for a given specklegram) in this context:

(i) Noise due to 'dark current' (I_D) - this increased with increases in the integration time duration (t_L) and appeared as increased 'background' noise.

(ii) Fixed pattern noise - from switching transients.

(iii) Amplifier noise.

As mentioned earlier (Section 4.4) the linear array that was used contained a series of 'dummy' diodes which were differentially amplified with the photodiodes, and this meant that the 'noise' associated with (i) and (ii) was somewhat reduced.

In order to decrease the noise associated with the waveform amplification, the gain of the oscilloscope was reduced and the 'sensitivity' of the array was increased to compensate for this. This was achieved by increasing

*These are in addition to the problems of 'crosstalk' (described in 4.3).

the integration time 't_L' (initially by a factor of 10) and increasing the illumination level (by using the laser of higher output power). These modifications produced an improvement in the displacement results obtained from the measured fringe spacings - such that all the results were now close to a maximum error of ±4%. A 'pay off' situation between increasing the integration time 't_L' and reducing the amplifier gain was observed and examined - as discussed later.

The array circuitry which was employed in this investigation had an overall scanning time of 520μs. [i.e. 256 photodiodes x 2 (one clock period* is 2μs) = 512 (+8 blanking pulses) giving a total of 520μs]. Initial integration time 't_L' was increased from approximately 0.5ms (at a clock frequency of 500kHz) to 5.0ms and in a final experiment to 35ms (at a clock frequency of 7kHz). For doubly-exposed specklegrams which generated interference fringes of higher spatial frequency (i.e. corresponding to the higher object displacement values used) the results obtained using a 5.0ms integration time were actually close to a maximum error of ±3% (compared to the displacement values recorded on the dial gauge).

The fringe resolution and measurement accuracy were found to be markedly reduced when the fringes were projected directly onto the array without the

*Sampling each photodiode takes 1 clock period.

cylindrical lens being used. When the higher power (8mW) laser was employed it was noted that it resulted in an improvement in the clarity of the video waveform on the oscilloscope (probably because it enabled the amplifier gain to be decreased and hence amplifier noise was reduced). Once the system was set up and operating it was found that the measurements could be quickly made and, with a digitized output, the system could be auto-mated - such that fringe spacing data is automatically processed (automatic read-out could be provided).

4.7. CONCLUSIONS.

This study confirmed the feasibility of using a linear photodiode array for measurement of interference fringes generated from doubly-exposed specklegrams. It also demonstrated the practicality of using a linear array in this context. The findings and observations in this respect have been substantiated by Kaufmann et al.[68,70] who also devised a fringe measurement system employing a linear photodiode array. (Their array had 512 photodiodes at 50.8μm centres compared to 256 photodiodes at 25μm centres used in this investigation). They only report the use of one 'clock' frequency (65KHz) and the beam diameter used to interrogate the speckle-gram (0.7mm) is slightly smaller than that employed in the experiments described here. Kaufmann et al.[68] also used a cylindrical lens in order to reduce speckle

'noise' in the projected fringe pattern. However, the optical system which they used was somewhat more complex than that employed in this investigation.

As indicated, a number of modifications were made to the system in order to improve the signal to noise ratio. In an attempt to reduce amplifier noise it was pointed out that the amplifier gain was reduced and the integration time 't_L' increased (in order to increase the 'sensitivity' of the array- to offset the reduction in amplification). According to the manufacturer's data[69], the integration time should not be increased beyond 30ms. because of significantly increasing the 'dark current' level. Nevertheless, as reported in the previous section, the integration time was actually increased to 35ms. in a final experiment. This was not found to produce a marked increase in the background 'noise' level. It did help to further improve the response and sensitivity of the array system but the detection of 'random' speckles also increased and so reduced the improvements which were obtained. An integration time of 5.0ms, for the array system used, is thus considered to be preferable.

It is not thought that reducing the diameter of the laser beam that was used to interrogate the specklegrams would have brought about any significant improvements in the fringe clarity and measurement. In fact, as Kaufmann et al.[68] point out, for specklegrams recorded

using an aperture ratio of f/4 the lower limit for the interrogating beam diameter is 0.7mm. If the beam diameter is reduced beyond this value, the speckle noise level becomes increasingly unacceptable.

Removal of the 'background halo' from the projected fringe pattern could help to improve the detection and measurement of interference fringes, in cases where fringes having a large spacing are projected onto the array or when fringe definition is particularly poor. Perhaps a polariser or filter could be used for this purpose. It could also be possible to modify the electronic system so that the filtering is achieved electronically.

It was pointed out in an earlier section that, as a sequel to the main investigation, a brief experimental study was undertaken concerning digitizing the output of the linear array system (such that computer analysis of the fringe data could be carried out directly). The study showed that an analogue to digital converter, used in conjunction with a microprocessor, could be usefully employed in this respect.(There are a large number of analogue to digital converters and suitable microprocessors now available for this purpose)

It is interesting that Kaufmann et al.[68,70] have devised a partially automated system for this purpose (using a punched-tape system and a fast Fourier transform computer sub-routine). More recently, fully automated read-out systems have been reported. For instance,

investigators such as Costa et al.[71] have described an automatic read-out system, using a serially-scanned photodiode array (which they have employed in the context of speckle interferometry - for thermal expansion measurement). Certain limitations revealed by this investigation and the overall accuracy of measurement using a linear array system could be significantly changed as array devices are further developed. It is suggested that linear photodiode array systems have considerable potential for exploitation in the context of speckle photography which has been identified in this study.

CHAPTER 5

MICROPROCESSOR/COMPUTER-CONTROLLED MICRODENSITOMETER AND COMPUTER-ASSISTED FRINGE MEASUREMENT SYSTEM

CHAPTER 5.

5.1. INTRODUCTION.

The research described in this chapter was concerned with the exploration and development of a computer controlled microdensitometer system for measurement of interference fringes (from photographic negatives of fringes generated from doubly-exposed specklegrams) with the provision of computer assisted analysis - using a specially formulated subroutine. This investigation was also concerned with the assessment of the overall sensitivity and potential of the integrated system developed for interference fringe measurement.

The detailed experimental investigation of the analysis and measurement of the interference fringes generated by doubly-exposed specklegrams using a microprocessor/computer controlled microdensitometer in conjunction with computer-assisted analysis has not been found to have been undertaken. In the context of speckle photography, Archbold et al.[9] have reported using a basic microdensitometer but only for determining the dependence of interference fringe contrast on the photographic density of specklegrams. However, Luxmore et al.[61,72,73] have employed a microdensitometer for fringe measurement - although this was not a precision computer-

controlled system (with digitized output) and the output data was not processed usingaspecially – devised subroutine.

An algorithm for fast digital analysis of interference fringes (not those specifically generated from doubly-exposed specklegrams) has been formulated by Snyder[74]. This was adapted for use with the microdensitometer data obtained in this investigation and its suitability assessed. Certain other subroutines, based on those developed by Pickering et al.[75] were also adapted and employed for the computer-assisted analysis of the interference fringe data.

5.2. BASIC PRINCIPLES OF THE (DIGITAL) MICRODENSITOMETER

The microdensitometer consists of a stationary optical system which focuses light from a white light source through an aperture on to the sample (e.g.photographic negative). Transmitted light intensity is converted to optical density by a photodiode detector. The optical density 'OD' of a light absorbing medium M is defined as the logarithm (to base 10) of the ratio of incident to transmitted light, when the medium is illuminated as indicated in Figure 5.2.1.

Thus $OD = Log_{10} I_i/I_t = Log_{10}(1/T)$ ..... (5.2.1)

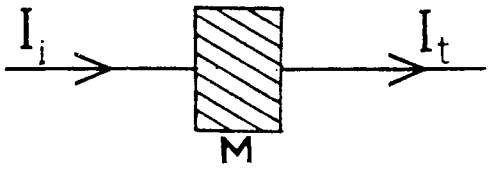

Fig.5.2.1. Optical transmission

Where the transmission factor 'T' = $I_t/I_i < 1$

i.e. when T = 1 then OD = 0

T = 10^{-1}" " = 1

T = 10^{-2}" " = 2 and so on.

Reflection losses are not taken into account and a practical microdensitometer thus measures the ratio of I_t/I_i from which the values of T and OD are calculated. The measurement involves illuminating a small area of the sample with a high intensity localised light source and digitizing the output of the photodiode which receives the transmitted light. (A practical microdensitometer has an optical system which collects both the specularly transmitted light and the diffuse scattered light - so the optical density measured is actually a mixture of these two). The density measured depends upon features of the optical illuminating and detecting systems (such as the detector acceptance angle) as well as on the sample. In the case of photographic samples, account may have to be taken, as pointed out by Dainty and Shaw[76] of the Collier effect* regarding optical density results.

In practice, images are digitized by recording the density at set positions on a regular grid. There are two basic forms of 'scanner'; the main difference between these is the method of mounting samples for scanning.

---

*An optical density non-linearity effect due to the scattering of light by grains in the processed film. (Termed the Collier coefficient).

These are 'flat-bed' and 'drum' scanners. (The former type was used in this investigation). A 'flat-bed' scanner has a flat glass plate onto which the sample is mounted and this plate can be translated through the optical path in two mutually perpendicular directions. Although the rate of movement is lower than that of a drum scanner(so the maximum data transmission rate is less) the sample can be 'stepped' in smaller increments - thus giving greater resolution.

When the microdensitometer is operated in the 'image scanning mode' (as in this investigation) the region of the sample measured when an optical density reading is taken is determined by the size of the detector aperture. In this mode the source aperture can be adjusted, as will be explained, to minimise the effects of non-uniform illumination of the sample. There are two important lens systems in the microdensitometer optical system (see Appendix 5). These are the 'influx objective' , which projects the image of the source aperture onto the sample, and the 'efflux objective', which defocuses the light passing through the sample onto the detector aperture (from where it passes to the photodiode detector).

Apertures are normally square, rectangular or circular and a range of both sampling aperture and detector aperture sizes are usually available. As Swing[77] observes, the larger the aperture then the less

fluctuations between consecutive readings - because there is an 'averaging effect' from viewing a proportionally larger amount of sample. (Some one-dimensional averaging is made possible by the use of a rectangular aperture.) It is not possible to use a sample aperture across which there is a large density gradient without some loss of accuracy (this follows from the logarithmic relationship between intensity and optical density, as indicated in Equation 5.2.1.). Choice of aperture size is also related to the 'step size' chosen for the sample movement between readings. The upper limit of aperture size which can be employed depends upon the resolution required (for features of a given image) and the granularity of the photographic emulsion sets the lower limit. All these and the other factors previously outlined were taken into account in undertaking the experimental investigations described later.

5.3. DETAILS OF THE DIGITAL MICRODENSITOMETER.

The microdensitometer which was employed in this investigation was the newly introduced Joyce-Loebl 'Microdensitometer 6'. This 'flatbed' microdensitometer was made available by S.E.R.C.* (Daresbury Laboratory). It has a solid state dual-beam photometric system (this

*Science and Engineering Research Council.

makes use of a two beam principle, by which the light source is monitored and any variations automatically compensated for when optical density measurements are made). The signal to noise ratio and overall stability of the system is enhanced by using silicon P.I.N. (positive-intrinsic-negative) photodiode detectors rather than photomultiplier tubes. Moreover, it has a large sample format with resolution down to 2.5μm (See Appendix 5 for fuller data). Figure 5.3.1 shows the unit in operation.

This microdensitometer was interfaced to a Data General 'Nova 3/12' minicomputer. An Intel'8085' microprocessor controlled all the basic microdensitometer functions under instruction from the minicomputer (including the table-drive [scanning] commands and the storage of the digital data [produced by an analogue to digital converter]).

The photodetector (2 photodiodes: area 5mm x 5mm) records the intensity of the light transmitted through the sample and this is converted internally to an optical density value (this is done using the standard logarithmic comparison - see Equation 5.2.1). Density (or transmission) data is measured digitally (as 10-bit binary words) and stored on magnetic tape.

A special interactive language (WIZARD) was employed with the minicomputer. (See Appendix 5)

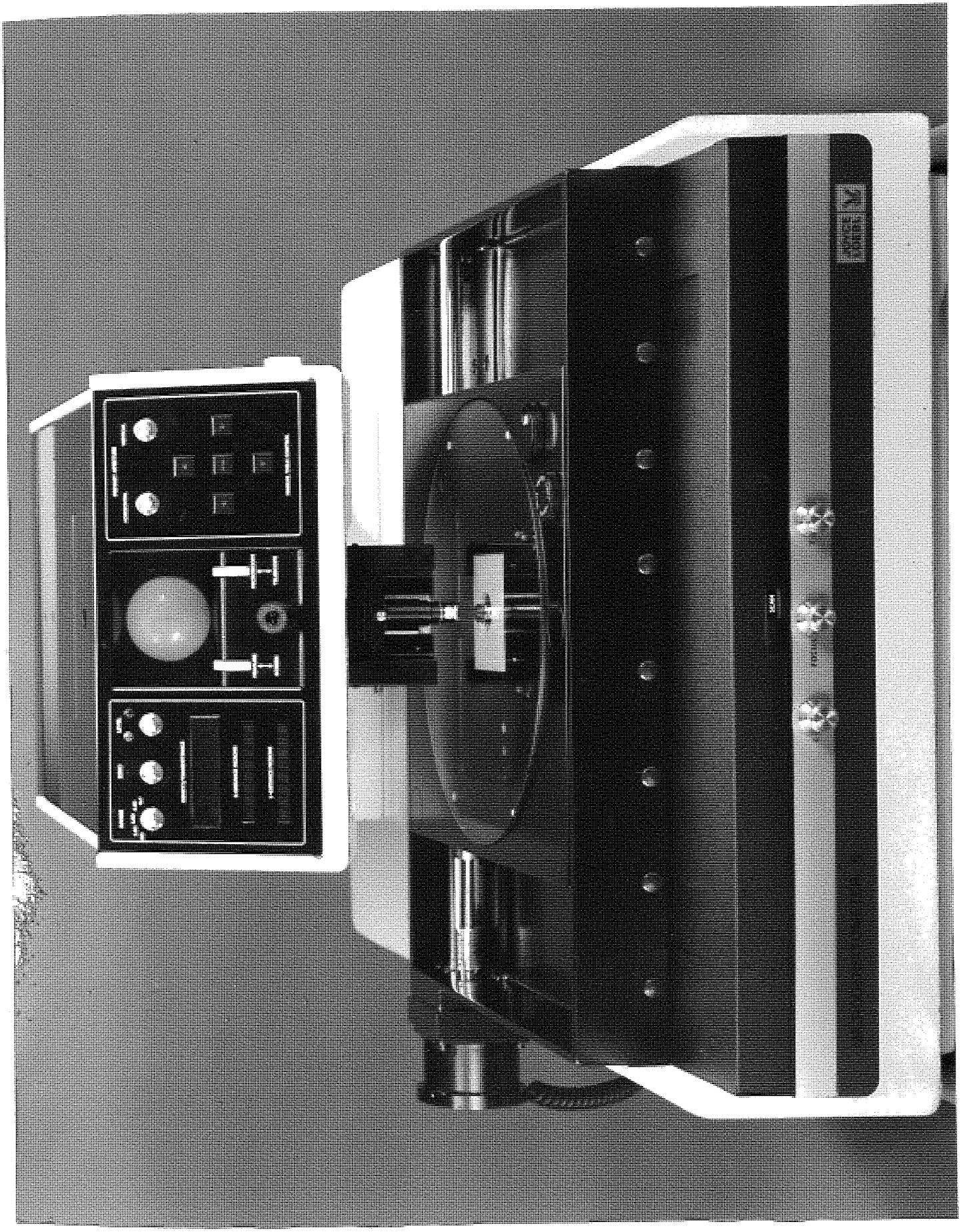

Fig.5.3.1. Microdensitometer system

5.4. EXPERIMENTAL METHOD.

(a) Microdensitometer.

The photographic negatives of the interference fringes to be measured (recorded on 35mm film) were each mounted, in turn, on a 6mm thick glass platen on the microdensitometer bed and held in position by a 1mm thick glass cover plate. To minimise the effects of possible non-uniform illumination the source aperture was adjusted (as recommended by the manufacturer) so that the fringe photographs were over illuminated by a factor of about 2 relative to the (hypothetical) reduced image of the detector aperture at the film sample. (This was kept as large as possible in order to reduce the effects of the random speckle patterns present on the photographic negatives of the interference fringes). Then the optical density range switch on the microdensitometer was set at the lowest range which would not be exceeded by the optical density of the photographic negatives (If it was set too high the effective accuracy would be reduced and if it was too low some optical density values could be truncated.)

As was outlined, the proprietary software for this microdensitometer system uses an interactive language called 'Wizard', and this allows considerable flexibility in programming the movement of the scanner table (i.e. setting the position of the scanner table, moving the table in the X and/or Y directions, and for taking

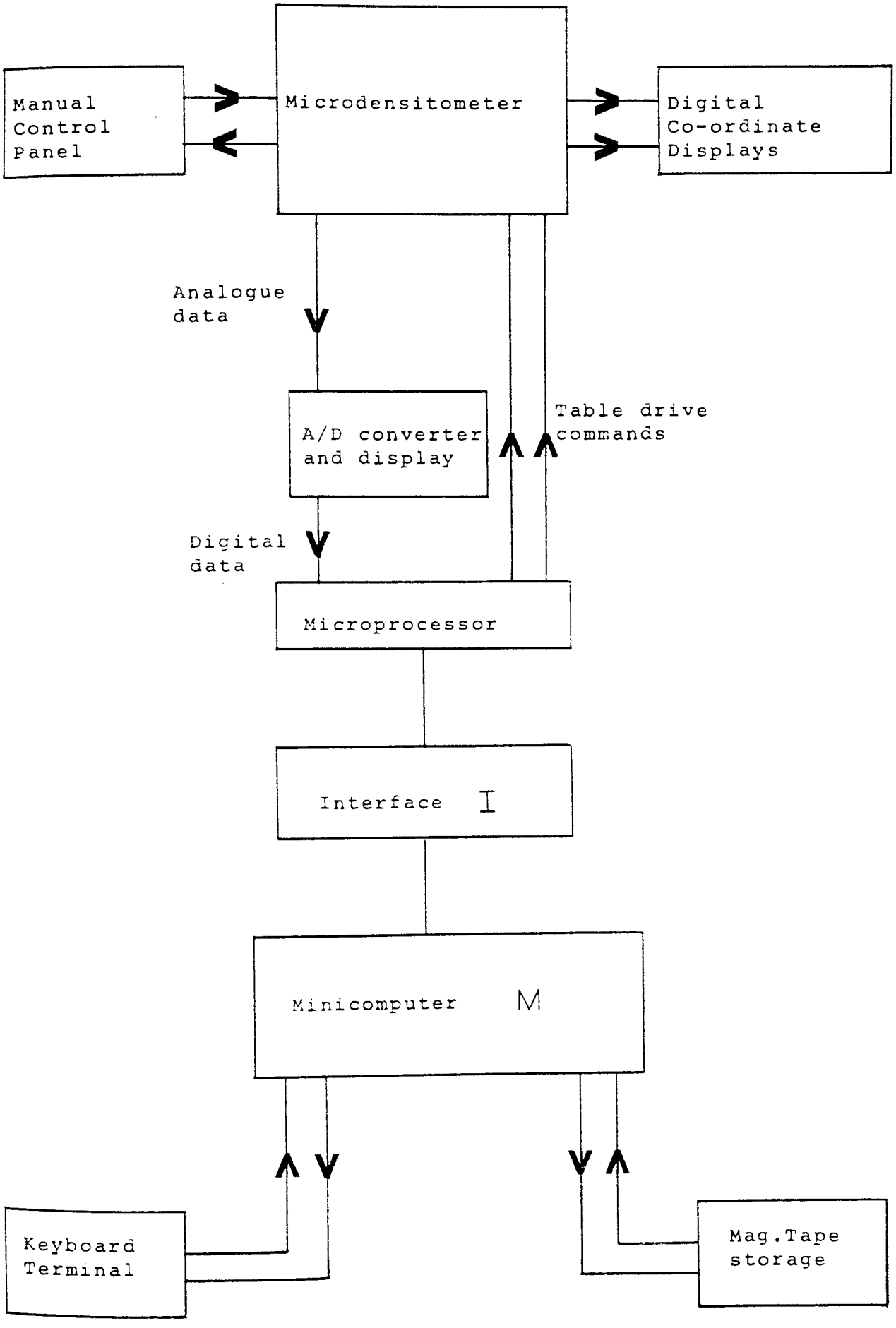

Fig.5.4.1. Schematic diagram of microdensitometer/ control system

density readings while the table is moving). A 'Wizard' program was employed with the microcomputer to instruct the microprocessor to control the scanning so as to provide full analysis of each fringe photograph. The system employed for this is shown, schematically in Figure 5.4.1. (Data obtained from each fringe photograph was stored on magnetic tape).

After undertaking a number of trials and tests the microprocessor was instructed to make the 'table drive' scan a rectangular area such that the longer sides of the rectangle enclosed all the fringes in the photographic negative. As these photographs had been recorded on 35mm film then, in order to analyse them, an area corresponding to 208 units in the 'X' direction and 304 units in the 'Y' direction was scanned using stepping increments of (raster size) 100μm - that is an area of 20mm x 30mm rounded to a multiple of 16 (for binary processing). Care was taken in mounting each film so that the fringes lay parallel to the 'x' direction as closely as possible. Scanning in the 'Y' direction, successive scans were made (parallel to the fringes) and the data obtained was subsequently averaged in this direction, as will be described. The raster size which was employed was chosen because it enabled all the fringes to be scanned in the scan length (See Figure 5.4.2.)

(b) Computer Analysis

A range of different spatial frequency interference photographs had been scanned and this data was stored on magnetic tape. The data from each file was subsequently analysed, using an I.B.M.'370/165' main-frame computer.* Initially, a modified form of the algorithm for fast

---

*All programs were written in 'Fortran' for this work. (See Appendix 6)

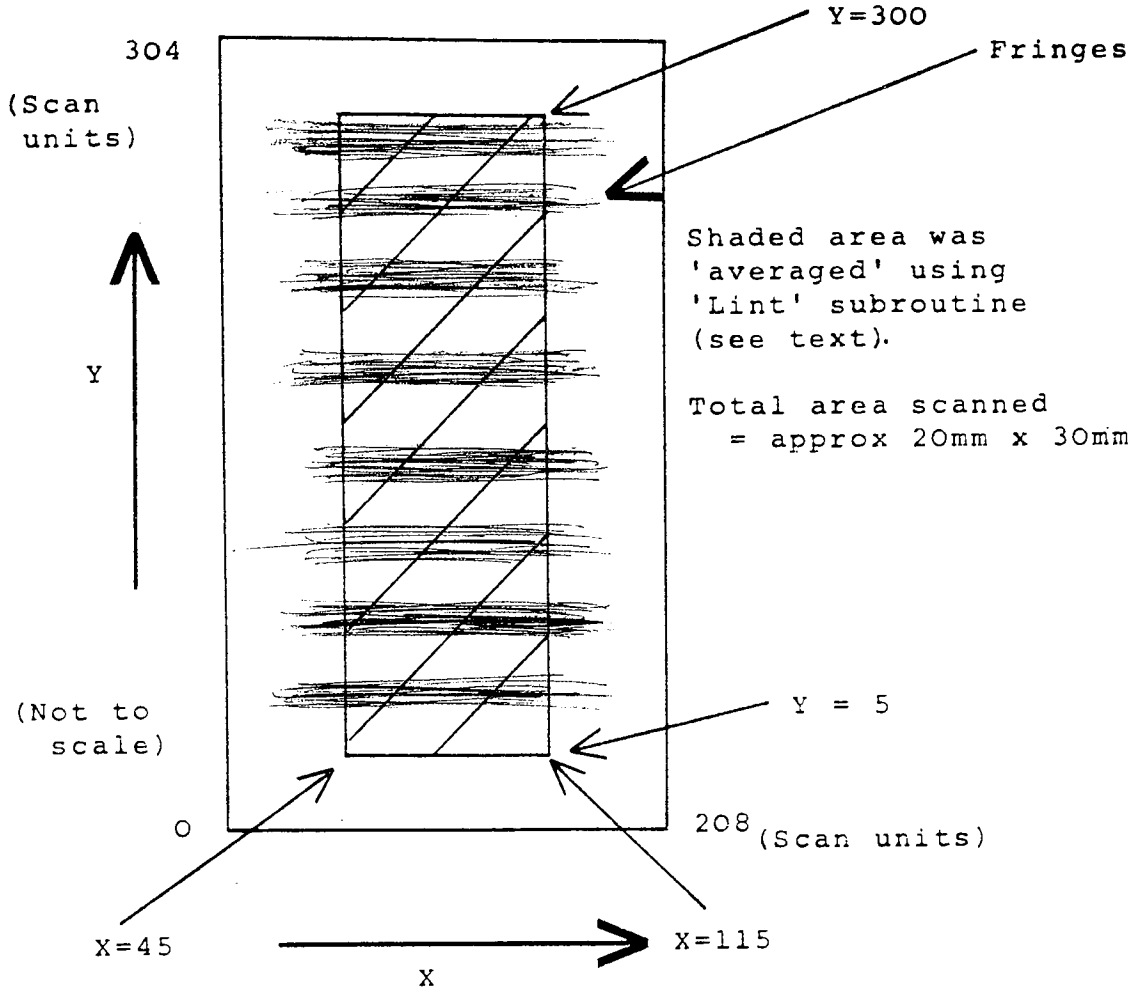

Fig.5.4.2. Area of Fringe Photograph Scanned.

digital analysis of interference fringes devised by Snyder[74] was tried but was not found to be satisfactory in this context. Consequently, the data for each fringe photograph was 'averaged' (in 'x' direction - as indicated on Fig.5.4.2.) using a subroutine based on a subroutine called 'Lint'. This subroutine employs deconvolution techniques based on a search Gaussian function. This search Gaussian is specified by a half-width at half-height and a tail cut-off which approximates the shape of the peaks which are to be located (the values employed are indicated on Figure 5.4.3.). Derivatives

of this Gaussian were used to calculate an overlap function with the intensity data at successive points. Then the resulting deconvolution function was inspected for evidence of peaks or troughs in the original optical density distribution.

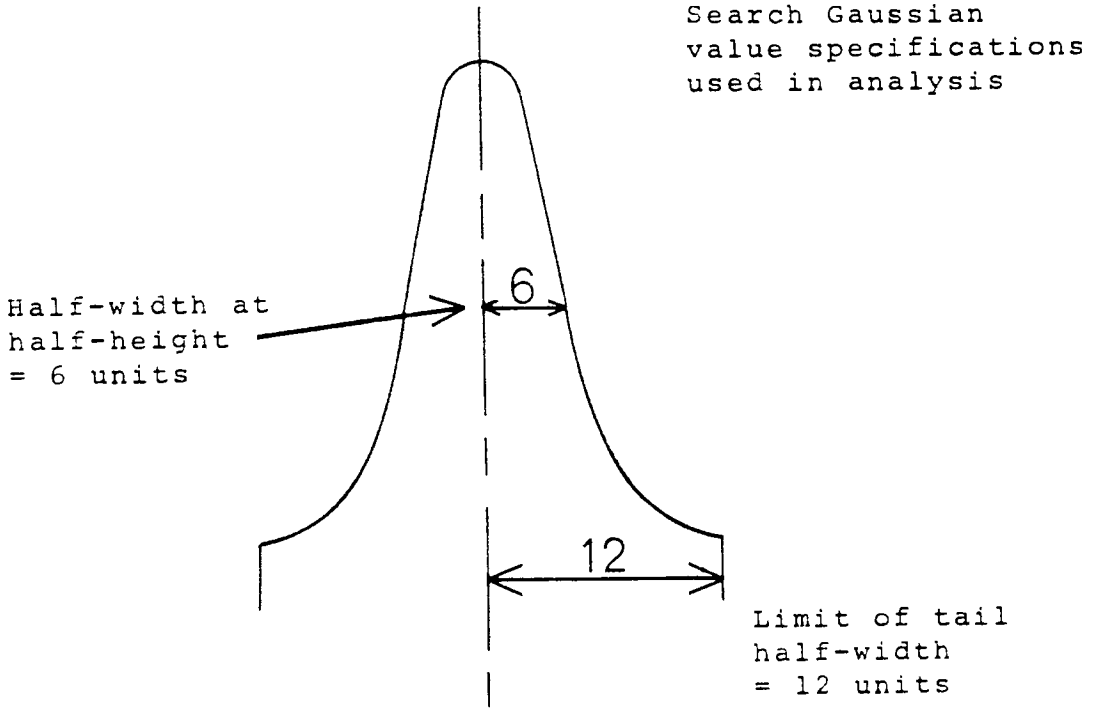

Fig.5.4.3. Search Gaussian Parameters.

The actual deconvolution of the linear profile of each fringe photograph obtained using the 'Lint' sub-routine was undertaken using a subroutine called 'Find'. (Both of these are part of the 'Gens' progam developed by Pickering et al.[75]). The deconvolution function employed* was a Gaussian 3rd derivative because this has

*Jansen and Brouwer: Analytical Chem, 45, pp.2239(1973).

the property that its product function with the profile passes from positive to negative as the Gaussian is moved along the profile and passes through a peak. It has an added advantage, over say a Gaussian 1st derivative, that sloping background, which can be approximated by a quadratic function, is removed and does not bias the peak positions. This produced an output, for each fringe photograph, which was a series of interpolated peak positions(see typical results in Section 5.5).

The weak peaks at either extreme of the pattern were discarded and then the mean and standard deviation for the distance between the peaks was evaluated- this then gave the mean interference fringe spacing in each case.

5.5. RESULTS OF FRINGE DATA ANALYSIS.

The data area that was 'averaged' in the x direction (See Figure 5.4.2, shown earlier) using subroutine 'Lint' produced a profile for each fringe photograph of 295 points perpendicular to the fringes, each point being the mean of 70 points (7mm) along the fringe direction. A typical graphical output (File 1,fringe photograph number 1) is given in Figure 5.5.1. As can be seen,this output trace confirms that this 'averaging' does resolve the interference fringes (see comments on this in Section 5.6.1.

As explained, interpolated peak positions were then

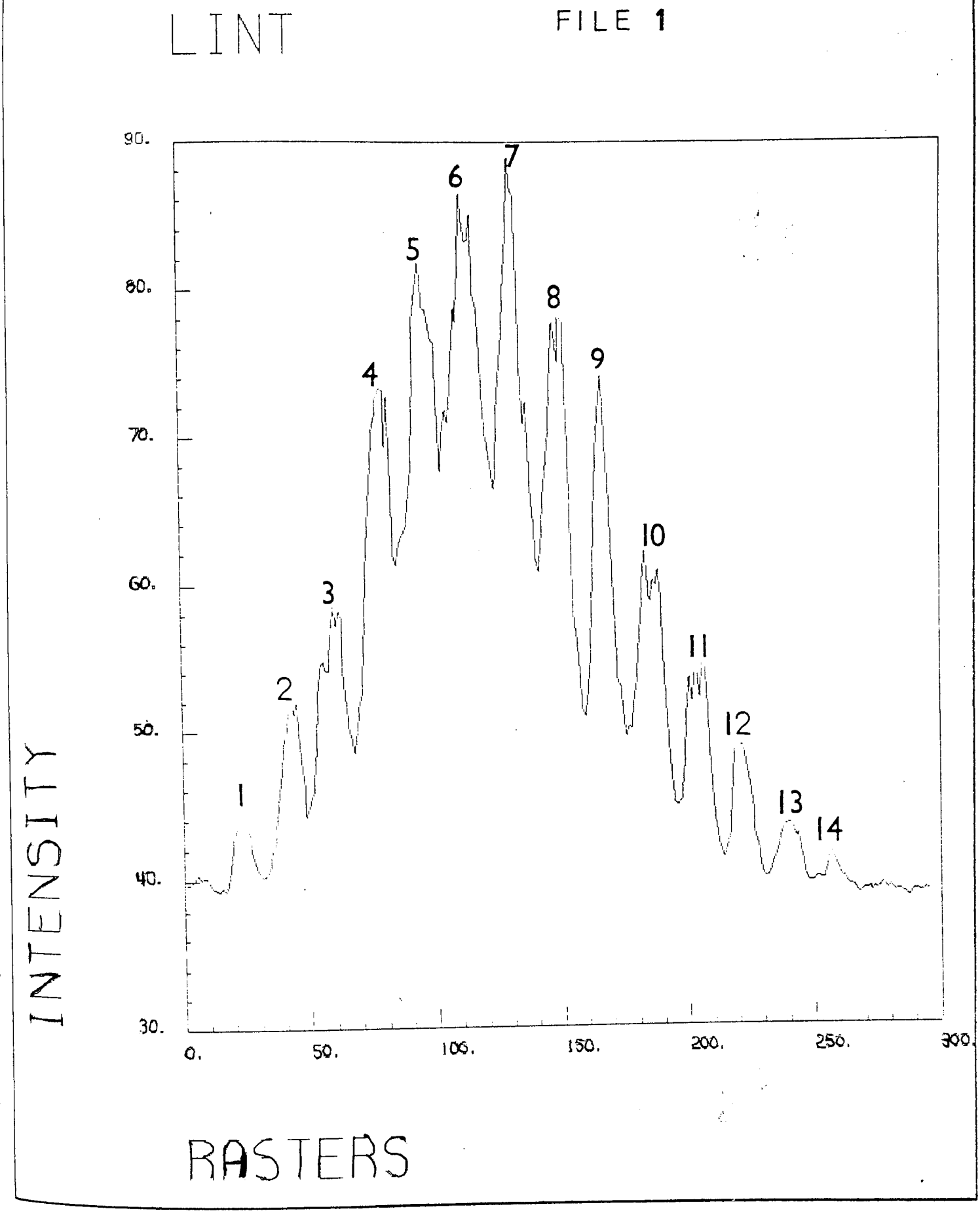

Fig.5.5.1. Graphical output (Fringe data analysis)

obtained using subroutine 'Find'. Table 3 gives typical interpolated peak positions (corresponding to Figure 5.5.1. i.e. File 1, fringe photograph number 1).

Peak No.	Position value	Peak No.	Position value
1.	2.27 mm	8.	14.93 mm
2.	4.23 "	9.	16.68 "
3.	5.92 "	10.	18.55 "
4.	7.81 "	11.	20.39 "
5.	9.58 "	12.	22.12 "
6.	11.32 "	13.	23,98 "
7.	13.11 "	14.	25.72 "

(Number of distinct peaks counted = 14.)

TABLE 3. Peak Position Values.

The mean value of the distance between each of the peaks (i.e. the mean of the 'position value' difference) and the standard deviation was calculated for each fringe photograph. As a check, and in order to discover any significant influence, the calculations were repeated using different Gaussian parameters (G.Ps). These were:

(i) Half-width at half-height = 5 units
Limit of tail half-width =10 units

(ii) Half width at half-height = 4 units
Limit of tail half-width = 6 units

Typical values for mean distance between peaks (i.e.

interference fringe spacing) for 5 different fringe spacing photographs (each one differing in spacing from the next by about 2%) are given in Table 4. The results obtained using the different Gaussian parameters that were employed are also given in this table.

File/photo -graph No.	G.P.(G.Param) = 6/12 Mean(mm)	Std Dev.	No.of reading	GP=5/10 Mean(mm)	GP=4/6 Mean(mm)
1	1.80	0.08	13	1.80	1.80
2	1.85	0.08	13	1.85	1.84
3	1.89	0.08	12	1.89	1.87
4	1.95	0.07	13	1.95	1.95
5	1.99	0.08	11	1.99	2.00

TABLE 4. Fringe Spacing Results.

As can be seen from the results obtained summarized in Table 4, the mean fringe spacings of the 5 different fringe photographs were 1.80mm, 1.85mm, 1.89mm, 1.95mm and 1.99mm respectively (using a Gaussian parameter of 6/12). These values are all with a standard deviation of about 0.08mm (i.e. a maximum error of about ±4% overall). The mean spacing values obtained using different Gaussian parameters, were, as can be seen from the table, only slighlty different in each case. Object surface displacements corresponding to these different fringe spacings were calculated, as before, and were comparable to the values obtained for the same doubly exposed specklegrams (such as the results calculated in

Section 3.9) described in Chapter 3.

5.6. CONCLUSIONS

This detailed investigation confirmed that a computer controlled microdensitometer could be employed to analyse interference fringe photographs of fringes generated from doubly-exposed specklegrams. It also showed that the digital output data could be processed such that the fringe spacing was obtained. In addition, this study demonstrated that computer subroutines can be devised for both the controlling of the microdensitometer scanning and recording as well as for comprehensive analysis of the fringe data - such that the whole process is automatic and very rapid.

The use of fringe photographs recorded with film larger than the 35mm film employed in this investigation could help to improve the overall accuracy of the fringe spacing measurement. Similarly, averaging over more than the 70 units along the fringe direction that was employed in this analysis could further enhance the accuracy of the measurement. However,this would take longer and produce much more data to be processed. It should be pointed out that averaging less than 70 units was also undertaken but this was found to yield proportionately lower accuracy results. Moreover, when a fine scanner resolution (<25μm) was employed, this was found

to make the fringe profiles more uneven in the Y direction and thus less satisfactory for analysis.

Although modified subroutines based on those devised by Pickering et al.[75] were found to be more suitable and practicable than that devised by Snyder[74] it is suggested that the latter could be used in some cases to good effect (e.g. for analysis of digitized data of fringes obtained from linear photodiode arrays - as described in the previous chapter). Further research could be undertaken to explore the effectiveness of different convolution functions in improving the accuracy of the fringe analysis. Nevertheless,it is considered that the odd order Gaussian derivative which was employed was well chosen since it reduces peak positioning to linear interpolation and corrects for sloping background (which was present in the fringe photographs). Even though the peaks (shown in Figure 5.5.1) are not Gaussian in profile the deconvolution function must be relatively blunt -since a sharp function would produce false peaks, because of the uneveness of the profiles obtained from fringe photographs in this context.

It may be possible to reduce the effects of speckle 'noise' by incorporating an adaptive filter in the processing routine.(The Snyder[74] subroutine contains a filter process that could be modified for particular purposes). Maddux et al.[78] have reported a fringe analysis system (not using a microdensitometer) that has

a 'software' filter which could be adapted for use with other systems.

The employment of a microsdensitometer for measuring the spacing of interference fringes from photographs has not been considered to be practicable by some investigators concerned with the analysis of fringes generated by doubly-exposed specklegrams. For instance, Luxmore et al.[61] have suggested :

> "....The most precise method of measurement used microdensitometer traces taken from photographs of the fringes, but this method was very tedious, a disadvantage that was considered to outweigh the advantage of greater accuracy".

It is suggested that this investigation has demonstrated that the use of a microcomputer control system (with appropriate command software) and computer-assisted analysis of the digitized output data means that the use of a microdensitometer is practicable and is not tedious. Furthermore, processing of fringe data can be carried out so rapidly that extremely detailed analysis of fringe photographs can be conveniently undertaken, although the cost of such a system is presently quite high.

CHAPTER 6

MOIRÉ PATTERN FRINGE MEASUREMENT SYSTEM

CHAPTER 6.

6.1. INTRODUCTION

The 'moiré fringe' effect between two transparent overlapping grids or gratings was first employed scientifically over a hundred years ago[79]. Since then, as Sayce[80] reports, the effect has been widely examined and various techniques have been devised for using the effect (e.g.in metrology). Nevertheless, the employment of the moiré fringe effect, using a reference grid, for determining the spatial frequency of fringes generated in speckle photography has not been reported. As an outcome of the preliminary investigations outlined in Chapter 3, it was considered that a system could be developed for this purpose. The system which was subsequently devised (Pickthorne and Rogers[81]) was found to be simple to use, provided very good sensitivity and was quite adaptable. Moreover, this system is much less complex or costly than either of the fringe measurement systems described in the preceding chapters.

6.2. BASIC THEORY OF MOIRÉ FRINGES.

When two grids (consisting of alternate transparent and opaque elements, of approximately equal spacing) are placed face to face with the elements of one grid at

a small angle to those of the other grid, no light is transmitted where the opaque parts of one grid fall on the transparent parts of the other grid. Consequently, when viewed against bright background illumination, a series of dark fringes crossing the grids is seen. These fringes are known as 'moiré fringes' and were given this name by French silk weavers who originally observed the effect with two overlapping layers of fine fabric. As Yokozeki[82] points out, moiré fringes may be divided into two types - coherent and incoherent. It is the former type which is of chief concern here.

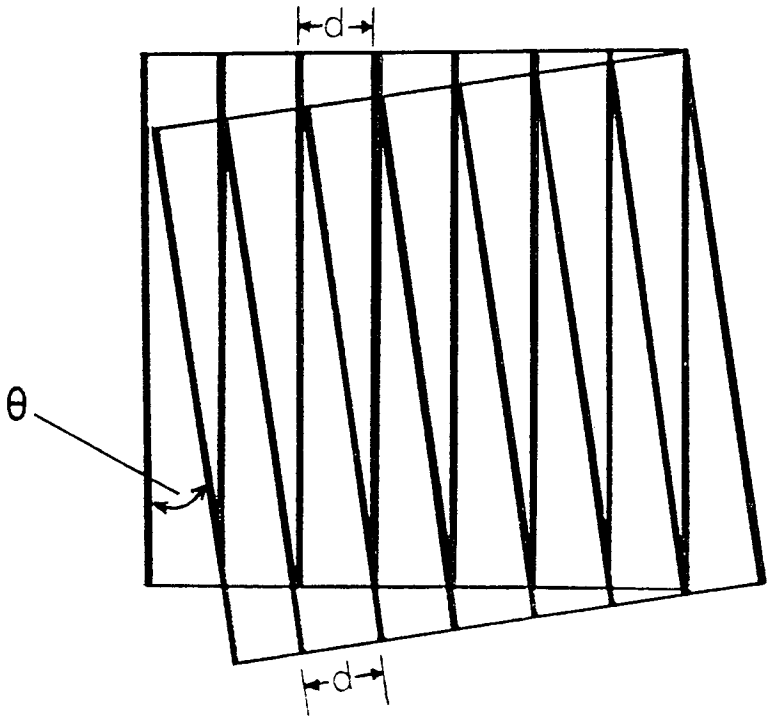

Fig.6.2.1. The Formation of Moiré Fringes.

Guild[83] has developed the work of earlier investigators concerning the moiré effect and has established

that moiré patterns are fundamentally diffractive effects. It can be seen from Figure 6.2.1. that, for grids having elements of spacing 'd' and lying at an angle θ to each other (θ assumed small), a set of moiré fringes is produced having a spacing S such that :

$$S = d/\theta \qquad \ldots\ldots\ldots\ldots\ldots\ldots \quad (6.2.1)$$

If one grid is kept stationary and the other grid is moved in the direction perpendicular to its elements, then it is observed that the moiré fringes move in the direction perpendicular to the fringes themselves. One moiré fringe will cross a point in the field of view as the grid advances a distance 'd'.

6.3. THEORY OF MOIRÉ PATTERN CALCULATIONS.

A simple method of calculating moiré patterns has been suggested by Rogers[84] who points out :

> "By the use of Ewald's reciprocal space* any particular problem in moiré production may be solved. In the case of gratings lying in parallel planes, the reciprocal space may be condensed into a reciprocal plane and the moiré patterns developed as difference vectors in this reciprocal plane".

This basic geometrical approach to moiré pattern calculations has been subsequently developed by Rogers.[85] To calculate the moiré pattern due to two linear grids, the construction involves drawing two lines from an

---

*Ewald,P.P.Phys.Z., 14, 465 (1913).

origin such that each is perpendicular to its corresponding grid and is of a length which is inversely proportional to the grid spacing.* When the triangle (or parallelogram) is completed, a difference vector and a sum vector are obtained. These vectors represent the spatial frequencies of the moiré patterns such that their directions are perpendicular to the moiré fringes and their lengths inversely proportional to the spacing of the fringes.

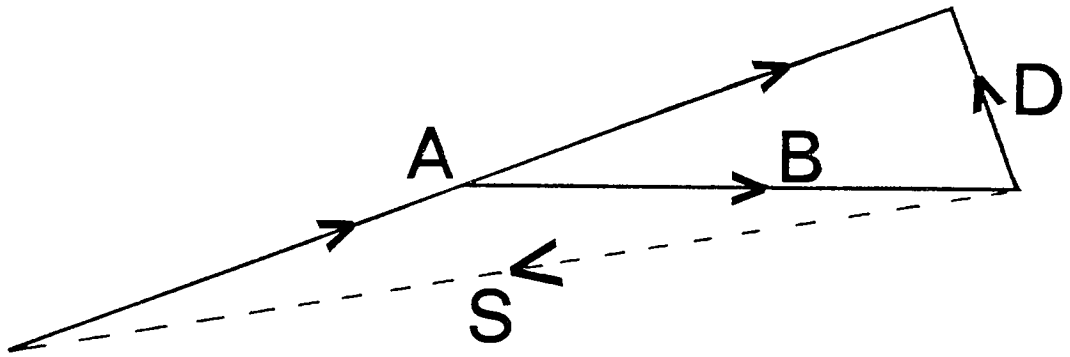

Fig.6.3.1. Moire fringe representation in frequency space.

In Figure 6.3.1, '$\underset{\sim}{A}$' and '$\underset{\sim}{B}$' represent spatial frequency vectors and, by extending vector '$\underset{\sim}{A}$' symmetrically about the origin, the sum vector '$\underset{\sim}{S}$' is displayed as the closing side of the triangle. The case illustrated

*i.e. directly proportional to the spatial frequency of the corresponding grid.

refers to linear grids with a plane, parallel monochromatic wave incident normally onto them. In this case, spectra arise in angular directions which correspond to the spatial frequency vectors. As the spectra are coherent with the original wave they are coherent with each other. Thus they can interfere, producing Young's interference fringes equivalent to the moiré fringes.

6.4. PRINCIPLES OF THE MOIRÉ PATTERN TECHNIQUE DEVISED FOR FRINGE MEASUREMENT.

As outlined earlier, when two grids, having nearly the same spatial frequency, are lying at a small angle to one another, they produce a low frequency moiré pattern. This pattern is a very sensitive function of the intergrid angle and of small variations in the frequency ratio of the grids. The same situation applies if one of the grids is replaced by a fringe pattern, such as the projected fringe pattern generated from a doubly-exposed specklegram.

The basis of the technique devised for fringe measurement is that a moiré pattern is generated between a reference (master) grid and the fringe pattern such that the orientation of the moiré pattern is related to the spacing of the fringe pattern. This means that the fringe spacing measurements can then be made in angular terms. As Pickthorne and Rogers[81] point out, this may be undertaken quite easily and the angles

measured with high accuracy.

This technique was developed from the geometrical approach to moiré pattern calculations suggested by Rogers[85] which was described in the previous section. In this case, it is the fringe pattern and reference grid which are each represented in spatial frequency space by a vector perpendicular to the original fringes (or grid lines) and of length inversely proportional to the fringe (or grid) spacing. This case is illustrated in Figure 6.4.1, where the vector '$\underset{\sim}{OA}$' represents the reference grid and vector '$\underset{\sim}{OB}$' represents the fringe pattern. The latter is lying at an angle 2β to the reference grid and the closing vector '$\underset{\sim}{BA}$' (which represents the moiré pattern in frequency and direction) lies at an angle α to the reference grid. By measuring the angles α and 2β, the ratio R, of OB to OA, can thus be found since, $\frac{OB}{\sin\alpha} = \frac{OA}{\sin(\alpha + 2\beta)}$

Then, as OA(which depends on the reference grid) is known, the spacing of the interference fringes is readily calculated as will be shown.

Angle α is relatively easy to measure but angle 2β is not so easy because it requires alignment of the interference fringes (which may be indistinct) along a fixed direction at the prescribed angle from the reference grid. However, by undertaking a <u>symmetrical</u> pair of measurements, a result can be obtained which is very

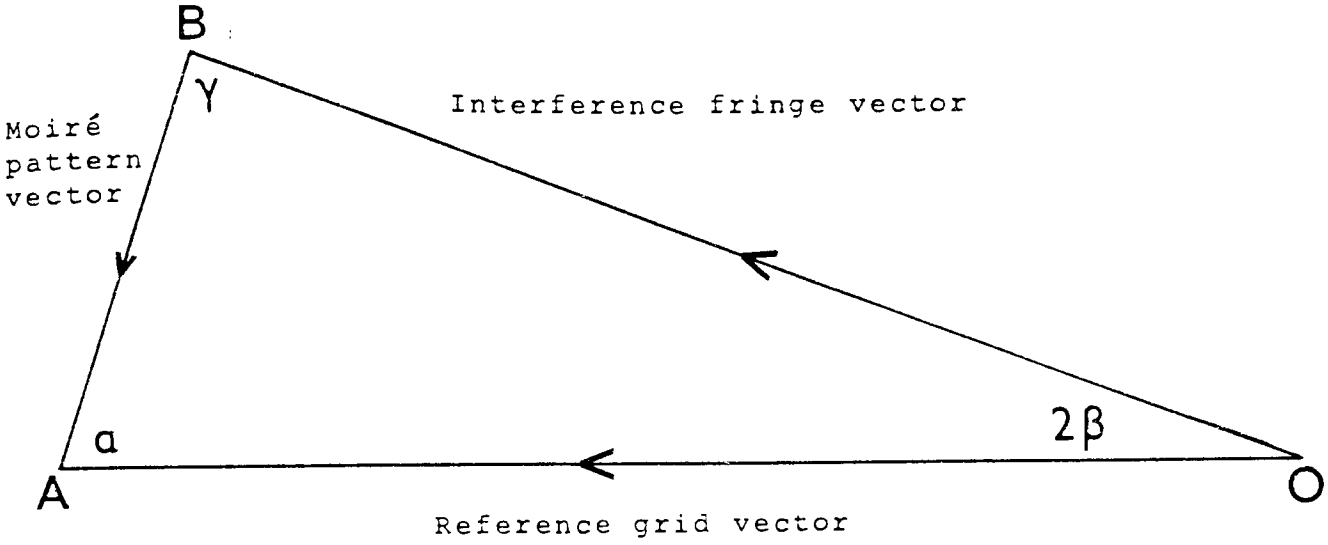

Fig.6.4.1. General case: moiré pattern representation.

insensitive to a small angular mismatch between the interference fringes and the reference grid.

Considerations of symmetry suggest that, as far as possible, the reference grid should be swung from a position to one side of the interference fringes, say by an angle '2β' and then to an equal angle '2β' on the other side. Small departures from symmetry will then have only a very small effect on the accuracy of the results (as will be shown), provided that the total angle (4β) is accurately known and is not large. This may be done by aligning the interference fringes (approximately only) along a fixed direction (e.g.vertical) and then swinging

the reference grid (between stops) by an angle +2β to the left of the interference fringes and then by an angle -2β to the right.

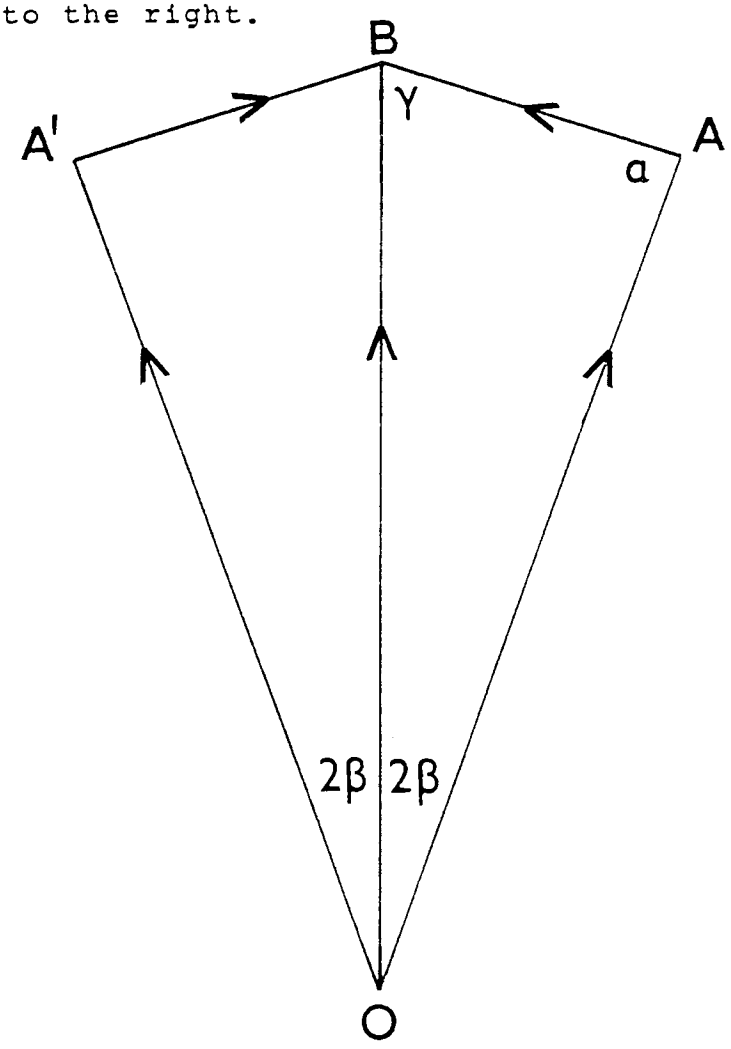

Fig.6.4.2. Symmetrical Technique.

In Figure 6.4.2 vector $\underset{\sim}{OB}$ represents the spatial frequency of the interference fringes (which are kept fixed in space). Vector $\underset{\sim}{OA}$ represents the initial position of the spatial frequency vector that represents the reference grid in its first position and $\underset{\sim}{BA}$ represents the moiré pattern spatial frequency. When the reference grid is swung into the symmetrical position it ends up

in the position that is represented by $\underset{\sim}{OA'}$ and then the moiré pattern goes over to $\underset{\sim}{BA'}$, as indicated.

Although all spatial frequency vectors are perpendicular to the grid lines generating them, by rotating the figure they may be regarded as parallel. As can be seen in Figure 6.4.2, the spatial frequency vector $\underset{\sim}{OB}$ is greater than $\underset{\sim}{OA}$ and , consequently, the moiré pattern rotates in a direction that is <u>opposite</u> to the rotation of the reference grid. However, if the rotation of the moiré pattern is in the same direction as the reference grid, this implies that $\underset{\sim}{OB}$ is <u>less</u> than $\underset{\sim}{OA}$. Thus it is necessary to note the direction of rotation when carrying out readings.

Since, in the symmetrical technique the <u>total</u> angles AOA'(4β) and ABA'(2γ) are recorded, then by halving these angles, this means that average values are obtained that are superior to those obtained using the direct measurement technique which was originally devised.

The triangle AOB is easily solved because :

$$OA/\sin\gamma = OB/\sin\alpha$$

If R is the ratio of the spatial frequencies OB and OA then, since $OB/OA = \sin\alpha/\sin\gamma$

$$\therefore R = \frac{\sin(\gamma+2\beta)}{\sin\gamma}$$

By expanding $\sin(\gamma+2\beta)$ and dividing through then :

$$R = \cos 2\beta + \cot\gamma . \sin 2\beta \quad \ldots\ldots\ldots\ldots\ldots\ldots \quad (6.4.1.)$$

As the angle 2β is a constant (fixed at a set value) therefore cos 2β and sin 2β are constants and thus R is simple to calculate.

If the moiré fringes rotate in the same sense as the reference grid cot γ is negative ($R<1$) and if they rotate in the opposite sense cot γ is positive ($R>1$). Since R is the ratio of the spatial frequencies and the actual spatial frequency vectors have lengths which are inversely proportional to the spacing of the grid or fringes, then $1/R$ is the ratio of the spacings. As $\overset{\frown}{OA}$ is already known (from the spacing of the reference grid) then the spacing of the interference fringes is easily determined.

6.5. EXPERIMENTAL INVESTIGATIONS

(A) Basic System.

Experiments were first undertaken using a system based upon the general, basic moiré fringe technique which had been intially developed (i.e. before the symmetrical technique had been devised). The system that was subsequently constructed consisted of a rigid metal plate 'P' with a large circular hole cut in it. This hole hada recessed rim on one side and a circular metal plate 'C', which had a lip that fitted against this rim, was mounted in the hole. Special clips held this circular plate in position but allowed it to be rotated within the main plate, as indicated in Figure 6.5.1. As can be seen the circular plate had a hole

cut in it (shown dotted) and the main plate was fitted with a support arm (so that it could be mounted on an optical bench. All the components were machined to a high tolerance to provide smooth movement without slipping or variations.

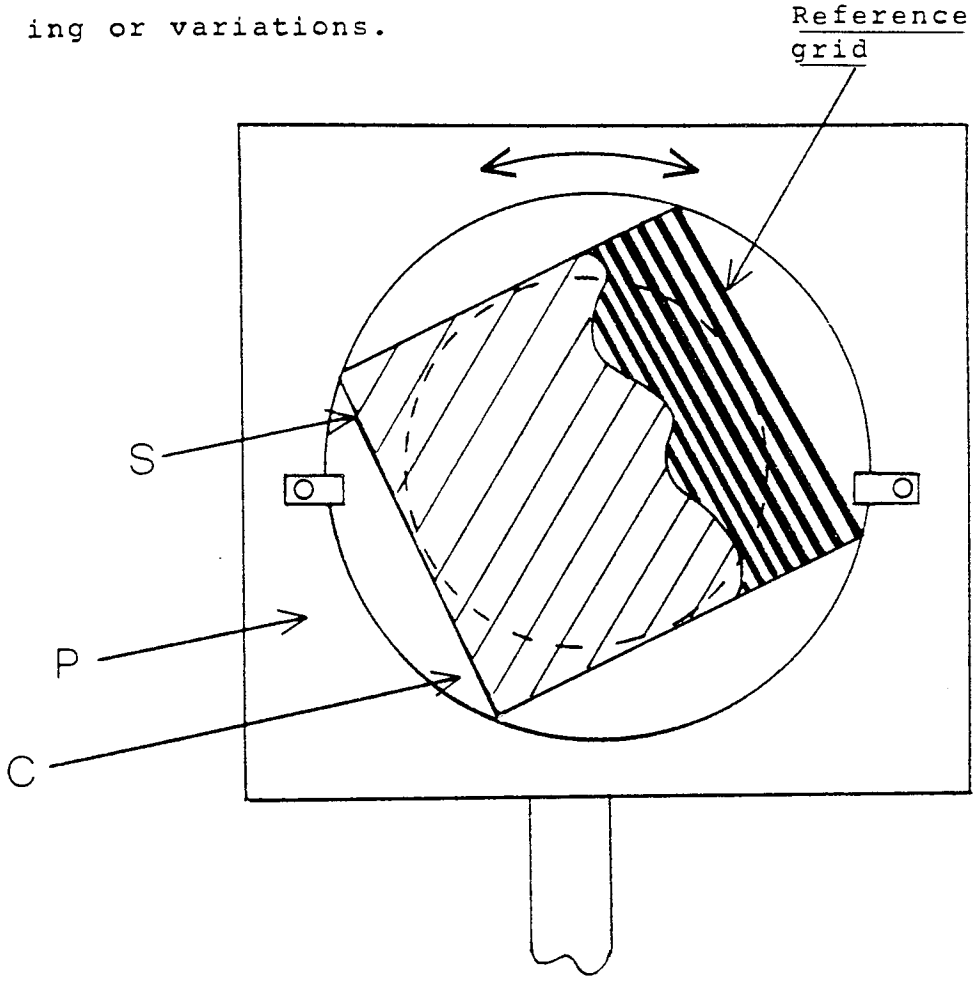

Fig.6.5.1. Part of the basic moiré fringe apparatus.

On one side of the circular plate, a square of acetate diffusing sheet 'S' (which acted as a screen) was attached. Next to this, on the outer face, a reference (master) grid was mounted. A transparent cursor was fitted to the main plate, as shown in Figure 6.5.2.

Interference fringes generated from a doubly-exposed

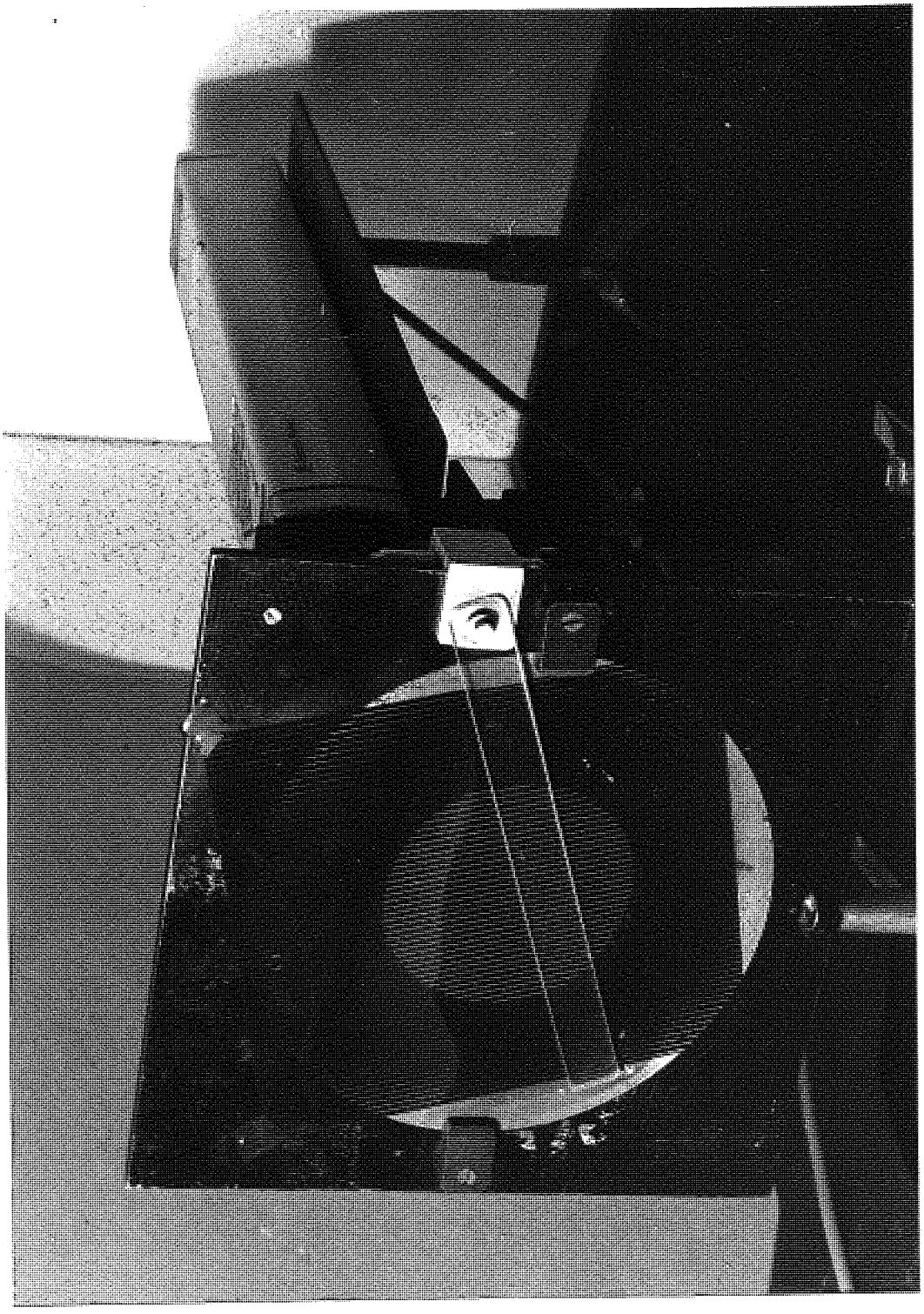

Fig.6.5.2. Basic moiré fringe system

specklegram, which was interrogated by an unexpanded laser beam (1mW), were projected onto the screen 'S'.(On the side furthest away from the reference grid and cursor). In order to match approximately the reference grid spacing the 'throw'of the projected fringes (i.e. the distance 'D' between the specklegram and the screen) was ajusted with the reference grid removed and the fringes viewed on the screen. To simplify the setting of the prescribed angle between the interference fringes and the reference grid the fringes were aligned with respect to a reference line on the main plate P and the reference grid was set at the required angle with this line. The only other angle then measured was between the moiré pattern and the grid. These angles were measured by the use of the cursor and a protractor (which was positioned on a reference line on the main plate). As a check, each reading was repeated with the reference grid moved through the corresponding angle in the opposite direction.

The alignment of the cursor with the moiré pattern was carried out with the background illumination lowered (to improve the visability of the moiré pattern) but when readings were taken on the protractor, a white light was directed onto this. Both the specklegram, which was fitted in a rigid holder, and the moiré fringe device were mounted on an optical bench so that the throw D could be precisely measured. Precautions were taken in

aligning the system to ensure that the projected interference fringes were incident normally on the screen.

Results were obtained using a variety of doubly-exposed specklegrams that had been recorded using a range of different lateral surface displacements. The image demagnification of each of these specklegrams had been previously measured to a high degree of accuracy using a travelling microscope. (This information was required so that the fringe spacing results, subsequently obtained, could be used to calculate the corresponding magnitude of the recorded surface displacements). In each case the specklegram was interrogated on a point by point basis on a 'grid' type format and the mean fringe spacing was calculated from the readings obtained.

(B) Symmetrical System.

As indicated in the previous section, a symmetrical technique for interference fringe measurement using moiré fringes was developed in order to improve the overall accuracy of measurement. This technique requires the reference grid to be swung, by equal angles, first to one side and then to the opposite side of the projected interference fringes. The system that was devised for this purpose is shown, simplified in Figure 6.5.3.

This system was made up of a thick rigid plate which was mounted on a strong metal arm that could be

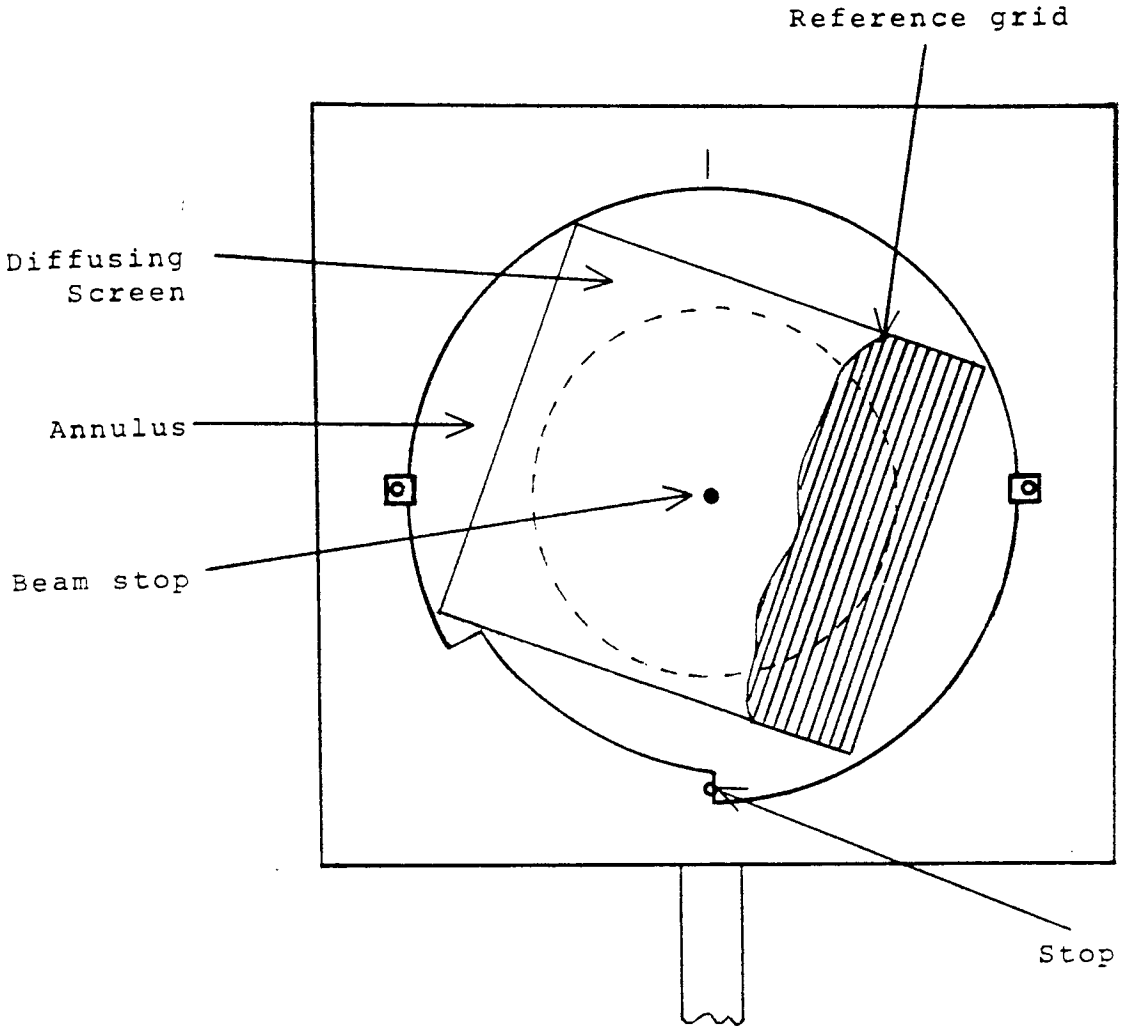

Fig.6.5.3. Part of the symmetrical moiré fringe system.

fitted into a holder on an optical bench (or held in a clamp unit). The plate had a large circular hole in its centre and shallow grooves were precision cut on either side of this hole. An annulus was made to fit into the groove on one side and this was held in position by two small clips. A slot was cut in the outer edge of the annulus and this was aligned with a stop on the main plate such that the annulus could be rotated by 20° either side of the vertical. (The choice of this angle will be discussed later). On the annulus a reference grid of known spatial frequency was mounted as

shown in Figure 6.5.4.

Both the main plate and the annulus were made from a material ('Tufnol') which has a low thermal expansivity and high resistance to oxidization so that accuracy would be maintained in different working environments and over a long period of use. A number of annuli were made to the same specifications so that these could be fitted with reference grids, covering a range of different spatial frequencies and rapidly interchanged as needed.

Directly behind the reference grid a thin glass diffusing screen was fixed to the main plate. Interference fringes produced by interrogating a doubly-exposed specklegram with an unexpanded laser beam (1mW) were imaged on this screen. The latter had a small black stop at its centre to remove the central undiffracted laser beam. Both the moiré fringe system and the specklegram (which was fitted into a special holder) was mounted on an optical bench. The throw 'D' of the projected fringe pattern was adjusted so that the fringe spacing roughly matched that of the available reference grid. This distance 'D' was then accurately measured on the optical bench.

The groove that was cut in the rim of the hole on the other side of the plate (furthest away from the specklegram) carried a circular protractor which was retained by spring clips. This could be rotated in the

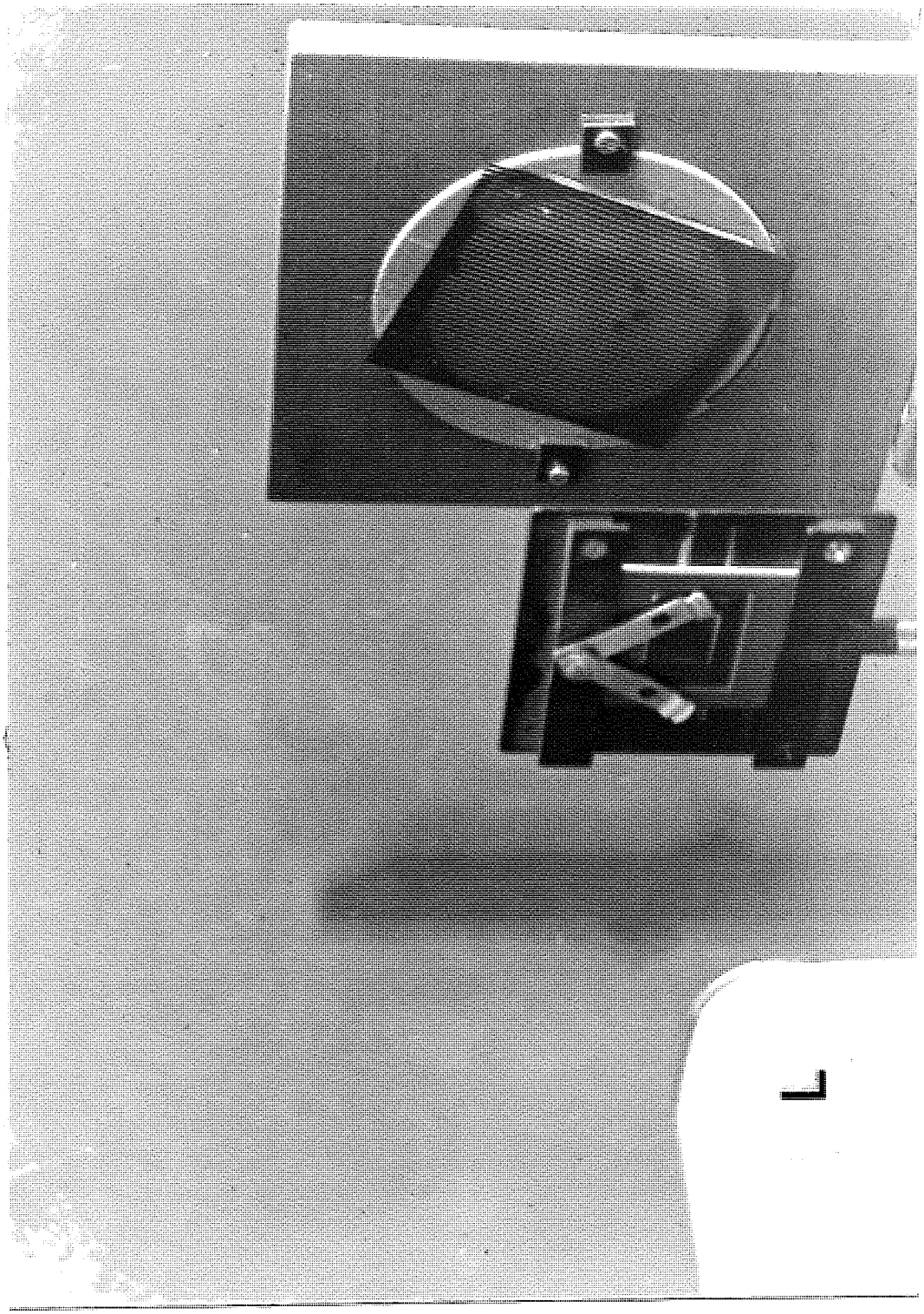

Fig.6.5.4. Symmetrical moire fringe system showing reference grid on annulus. (In practice the specklegram is close to the laser 'L').

vertical plane and had a transparent bar across its centre, as shown in Figure.6.5.5. The bar was aligned with the moiré pattern and the angle read off against a vertical reference on the main plate. A second reading was taken when the reference grid had been moved to the symmetrical position on the opposite side of the vertical. The direction in which the moiré pattern rotated when the reference grid was moved was also noted.

Further readings were taken for each specklegram (which were all analysed on a point by point'grid' basis) and the mean value of these readings was used in the calculation of the interference fringe spacing. As when the basic moiré system was used the background illumination was kept relatively low while the bar was being aligned with the moiré pattern and then a lamp was directed onto the scale to assist the reading of the angle. For comparison purposes, a laser of higher power (8mW) was later used to interrogate the specklegrams (it was found that the background illumination did not require to be significantly lowered in this case).

Measurements were taken using the symmetrical system of a number of doubly-exposed specklegrams (of known object demagnification ratio) which were recorded for a range of lateral surface displacements. In addition, to assess the sensitivity of the system, a typical specklegram was interrogated with a glass block placed between the specklegram and the screen. It was then

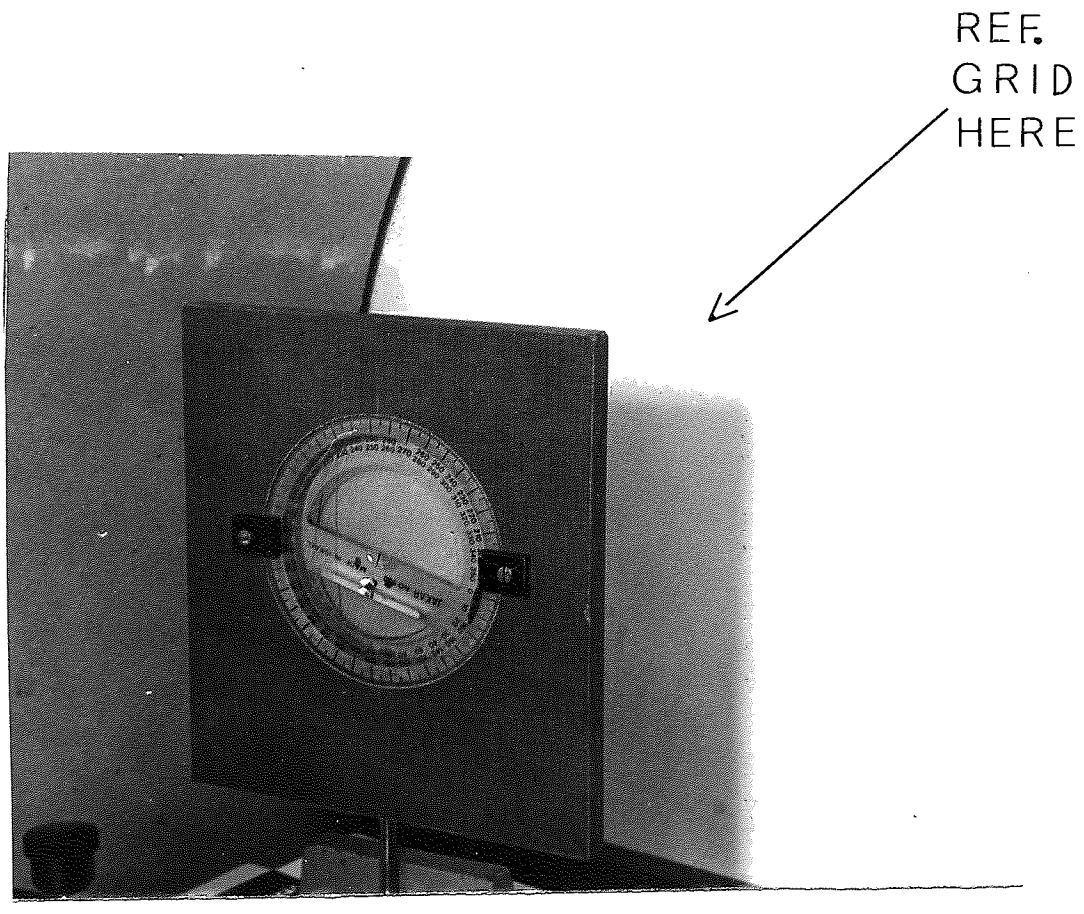

Fig.6.5.5. Part of front of symmetrical moiré fringe system. (Showing protractor and transparent bar)

interrogated with the glass block removed (so that the 'throw' and hence the interference fringe spacing was changed by a small amount). Symmetrical readings were recorded in each case along with the thickness and refractive index of the glass block. Since all other conditions were kept constant in each case the fringe spacing results could thus be compared along with the ratio of the two throws used.

6.6. RESULTS OF EXPERIMENTAL INVESTIGATIONS.

(A) Basic system.

The following typical results, which were obtained with the basic system, are for reference grid and moiré pattern angles measured with a simple cursor and protractor as shown earlier. This enabled angular readings ($\pm 1^{o}$) to be taken quite easily but with this system errors could occur, as explained, in the alignment of the interference fringes along a fixed direction at the prescribed angle from the reference grid. Using the nomenclature given in Figure 6.4.1, the mean values obtained for a typical doubly-exposed specklegram (which was recorded for a lateral surface displacement of 0.150mm measured with a sensitive dial gauge) were as follows :

Results

Angle $\alpha = 70^{\circ} \pm 1^{\circ}$

Angle $2\beta = 20^{\circ} \pm 1^{\circ}$

Throw D = 225mm + 1mm.

Spatial frequency of the reference grid used was: 0.5 cycles mm^{-1}.(i.e. 2.0mm spacing). The moiré pattern rotated in the same sense as the reference grid.(i.e. R, the ratio of the spatial frequencies, is less than 1).

Referring to Figure 6.4.1. (Section 6.4) it was shown that :

$$\frac{OB}{\sin\alpha} = \frac{OA}{\sin(\alpha+2\beta)}$$

and $R = OB/OA$

$$\therefore \quad R = \frac{\sin\alpha}{\sin(\alpha+2\beta)} = 0.9397$$

However, R is the ratio of the spatial frequencies. Thus 1/R is the ratio of the spacings = 1.064. Now, the reference grid spacing = 2.0mm. Hence the interference fringe spacing = (2.0 x 1.064)mm

= 2.128mm.

[Using this result and the measured value of the throw D given above, along with the known speckle-gram demagnification ratio, the calculated surface displacement was found to be 0.150mm, compared to the measured value of 0.150mm.]

Figure 6.6.1 shows typical fringes with the cursor set along the moiré fringe angle. This was recorded with

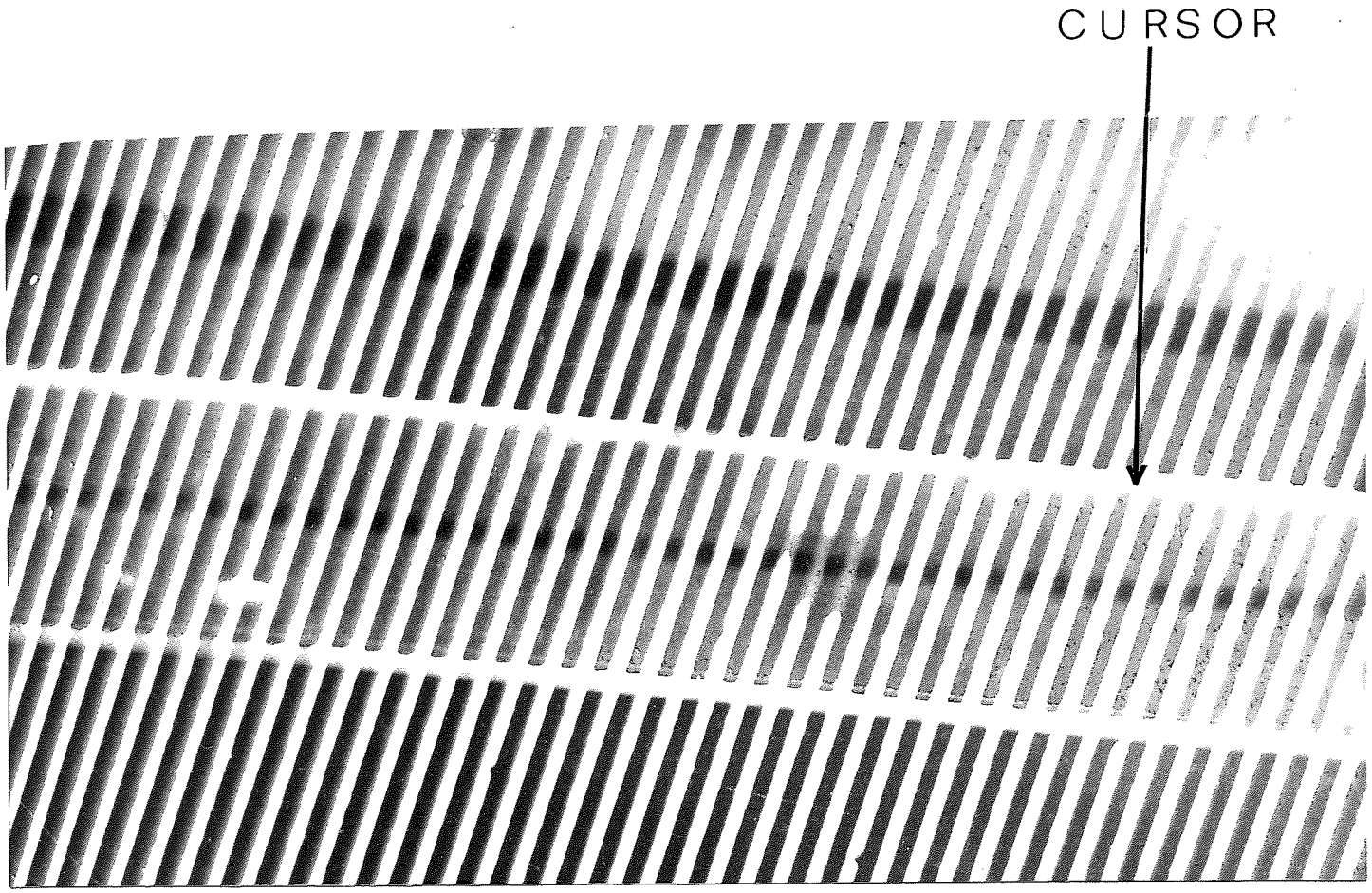

Fig.6.6.1. Moiré fringes : basic system

a 35mm S.L.R. camera using an exposure of 4 seconds with an aperture of f/2.8. It was found that Ilford Pan F developed in 'Phenisol' (1:4 dilution) at 20° for five minutes produced superior photographic negatives. The photograph shown was printed on Number 1 bromide paper using a 150mm enlarger lens and Kodak Universal developer (1:7 dilution) at 20°C. A 50mm enlarger lens was tried but, because it produced quite high magnification, the moiré fringes could not easily be discerned on the photographs

(B) Symmetrical system.

With the system which was devised, the angle 2β was fixed (at 20° either side of the vertical) and the only angle which it was necessary to measure was the angle γ (shown earlier in Figure 6.4.2). As explained in Section 6.4, the total angles (i.e. 4β and 2γ) were actually recorded in order to reduce the effects of errors in measuring these. The angles could be read to ±0.5° using the system that was constructed and the only other information which it was necessary to record was the direction in which the moiré pattern rotated with respect to the rotation of the reference grid.

The results which follow are representative of a large number of experimental investigations that were undertaken using this symmetrical system. In this case, the results were obtained using an 8mW output power laser

rather than a 1mW laser(so that the moiré patterns could subsequently be photographed* more satisfactorily). These results are mean values obtained from the analysis of a doubly-exposed specklegram recorded for a known surface displacement (and of a known demagnification ratio). The reference grid which was employed in this analysis had a spacing of 2.00mm.

Angle $2\beta = 20^{\circ} \pm 0.5^{\circ}$
Angle $2\gamma = 128^{\circ} \pm 0.5^{\circ}$
Hence, angle $\gamma = 64^{\circ} \pm 0.25^{\circ}$
The moiré fringes rotated in the same sense as the reference grid (thus R<1).

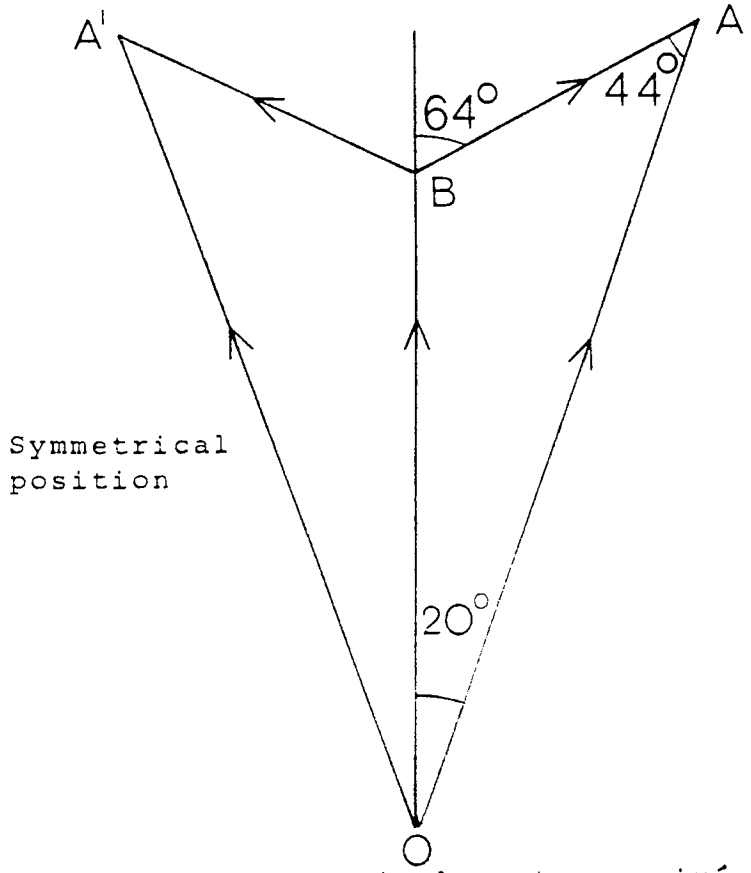

Fig.6.6.2. Symmetrical system: moiré pattern analysis.

*For the purpose of illustration not measurement.

Solving the triangle shown in Figure 6.6.2 gives:

$$R = \frac{\text{Sin}44^\circ}{\text{Sin}64^\circ} = 0.773 \text{ (ratio of spatial frequencies)}$$

$\therefore$ the ratio of the spacings $1/R = 1.294$

Thus 1.294 x reference grid spacing gives the spacing of the interference fringes = 2.588mm.
This value differs from the result calculated (using the known surface displacement, throw and demagnification) which was 2.564mm, by less than 1%.

Figure 6.6.3 is an enlarged photograph of the fringe pattern showing part of the transparent bar of the protractor aligned with the moiré fringes. The fringes with the reference grid moved over to the symmetrical position are shown in Figure 6.6.4.

To examine the sensitivity of the system, as explained earlier, a glass block was introduced between the same specklegram and screen (with all else kept constant) in order to produce a small change in the interference fringe spacing. This only produced a change in the spacing of 7% but the change in angle that resulted in this case, which was 8.25°, was easily observed. The results obtained for this experiment (see Appendix 7 for fuller details) clearly indicate that an overall accuracy of about ±1% can quite readily be achieved (i.e. in the context of the fringes generated by doubly-exposed specklegrams and their use in calculating lateral displacement)with the symmetrical system.

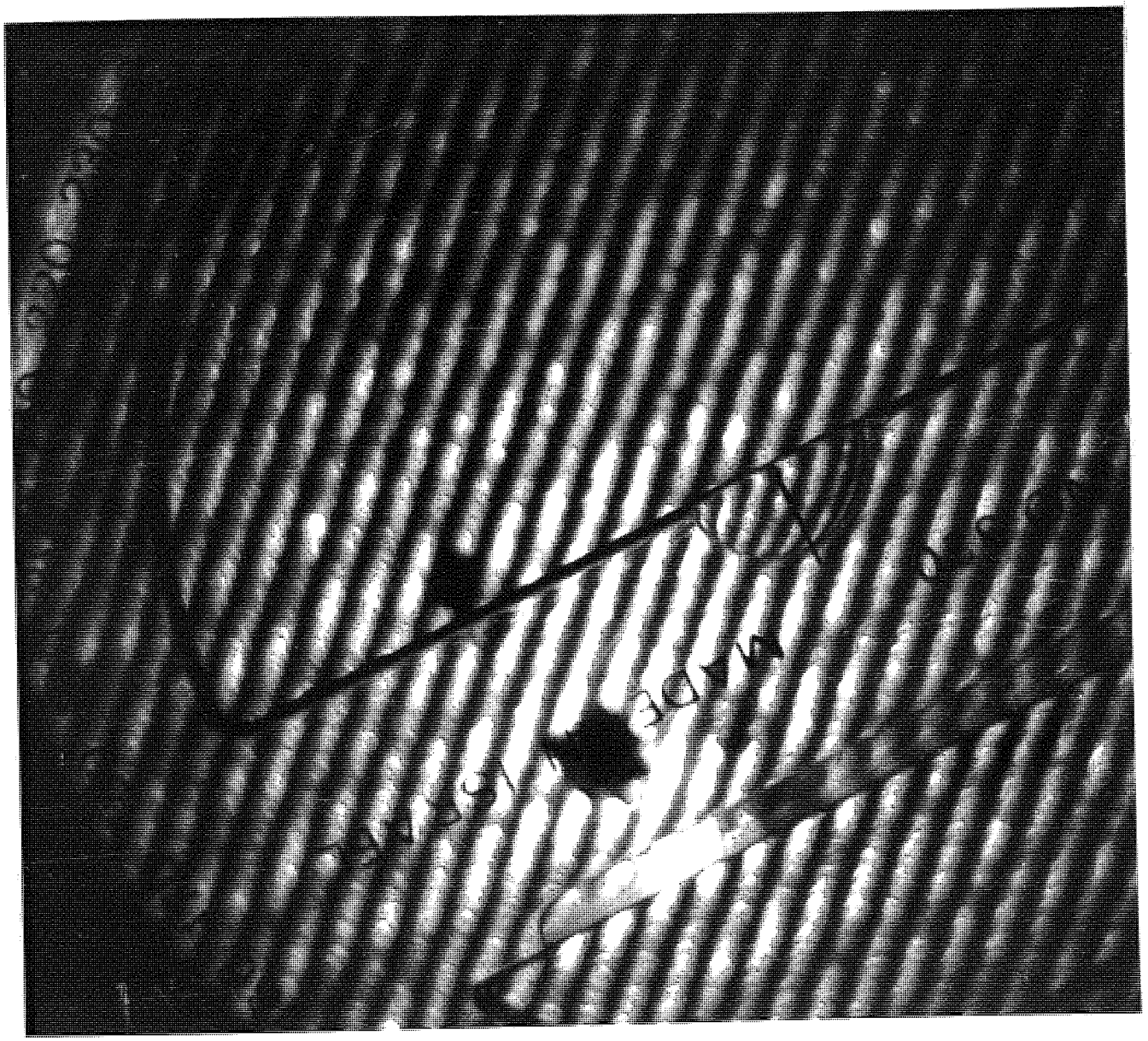

Fig.6.6.3. Protractor bar aligned on moiré fringes

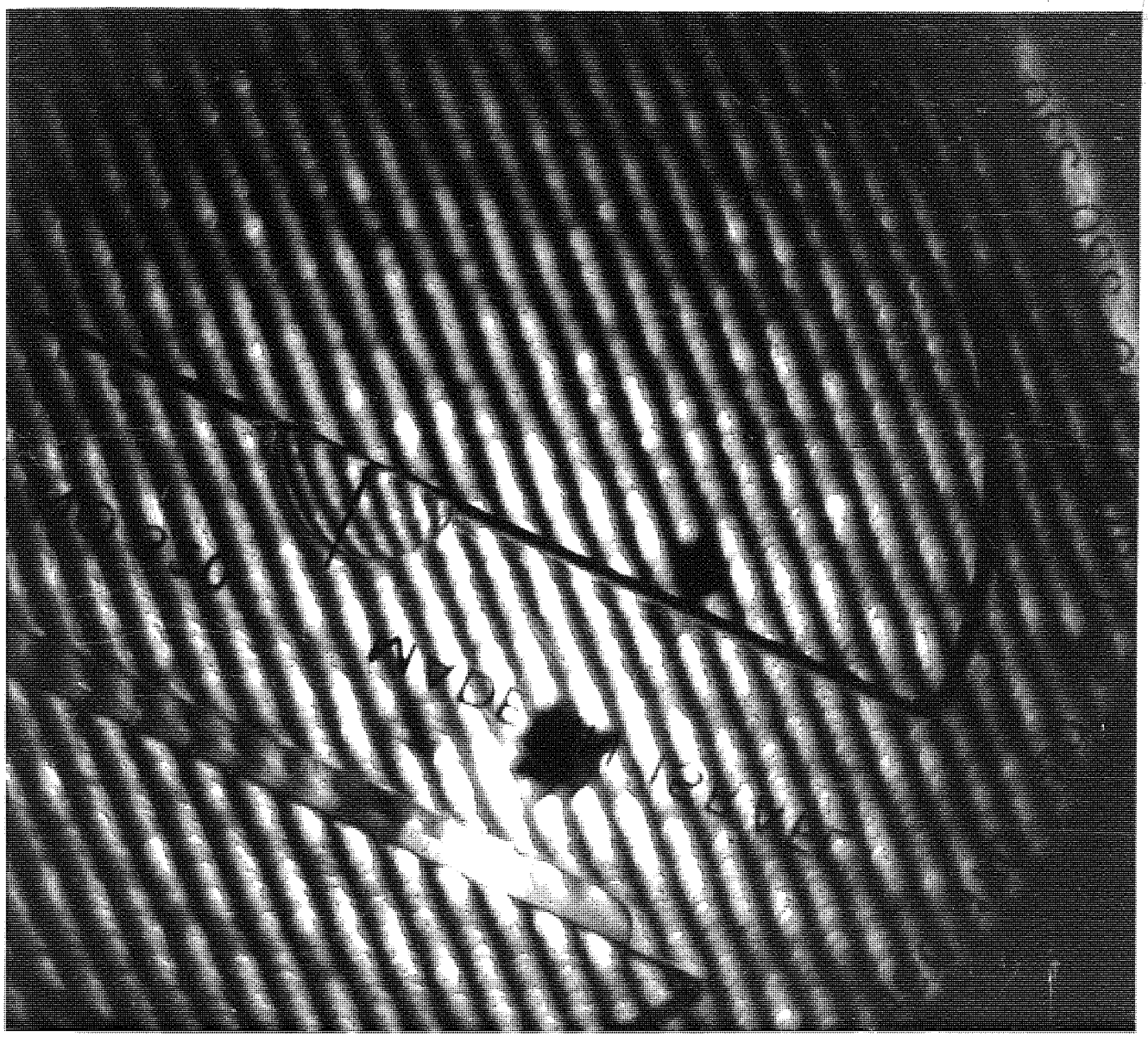

Fig.6.6.4. Corresponding moiré fringes in symmetrical position

6.7. CONCLUSIONS

The systems based upon a moiré pattern technique which were devised for the measurement of fringe spacings were not only found to be simpler and more portable than the methods reported in the previous two chapters but also considerably cheaper to fabricate and maintain. In addition, the symmetrical system was found to be particularly sensitive and suitable for measuring the spacing of indistinct fringes - such as occur in speckle photography.

Regarding the basic fringe measurement system(see Figure 6.4.1. shown earlier) if the vector representing the reference grid is not too different (e.g. about ±25%) from that representing the interference fringes (which means that the two spatial frequencies are reasonably close) then this method is most sensitive. In turn, this depends upon the magnitude of the angle 2β between the reference grid and the interference fringes. As can be seen from Figure 6.4.1, if this angle is small, then the sensitivity will be high. However, this means that the spatial frequencies of the interference fringes and reference grid must only differ by a small amount (e.g. ±5%). It is possible to achieve this by having a wide range of different spatial frequency reference grids available and/or using carefully adjusted 'throws' to match the interference fringe spacing to that of the reference grid. Nevertheless, in practice, it was found that using

an angle of $2\beta = 20^{\circ}$, which allowed a difference of ±20% in the reference grid and interference fringe spatial frequencies, was quite satisfactory. Moreover, this enabled a reasonably large throw (between 200 and 300mm) to be generally employed - thus reducing the significance of small errors made in the measurement of the throw, and also meant that a large number of reference grids was not required (e.g. a grid of spatial frequency 0.5 cycles mm^{-1} could be used with interference fringes of spatial frequencies from about 0.4 cycles mm^{-1} to over 0.6 cycles mm^{-1} without needing to adjust the throw - which would obviously enable the range to be extended).

The basic system requires that the interference fringes are aligned along a fixed direction at the prescribed angle (2β) from the reference grid. As was explained, this may not be easy and can lead to errors. Thus if the ratio of the spatial frequencies R is fixed and the angle 2β is incorrectly set, such that there is an error of $\delta\gamma$ in the angle γ between the moiré pattern and the fringes. This error is :

$$\delta\gamma = \left(\frac{\partial\gamma}{\partial\beta}\right)_R \delta\beta \quad \ldots\ldots\ldots\ldots\ldots\ldots (6.7.1.)$$

However, with the symmetrical system this problem and the attendant errors were considerably reduced by aligning the interference fringes (approximately only) along a fixed direction (vertical) and then swinging the reference grid between angles $+2\beta$ and -2β. (The use of

a precision machined annulus and a slot/stop system meant that these angles could be accurately set without needing to be measured each time.) The total angle 2γ through which the resulting moiré pattern swung was still a very sensitive function of the ratio of the spatial frequencies but was less sensitive to small errors in the original interference fringe settings. This is because, if the two original angles were $2\beta + \delta\beta$ and $2\beta - \delta\beta$ either side of the symmetry point, then corresponding errors in the moiré pattern angles will compensate for this. In other words, the errors $\pm\delta\gamma$ in the value of γ will cancel in the total angle 2γ provided that the error $\delta\beta$ is small enough to leave $\left(\frac{\partial\gamma}{\partial\beta}\right)_R$ unchanged. The actual error depends upon $\left(\frac{\partial^2\gamma}{\partial\beta^2}\right)_R$ which is very small. If the magnitude of angle 2β which is used is 20° this means that the resulting error in R will be less than 1%, provided $\delta\beta$ is less than 3°. It was found in practice that the settings could easily be made to the nearest degree and so such errors were negligible.

Concerning the alignment of the projected interference fringes with respect to a fixed direction, it was subsequently noted that this could also be undertaken using such moiré patterns. This was done by aligning the reference grid along a reference line and then adjusting the angle of the projected fringe pattern such that the resulting moiré pattern fringes were halfway between the two limits of infinite spacings - the interference

fringes are then aligned with the reference. In addition, it was noted that the throw 'D' could also be accurately measured with the use of moiré patterns. This may be undertaken by employing a standard reference grid in place of the specklegram and projecting an image of this onto the screen of the fringe measurement system. In this case, the spacing is already accurately known and so the results can be used to calculate 'D' instead.

In addition to the use of the system for the measurement of projected images, fringe systems or grids, the system could be used as an angular amplifier. For example, it is evident, as Pickthorne and Rogers[81] have outlined, that it could be employed for the detection of small angular motions over a limited range.

The effectiveness of the symmetrical system was examined, in conjunction with its use with single illumination beam speckle photography, with regard to certain practical and applied problems in industrial and engineering contexts. These investigations, which are described in the following chapters, provided a comprehensive basis for the assessment of the system and revealed further possibilities for its use.

CHAPTER 7

INVESTIGATION OF RAIL CONTAMINANT THICKNESS USING SPECKLE PHOTOGRAPHY

CHAPTER 7.

7.1. INTRODUCTION

In the context of railway engineering, very little information is available regarding the thickness of contaminant films present on the track, when the wheel and rail are in contact. There is also little known regarding the influence of wheel loading and the duration of the loading on the thickness of such films. Current and proposed developments (now that the Advanced Passenger Train is to be replaced) with respect to safety, performance, efficiency and maintenance make the need for this information particularly important.

Some attempts have been made by British Railways Research Department to obtain such information but various problems, requirements and difficulties concerning the examination and analysis of the thickness of contaminant films and the very small changes due to load changes have meant that the necessary information has not been satisfactorily obtained. However, as will be discussed, it was considered that laser speckle photography combined with a highly sensitive and adaptable interference fringe measurement system could be successfully employed for this examination and analysis.

An initial investigation was undertaken to determine if single illumination beam speckle photography in conjunction with the sensitive and accurate moiré pattern fringe measurement system that was detailed in the previous chapter, could be used for the purposes outlined. Having established that the system could be employed, a detailed investigation, involving the study of the thickness of different contaminant films in the wheel/rail contact region with a variety of loading conditions, was then carried out. Much of the applied experimental work was undertaken at the British Railways Board Research Department where special equipment and facilities were provided.

7.2. OUTLINE OF INVESTIGATION.

As will be explained, certain thin contaminant films on railway track are thought to affect the interaction of the railway wheel and rail. The thickness of these films is believed to influence their effects in this respect and this thickness (and changes in thickness due to different loads) has not been determined in the wheel contact region. It was initially intended to investigate the use of speckle photography and the symmetrical moiré pattern fringe measurement system for the analysis and measurement of the thickness of a common contaminant film between a simple wheel/rail arrangement. If this proved satisfactory the intention was then to build upon this experience and undertake a detailed study using an actual full-size railway wheel and appropriate loading system.

The chief objective in this respect was the obtaining of information concerning the thickness of commonly occurring contaminant or debris films for typical wheel loadings and respective changes in thickness for given changes in applied load.

The proposed development of a faster version of the High Speed Train (H.S.T.) and also increases in loadings of freight trains will mean that contaminant films may be subjected to rapidly changing loads sustained for some time. A further objective was thus to investigate these factors and explore their influence on the thickness and changes in thickness, of common contaminant films. In addition, it was intended to examine the resulting lateral displacement at the wheel bearing for the different wheel loadings and contaminant films.

All this information would mean that a fundamental picture of the thickness, changes in thickness under different loading conditions and loads,of common rail contaminant films could be provided. Although some of the relative differences and changes in thickness may be quite small, the sensitive moiré pattern fringe measurement system should enable these to be detected and accurately determined.

7.3. THEORY AND PRINCIPLES OF INVESTIGATION.

The ability of a rail traction unit to drive a

wheel and the breaking system to provide a braking effect are both influenced by the contact conditions between the wheel and rail. As Kalker[86] explains, theoretical predictions of the force which can be transmitted through the contact requires knowledge of the contact size. Timoshenko and Goodier[87] point out that contact size is determined by the geometry and elastic deformation of the contacting solids. For a railway wheel and rail the contact area is elliptical in shape as shown in Figure 7.3.1. The railway wheel has a steel'wear band' which is harder than the rail and the deformation is relatively small.

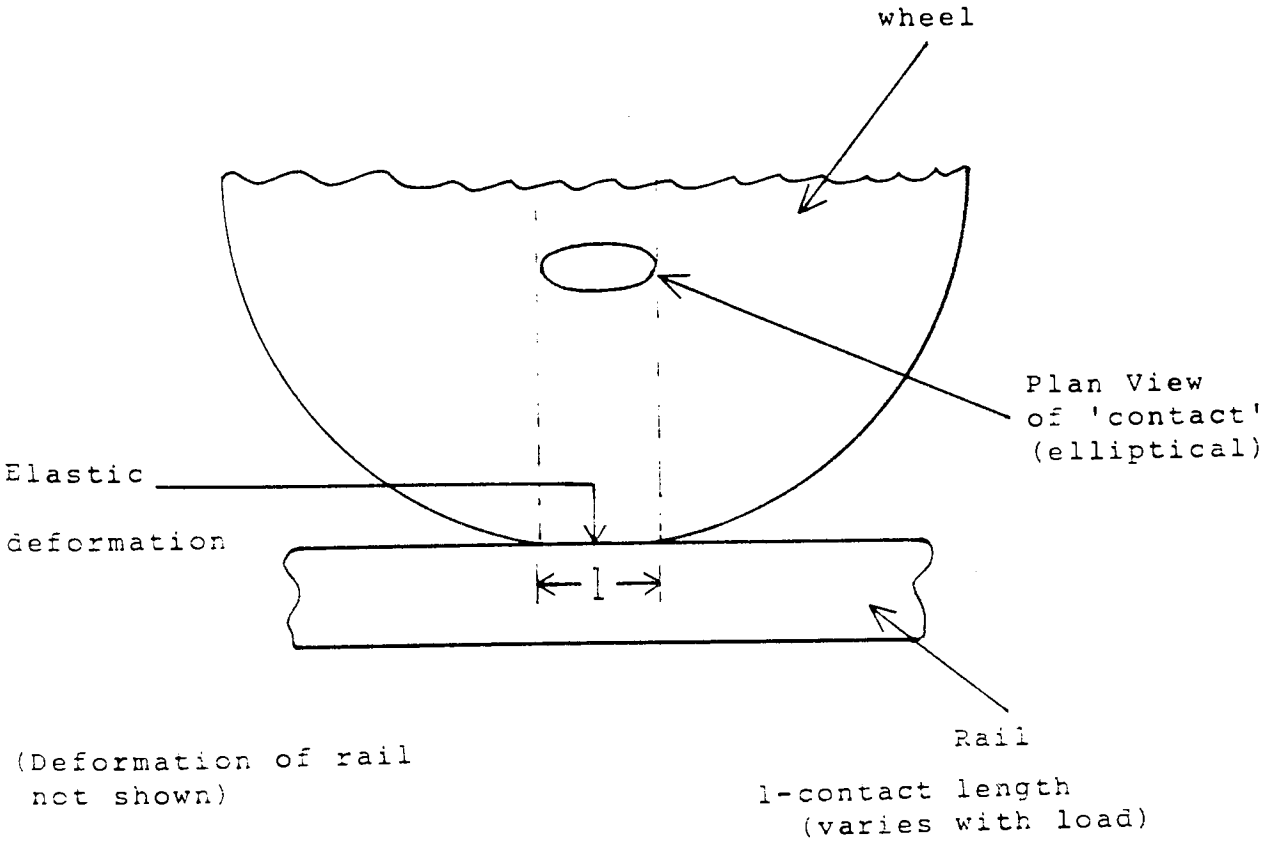

Fig.7.3.1. Static Contact conditions : clean surface.

According to Smith[88] various contaminant (debris) films such as water and iron oxide, oil (of

various types), oil and iron oxide and coal dust* frequently exist on railway track. If there is a contaminant layer present between a railway wheel and rail then, as Johnson and Roberts[89] report, the nature and thickness of this layer can influence the force that can be transmitted through the contact. The thickness 't' of this layer for a particular wheel geometry depends upon the type of contaminant and the load on the wheel (i.e. the compressive force between wheel and rail) as shown in Figure 7.3.2. It is also possible that the magnitude of 't' will depend upon the frequency of changes in the compressive force (i.e. as successive wheels pass over the layer). In addition, it may be influenced by the duration for which the force is sustained. Cameron[90] indicates that certain films may be squeezed out, by a particular force, in a very short time. This depends on the viscosity of the film which, in turn, depends upon pressure and temperature. However, other films (containing elastic particles) will not be squeezed out under such conditions and will compress.

If the load (force) on a railway wheel is changed then the displacement due to elastic deformation at the wheel/rail contact will change (there will be displacement also at the wheel bearing). It is possible to measure the respective lateral displacements in this context using

---

*On track used by coal-carrying freight trains.

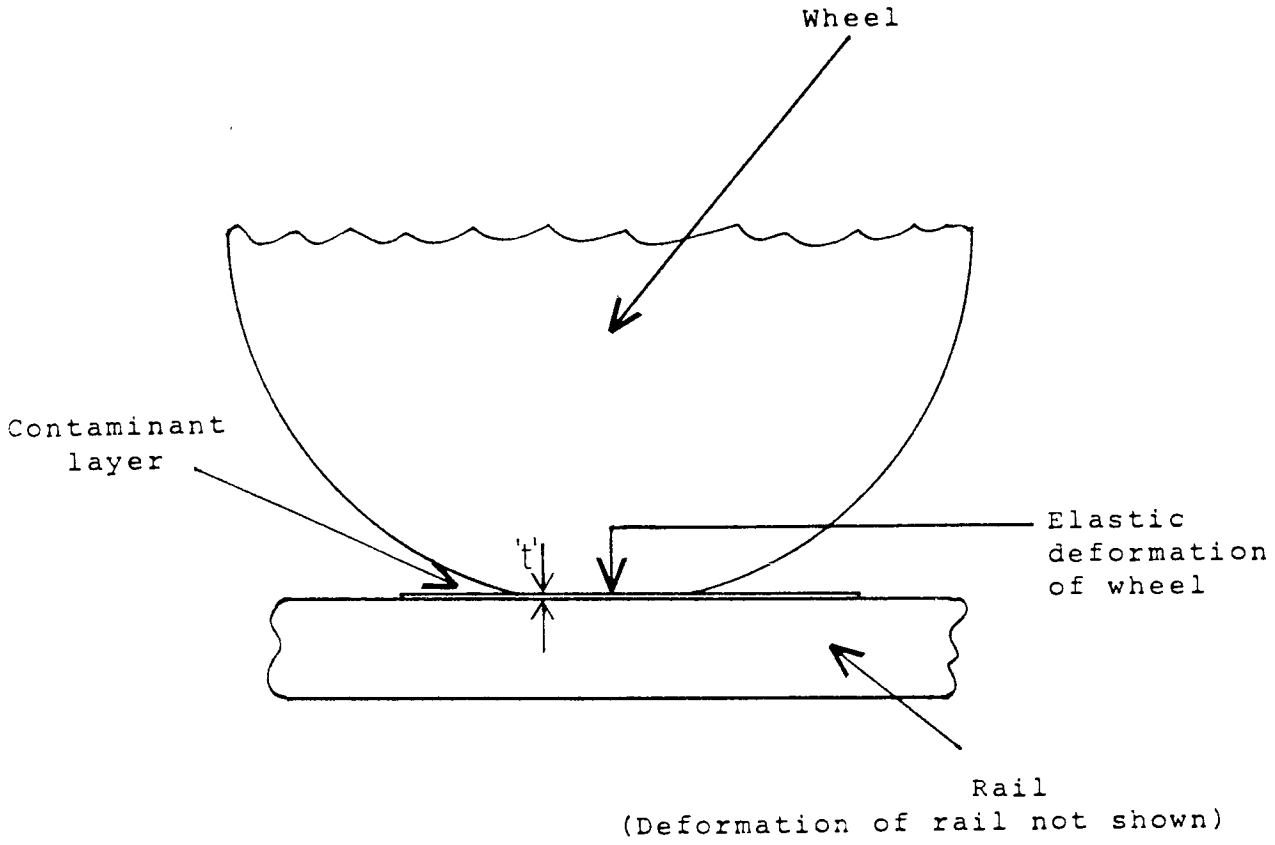

Fig.7.3.2. Static Contact conditions: contaminant present.

speckle photography. Thus, if a contaminant layer is introduced between the wheel and rail the change in thickness of this layer with the same change in load will produce a corresponding difference in the wheel/rail lateral displacements measured by speckle photography. This difference is equal to the change in thickness of the contaminant layer, as indicated in Figure 7.3.3.

Hence, the thickness of a contaminant film under typical wheel load conditions may be determined by comparing the lateral displacements, with and without the contaminant , when the load is increased from a typical

value to one which will significantly compress (or squeeze out) the contaminant so that only an insignificant amount remains. This method can also be applied to cases where changing loads or loads maintained for some time rather than than a particular (typical) load are of interest-in terms of their influence on contaminant layer thickness. The

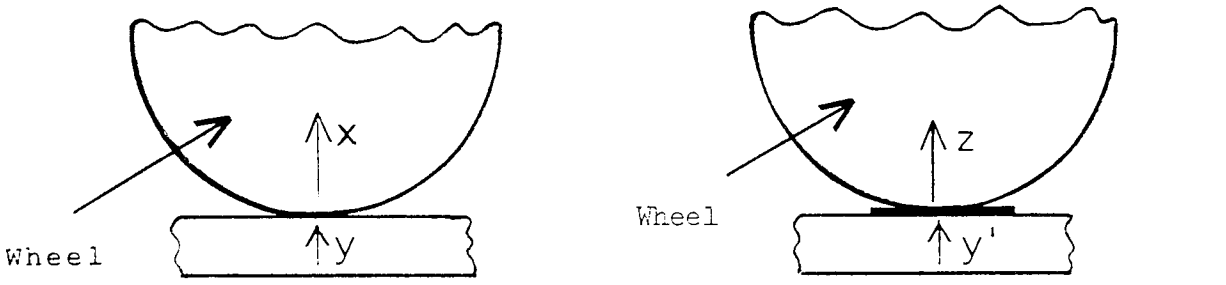

Without film

With film of thickness 't' (t=z-y')

Fig.7.3.3. Displacement with and without contaminant film.

lateral displacement of the wheel bearing and the corresponding influence of load and contaminant layers can similarly be measured and assessed.

7.4. METHOD OF INVESTIGATION.

A preliminary study was carried out to assess the experimental requirements and possible problems concerning the measurement of contaminant film thickness using single illumination beam speckle photography. This

involved a basic investigation with a simple small-scale wheel and rail section. With this arrangement the loads were applied directly to the wheel and double-exposure photographs were recorded of the wheel/rail interface before and after loading. Corresponding doubly-exposed specklegrams were recorded after a typical thin layer of contaminant material had been introduced between the wheel and rail. The information and experience gained from the preliminary studies reported in Chapter 3, regarding such factors as optimum surface illumination positions, camera settings, film processing and so on was fruitfully exploited in relation to this initial investigation. Various exploratory experiments were undertaken with this simple wheel/rail arrangement and the information obtained utilized when subsequent experiments were carried out with a full-size test rig. The measurement and analysis of the resulting doubly-exposed specklegrams using the symmetrical moiré pattern fringe measurement system was found to be quite satisfactory and so it was decided to proceed to more detailed research.

In the main investigations, a test arrangement which consisted of a full-sized railway wheel complete with normal axle and bearing mounted on a steel girder chassis was employed. A section of rail was rigidly mounted in a holder and held in position under the wheel. Different applied forces between wheel and rail could be introduced, as shown in Figure 7.4.1, by a

hydraulic ram which acted on the rail section holder. Technical assistance concerning this test rig, wheel and rail surface finish and the associated factors of contaminant film condition and position was provided by British Railways research engineers, as was the test equipment.

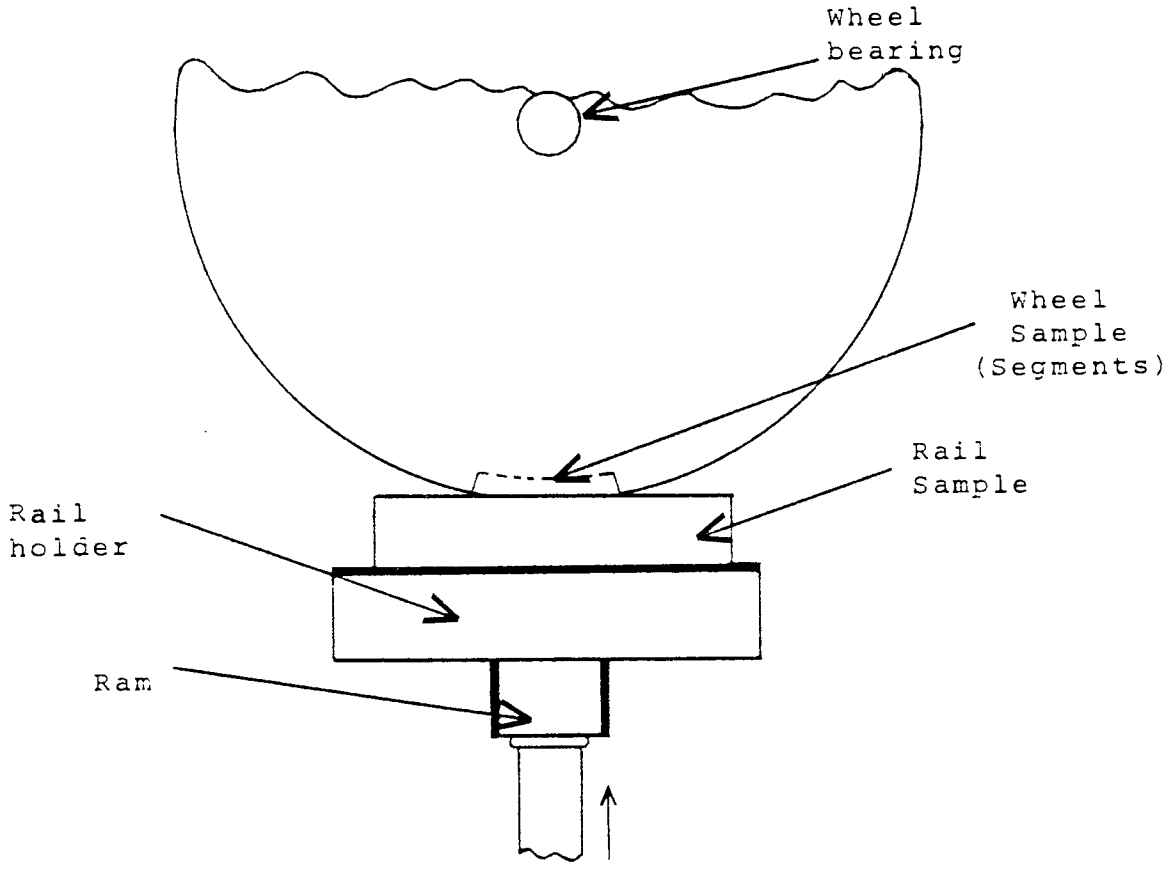

Fig.7.4.1. Simplified full-scale wheel rig.

The rim of the wheel ('tyre'section) had a section cut out in the region of the wheel/rail contact. Different wheel segments could be rigidly mounted in this section as required. By lowering the rail section, using the hydraulic ram, contaminant layers such as water and iron oxide could be introduced between the wheel and rail.

The hydraulic loading system was designed to enable considerable forces, typical of those encountered in actual railway operating conditions, to be provided between the wheel and rail. A pressure transducer was fitted to the system in order that the force which was being applied could be monitored. This system was capable of providing a sustained force, without significant variation, for several hours. As can be seen from Figure 7.4.2, the whole wheel rig system was accessible yet robust and rigidly constructed.

Both the laser and recording camera were firmly mounted adjacent to the main chassis such that there was no relative movement with respect to the test system. When the necessary adjustments to the camera and laser had been made, a light 'blackout' unit was put in position before the wheel/rail interface. The camera used in this investigation was a 35mm. S.L.R. camera with a 6 element lens system. An aperture ratio of f/4 was employed for all recordings and a helium-neon laser of 8mW output power, with a beam expansion system similar to that described in Section 3.3, was used to illuminate the interface area. Remote cables, outside the blackout unit, were used to operate the camera shutter and a beam cut-off shutter - which was used to cut out the illumination between each double exposure. Actual wheel/rail contact length 'ℓ' was approximately 3.5×10^{-3}m and equal regions either side of the contact were included in the illuminated

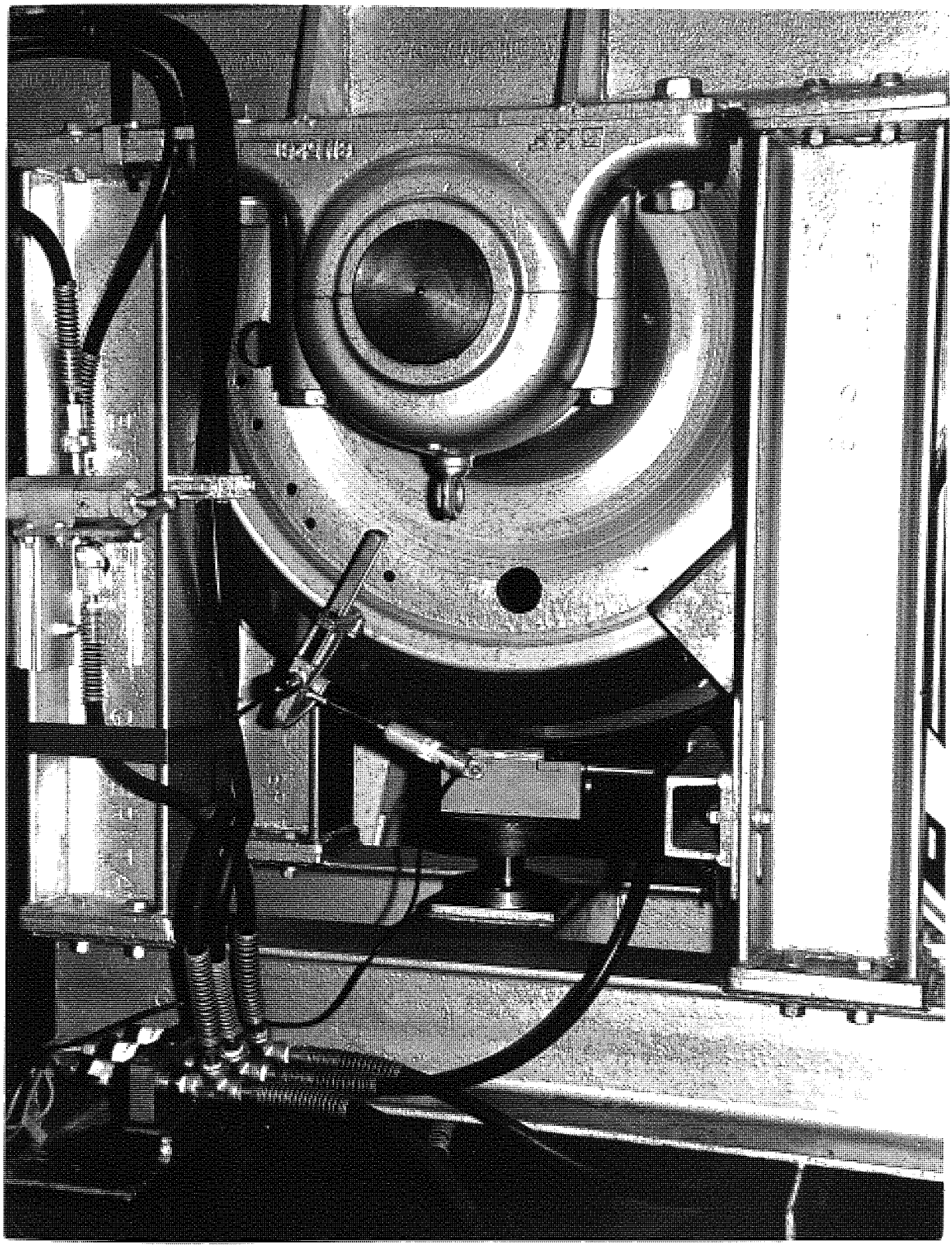

Fig.7.4.2. Part of main test rig

area recorded photographically. The wheel segment and rail section both had non-specularly reflecting surfaces. Once the camera and laser had been set up, as indicated in Figure 7.4.3, they were clamped in position and remained fixed for the duration of the investigations.

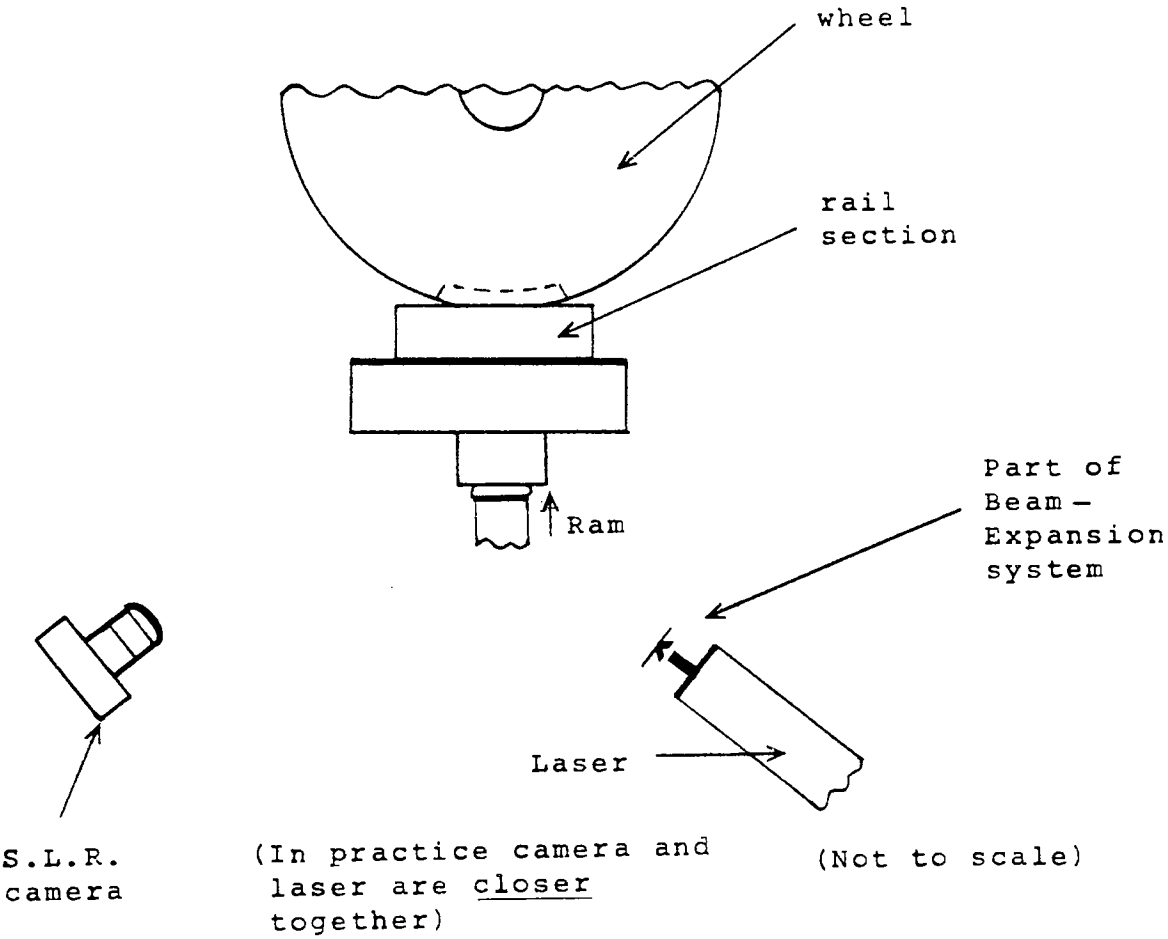

Fig.7.4.3. Simplified arrangement for speckle photography of wheel and rail.

A small force was applied (via the hydraulic ram) which was known to just bring the wheel and rail into contact. Then a single exposure photograph was recorded using Agfa-Gevaert 10E75 film. After increasing the

force to 40kN a second (double) exposure was recorded. The recorded image size was almost the same size as the interface area being photographed and exposures of 15 seconds for each exposure were found to be most effective. This procedure was repeated when doubly-exposed specklegrams were recorded for different contaminant films introduced between the wheel and rail. As outlined earlier, in order that contaminant film thickness for typical wheel load conditions could be determined a second set of specklegrams was recorded each time. For these the initial exposure was recorded when the applied force was 40kN and the second after the force had been increased to 50kN (which squeezed most of the contaminant layer out). An ambient temperature of 20^{o}C ($\pm$1^{o}C) was maintained during the photographic recordings and also the same initial contaminant layer thickness (1mm) and applied wheel/rail forces were employed in each experiment.

Corresponding doubly-exposed specklegrams were recorded at the lower edge of the wheel bearing so that the relative lateral displacements could be measured. The camera and laser were kept in the same respective positions but raised vertically and mounted on the same level as the bearing. All settings, recording conditions and exposure times were the same as those used for the wheel/rail examinations. In all cases a few seconds was allowed for the system to settle down before the second exposure was recorded.

A further series of experiments was carried out with regard to contaminant film thickness, in which the effect of the load (force) being successively applied and removed was simulated. (As when a wheel passes over the film and a further wheel follows and so on.) Experimentally, this was achieved by applying and quickly removing a force of 40kN having taken the first exposure before the force was initially applied and the second exposure (when the force was 40kN) after the process of applying and removing had been repeated 30 times. (The latter figure was reported as being fairly representative of actual minimum conditions). In addition, experiments were undertaken to explore the possible influence of sustained loads on contaminant film thickness. In this instance, the first exposure was recorded as before but the second exposure was not recorded until the applied force of 40kN had been maintained for 5 minutes.

The treatment and processing of the doubly-exposed photographs was carried out (with Kodak D19 developer) using the measures outlined in Chapter 3 which had been found to produce specklegrams of high contrast and definition. Precise measurements were made of the respective image and object sizes so that the demagnification ratio could be accurately calculated.

As indicated earlier, a sensitive and adaptable fringe measurement system was required for this investigation and the symmetrical moiré pattern system was

considered to be most suitable for this purpose. The specklegrams were fixed into a rigid holder which was held in a base clamp. It had fine, calibrated adjustments in both horizontal and vertical planes so that small known movements of each specklegram could be made with respect to the interrogating beam, as shown in Figure 7.4.4. This meant that the specklegrams could be interrogated in precise steps and corresponding regions on each specklegram could be accurately located. An unexpanded laser beam (1mm diameter) provided by an 8mW output power helium-neon laser was employed to interrogate the specklegrams. The symmetrical moiré pattern fringe analysis apparatus was fitted into a base clamp mounted on a small optical bench along with the specklegram holder. Adjustments to the 'throw' D were conveniently and quickly made and then D was measured using the moiré fringe technique described in the previous chapter.

Each doubly-exposed specklegram was interrogated on a grid type format, on a 5mm raster, and the moiré fringe angles accordingly measured. The precision specklegram adjustment arrangement enabled the wheel and rail contact regions to be isolated and the respective lateral displacements were then determined so that the various contaminant film thicknesses could be found. Similarly, the wheel bearing displacements were determined in each case using this system. Owing to the fact that the moiré

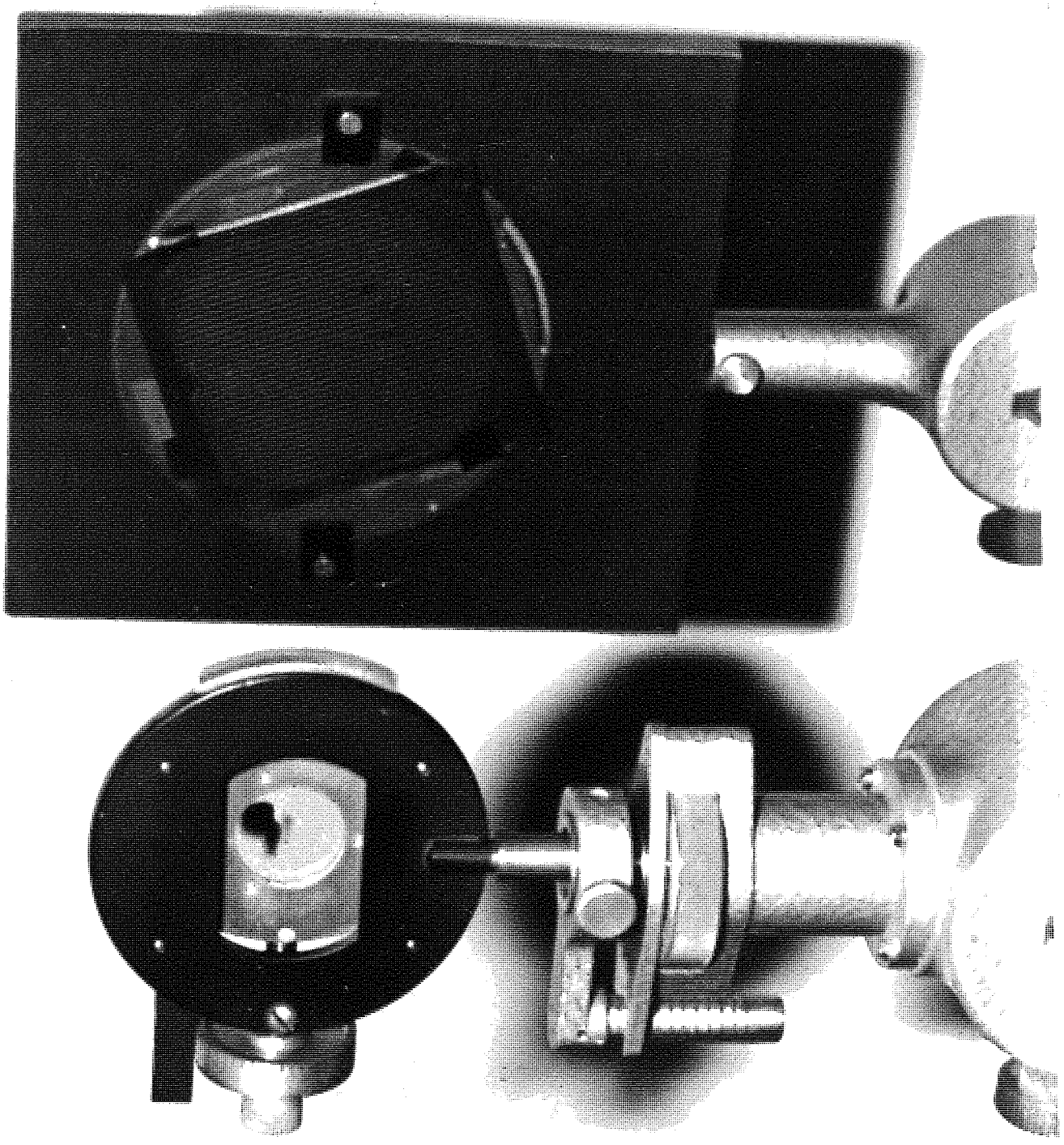

Fig.7.4.4. Precision specklegram translation apparatus (Laser not shown)

pattern system allowed a difference of ±20% between the reference spatial frequency and that of the interference fringes without significant loss of precision, it was not found necessary to adjust the throw very much for a particular set of experiments.

7.5. RESULTS.

Mean interference fringe spacing values for the lateral displacement of the wheel at the wheel/rail contact were obtained, using the moiré pattern system, from doubly-exposed specklegrams recorded with and without contaminant films present. These were in corresponding sets such that the first set was of a wheel/rail contact force increased from a small initial (contacting) force to a force of 40kN and the second set was for a force initially of 40kN increased to 50kN for the second (double) exposure. The conditions and region of contact for which the displacement was measured were all kept the same. Thus the respective differences between each set, compared to the set recorded with no contaminant present, were proportional to the relative film thickness for a typical wheel/rail force of 40kN. Using the differences in fringe spacing obtained in this way, the actual lateral displacements, and hence relative contaminant film thicknesses were calculated using the equation given earlier in Section 3.9. Table 5 gives the results obtained for common rail contaminant films of the same

initial thickness and temperature.

Contaminant	Relative thickness for wheel/ rail force of 40kN.
Water and iron oxide	0.12×10^{-3}m ± 1%
Oil and iron oxide	0.16×10^{-3}m ± 1%
Oil	0.08×10^{-3}m ± 1%
Coal dust	0.10×10^{-3}m ± 1%

TABLE 5. Contaminant layer thickness results.

The wheel displacement results without a contaminant layer present were :

0.06×10^{-3}m (40kN wheel/rail force)

0.08×10^{-3}m (50kN " " ")

These values agree with theoretical values calculated by British Rail research staff. The corresponding displacements at the wheel bearing were found to be :

0.21×10^{-3}m (40kN applied force)

0.25×10^{-3}m (50kN " ")

Wheel bearing movements measured when contaminant layers were present were all found to be related to the change in thickness of the contaminant layer. The elastic deformation of the rail was not measured but it could be

examined in future investigations.

In keeping with sensitivity and overall accuracy of the symmetrical moiré pattern system, the displacement results (calculated from the fringe spacing values obtained) are all within a ±1% error.

No significant differences in displacement results and relative film thicknesses were detected for the cases when the applied wheel/rail force was repeatedly applied and removed or when the force was sustained for 5 minutes before the second exposure was recorded. Figure 7.5.1. shows (for corresponding doubly-exposed specklegrams of coal dust contaminant film) the moiré fringes obtained in the same symmetrical position for (a) applied force repeatedly removed/applied (b) applied force sustained. As can be seen the moiré fringe angles are virtually identical.

Finally, it should be pointed out that, when a rain water containment layer was introduced between the wheel and rail, and a doubly-exposed specklegram recorded before and after applying a 40kN force, the results showed that the film had virtually zero thickness after the force was applied. This is in keeping with predicted results for this particular wheel radius (0.5m) and applied force, calculated by British Rail Research Department.

Fig.7.5.1. Moire fringes for coal dust contaminant

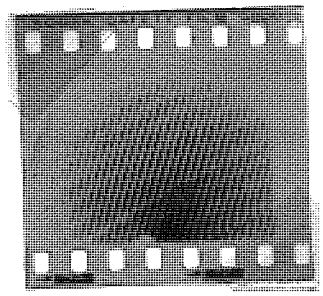

(a) applied force repeatedly removed/applied

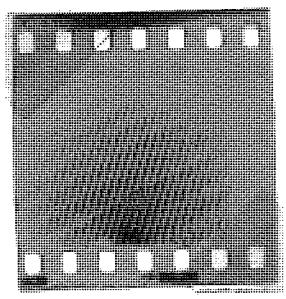

(b) applied force sustained

7.6. CONCLUSIONS.

The employment of single illumination beam laser speckle photography for this investigation proved most satisfactory. Various methods of non-contact measurement had been explored or considered for this purpose by the British Railways research section but had been found to be not sufficiently sensitive and adaptable or were impracticable. Moreover, since speckle photography is relatively insensitive to small movements towards or away from the camera then displacement of the wheel at right angles to the lateral displacement, due to the elastic deformation of the wheel and rail at the contact, does not impose difficulties in interpreting results. However, it was the use of the moiré pattern fringe analysis system which was particularly important for this investigation since it enabled comprehensive analysis of the interference fringes to be carried out over the whole contact region quickly and precisely. The sensitivity of this system was especially valuable because corresponding differences in interference fringes generated from doubly-exposed specklegrams recorded under normal and higher wheel loadings were frequently very small. Nevertheless, these differences were detected and measured with good accuracy.

This investigation provided definitive information concerning the relative thicknesses of common rail contaminant films under typical wheel/rail load conditions.

The findings indicate that, except for a water film (which was virtually all squeezed out) the various contaminant films were of sufficient thickness to modify the contact area and influence wheel/rail interaction. Furthermore,the results which were obtained for the wheel bearing displacements corresponding to different wheel/rail contaminant films show that the change in bearing displacement is directly proportional to the change in film thickness with change in wheel load. This is considered to be due to the contaminant film altering the contact area over which the load is distributed as its thickness changes. In addition, the investigation also confirmed the theoretically predicted magnitudes of the lateral displacement of the wheel (at the contact) due to elastic deformation under typical and higher wheel loadings.

Further investigations could be undertaken which could build upon the findings reported here and explore the possible influence of rail and wheel surface roughness and also ambient of temperature on contaminant film thickness. Moreover, the effect of wheel geometry in this context could be examined by changing the wheel segment for ones of different profiles. Although the respective differences in the resulting interference fringes could be quite small the moiré pattern system should enable these differences to be determined. This property of the fringe measurement system, along with certain others

outlined in the previous Chapter, was of specific importance in relation to the final applied investigations which are next reported.

CHAPTER 8

INVESTIGATION OF MACHINE MONITORING AND STRUCTURAL ANALYSIS USING SPECKLE PHOTOGRAPHY

CHAPTER 8.

8.1. INTRODUCTION

Significant changes are beginning to emerge in both automobile manufacturing technology and vehicle structures. Associated with these innovations are certain applied problems and special demands for information. In some cases, the requirements are for sensitive measurements or examinations to be undertaken and in others, detailed investigations of such factors as component reliability or structural defects are necessary. Specific applied technical problems in each of these two main contexts were identified with respect to developments currently taking place in the British Leyland Technology (B.L.T.) car division. Various measures had been adopted in order to resolve these problems but these had not been proved to be completely satisfactory in relation to the particular requirements demanded.

Following initial enquiries and experiments, it was considered that single illumination beam laser speckle photography supported by a reasonably simple,portable and highly sensitive interference fringe measurement system could be used to good effect with regard to the above two cases. In view of the interference fringe measurement

requirements, it was decided, on the basis of the evidence and findings reported in Chapter 6, that the symmetrical moiré pattern fringe measurement system would be most appropriate and suitable. The subsequent investigations of these diverse problems provided valuable opportunities for exploring the use of both speckle photography and the interference fringe measurement system in conditions which imposed various demands and restrictions not previously encountered. Consequently, this enabled an appraisal to be made, with particular reference to manufacturing and vehicle testing environments, of the complete measurement and analysis system.

8.2. OUTLINE OF APPLIED PROBLEMS INVESTIGATED.

(A) Monitoring of prototype production machines.

The increasing complexity of numerically controlled (N.C.) multiple-operation machines and the development of sophisticated 'robots' means that machines are becoming more expensive. For this and other reasons as Collacott[91, 92] and Williams[93] observe, so called 'machine health monitoring' is becoming more important. At British Leyland Technology, various investigations in this context have been undertaken by the Materials and Manufacturing Technology section in relation to certain prototype multiple-operation machines. With regard to the monitoring of several multiple-operation automatic machines which were being developed difficulties had been experienced in

detecting the development of faults and deterioration in performance in good time. In the actual production context, this could lead to serious disruption of the manufacturing process and poor quality products which could have to be rejected. However, if means of detecting potential faults due to wear, aging and other factors could be provided that would enable earlier indications to be given in this respect, then regular monitoring with such means should help prevent these serious stages being reached and remedial measures could also be taken much earlier.

The monitoring method and system would need to be sensitive, relatively portable and robust to enable it to be suitably employed in a large-scale production engineering environment such as that in an automobile manufacturing plant. An electronic continuous monitoring system had been devised for use with the particular prototype automatic production machine but had been found to be unreliable and unsatisfactory when used in an actual production context. Nevertheless, initial evidence concerning the employment of single-beam speckle photography and the moiré pattern fringe measurement system suggested that this could used in this context. It was considered that, because of the good reliability and reproducibility of the speckle photography/moiré pattern system as well as the high sensitivity, it could be possible to make 'time domain' measurements to determine variations over

time. Thus periodic monitoring of key machine units should be adequate to provide the necessary advance information on machine deterioration and condition. This information could be obtained fairly quickly, could be easily re-checked and would not be difficult to interpret, as will subsequently be explained. Since continuous monitoring would not be necessary when using this technique, one monitoring unit could actually be employed with a number of automatic production machines thus significantly reducing overall monitoring costs. In addition, because of the relative flexibility and adaptability of this method it could readily be employed with successive prototype machines and with modified machine systems.

(B) Automobile structure and component analysis.

New vehicles are being developed by British Leyland Technology car division that have very advanced and specialised structural and main component specifications. Stringent requirements have been detailed concerning the testing and examination of certain major components and sections of these vehicles. Investigations are being carried out in order to obtain information regarding manufacturing or design factors which may ultimately result in the creation of localised stress concentrations or structural weaknesses. It was with the obtaining of such information for a relatively large and complex vehicle component that certain technical difficulties had been

experienced. This particular problem was the one which was chiefly investigated in this case, as will shortly be indicated.

For complicated structures subject to complex loading patterns stresses may be derived from the study and measurement of the strains that are related to very small dimensional changes in the structures or components. Within the range of the elasticity of a particular material stress is directly proportional to strain. The latter may be simply expressed as $\Delta x/x$, such that Δx is the increase in the original length x. Strain is a dimensionless quantity and is often conveniently expressed as microstrain or 'μ' strain (where μ is 10^{-6}). Moreover, as Vest[31] observes :

> "Strain is a kinematic quantity related to the derivatives of displacement."

Thus, as Archbold et al.[52] have explained, since speckle photography is a simple technique for measuring displacement in the plane of a surface it thus enables the strain field to be determined in two dimensions. Furthermore, Erf[94] points out that measurements of the in-surface displacement followed by differentiation provides the strain magnitude. Therefore, it was considered that speckle photography could be employed for the examination of surface strain of the vehicle components in question.

Following preliminary investigation, the viability of speckle photography in this respect was confirmed. However, it was noted that an accurate and sensitive method

of measuring the interference fringes obtained from the doubly-exposed specklegrams would be necessary and, as will shortly be indicated, the moiré pattern fringe measurement system was consequently used for this purpose. This system could also be quickly modified to enable interference fringe angles to be respectively measured, as will be later described.

8.3. EXPERIMENTAL METHOD.

(A) Monitoring of production machines.

Initial experiments were undertaken to see if small lateral displacements could be detected and measured using single-beam speckle photography in an industrial production environment. Small, known displacements of a coarse ground steel surface produced by the displacement system described in Chapter 3 (Figure 3.2.2.) were used for this purpose. The system was clamped to a machine bed and the laser and recording camera were mounted on a steel workshop table adjacent to this. A black plastic sheet was placed over a simple wire frame which was arranged around the set-up so that ambient light levels could be reduced during photographic recording. This was subsequently modified and a cowl arrangement which could be used to provide safe and sufficient background light reduction for a variety of machines was devised. Originally a 1.5mW output laser was employed to provide surface illumination but an 8mW output power helium-neon laser was later used

and this enabled photographic exposure times to be significantly reduced.

Following these initial experiments an investigation was carried out to see if small lateral displacements and small changes in displacements of certain machine operating units, due to wear or the development of faults, could be detected using speckle photography and a sensitive interference fringe measurement system. The machine system employed for this investigation is shown in Figure 8.3.1. This consisted of four automatically controlled drilling units each fitted with an electrical power level monitor which could detect small differences in power levels due to such factors as drills becoming blunted. Unit number 1 had only been operated for a few hours before the monitoring investigation commenced as had unit number 3. However, unit number 2 had been operated for the equivalent normal production use of several tens of thousands of hours and unit number 4 had been modified to simulate the onset of deterioration in the drill pressure feed unit. All other factors were kept the same for each unit and all were fitted with identical new drills.

The recording camera, laser and beam expansion system were held by magnetic clamps on 'I' section bars bolted onto a heavy steel plate resting on a rigid steel trolley (fitted with pneumatic tyres). This plate had a 50mm thick foam rubber cushion between it and the top of the trolley as a further precaution to prevent any vibrations

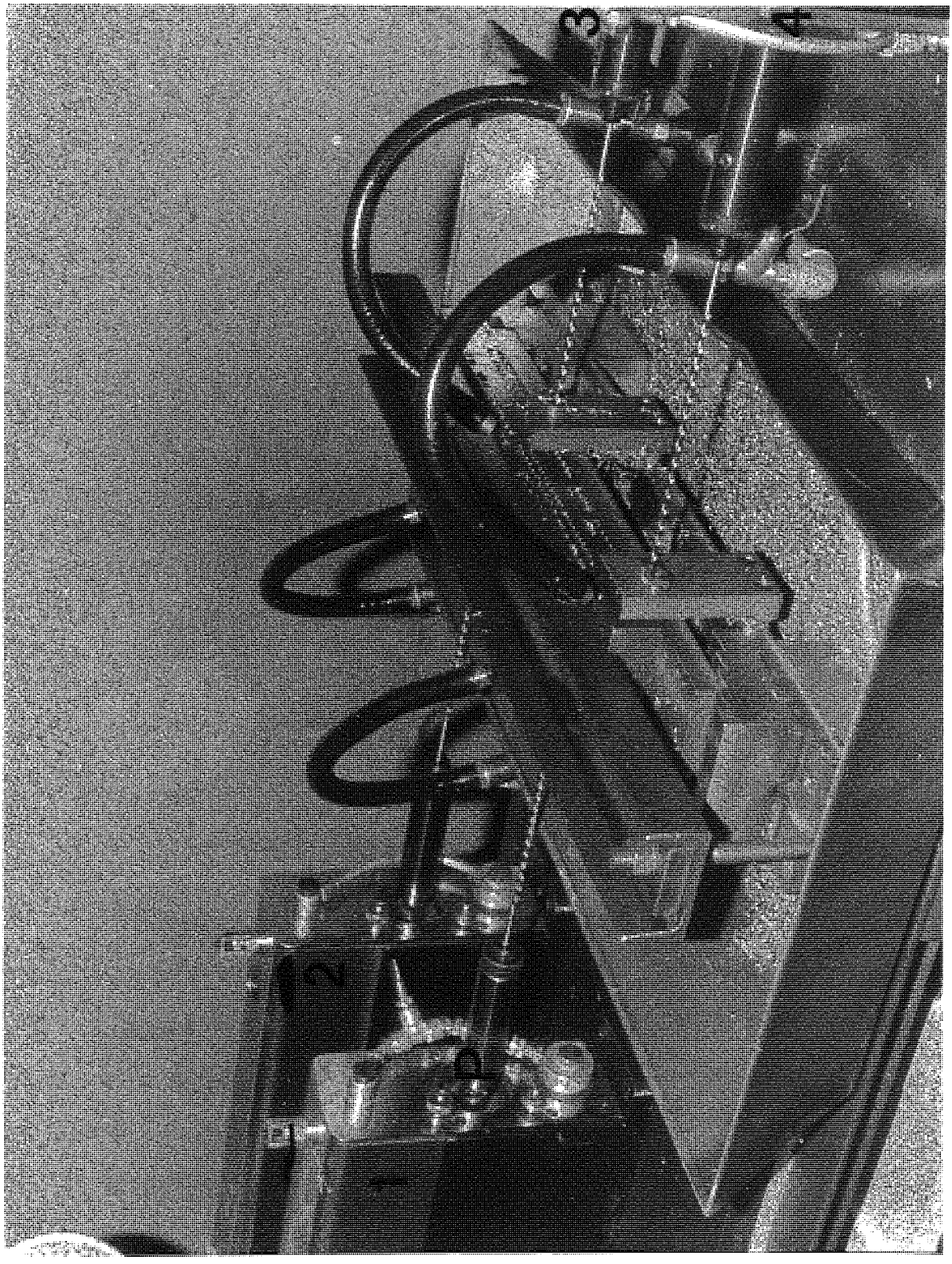

Fig.8.3.1. Basic test machines monitored using speckle photography

being transmitted through the floor. Each 'I' section bar protruded a short distance beyond the edge of the steel plate so that the recording camera and laser could be positioned relatively close to the machine section being photographed, as required. The trolley could be adjusted to different heights and the wheels could be locked in position. Remote cables were used to operate the laser beam cut-off shutter and the 35mm S.L.R. camera shutter. A camera aperture ratio of f/4 was employed and the camera position and illumination angle that had been found in the preliminary studies to produce specklegrams of high contrast and definition was used.

When the camera and laser had been adjusted and positioned a cowl was fixed over them and extended over the region of the machine being photographed. This was made of flameproof blackout material fitted on an adjustable frame. Small magnets were used to hold it in position and prevent it getting caught up on the machine. Commencing with Unit number 1 the section at the base of the quill 'P', shown in Figure 8.3.1. was photographed before a drilling operation started using an exposure of 15 seconds. A second, double-exposure was recorded at the end of the drilling operation before a new operation commenced, using the same exposure. The intention was to detect any relatively significant displacement in this non-specularly reflecting operating section, as will be explained, since this could be associated with deterioration

and unsatisfactory operation. This was repeated for each of the drill units in turn and care was taken to ensure that the machine temperature, ambient temperature and other variables which could influence the displacement examination did not vary significantly during the recording of the successive specklegrams. Agfa-Gevaert 10E75 film was used for the recording and a demagnification ratio of approximately x2 was employed in each case.

After the drilling units had each been operated for the equivalent of 1000 hours production use a second set of doubly-exposed specklegrams was recorded as before. A further set was recorded after the units had been operated for the equivalent production use of another 1000 hours. All the photographs in each set were carefully numbered so that they could be identified. They were all processed using Kodak D19 developer and the measures outlined in Chapter 3, which had been found to yield high quality specklegrams, were employed. In this investigation, the processing was undertaken in the 'works laboratory' but arrangements could be made for this to be done on the spot if required. Analysis of the resulting interference fringes generated by the specklegrams could also be carried out on the shop-floor if this was needed.

An interrogating laser beam of 1mm diameter provided by an 8mW output power helium-neon laser was used at normal incidence to each specklegram in turn. The latter

were mounted in a co-ordinate slide which had micrometer adjustments in the vertical and horizontal planes. Identical regions on each doubly-exposed specklegram were examined on a grid type format and, using the symmetrical moiré pattern fringe measurement apparatus, the interference fringe spacings were determined and the mean value recorded in each case. In those cases where there was a lateral displacement of the section P, the magnitude of the displacement was calculated, as will be shortly described.

A new N.C. multiple-operation machine that was being developed by B.L.T. was also monitored to determine if the speckle photography displacement measurement scheme could be used in connection with the 'health monitoring' of more complex machines. This machine and the associated control system is completely new and a confidentiality undertaking has been imposed by B.L.T. (See Appendix 8). Nevertheless, in the context of this investigation it can be said that the same basic method and apparatus used in monitoring the automatically-controlled drilling units was employed, with minor modifications to aid adjustment and positioning of the laser and camera in relation to less accessible units of this machine. Monitoring was carried out as before (i.e. exposures were taken prior to the commencement of an operation and again at the end, before a successive operation) when the machine had been in operation for the equivalent of thousands of hours of

production use. In this case, not all units or sections of the machine were monitored using this system of speckle photography for reasons which will later be explained. However, it was found that useful monitoring data could be obtained with the aid of this system of recording and interference fringe analysis.

(B) Automobile structure and component analysis.

Preliminary experiments using single illumination beam speckle photography and the moiré pattern interference fringe measurement system were carried out with regard to simple surface strain examination. It was found that this could be undertaken with the materials and surface finishes of the automobile unit and components for which a more detailed investigation was to be carried out, without the need to treat the surfaces to obtain high contrast speckle patterns. In addition, it was noted that a relatively large area of surface could be photographed without a serious loss of sensitivity due to increased demagnification ratio. These and other findings, which will later be outlined, were taken into account when undertaking the examination of the vehicle unit and associated components.

The particular unit which was investigated was the rear suspension assembly of a vehicle being comprehensively tested by B.L.T. Detailed information concerning this is restricted by a confidentiality undertaking but it does not

apply to the details necessary in this context. This assembly and associated components had previously been examined by various means, including the use of brittle lacquers, in order to identify possible localised stress concentrations and potential weaknesses. However, the quality of the data obtained was not considered satisfactory and so it was decided to explore the use of speckle photography in this respect, as previously outlined. This work was mainly undertaken in an automobile structure testing and analysis laboratory using a typical rear suspension assembly.

The main suspension assembly was firmly clamped on a base unit which was bolted to an air suspension optical bed. Illumination of the surfaces which were photographed was provided by a 15mW output power helium-neon laser fitted with a beam expansion system. A laser of this particular output power is not essential for this purpose (an 8mW output power laser was used in the preliminary experiments) but its availability was exploited so that relatively short exposure times could be used for convenience. Photographic recording was carried out with a 35mm S.L.R. camera fitted with a 10mm extension tube. An aperture ratio of f/4 was employed and Agfa-Gevaert 10E75 film was used for the recording. The actual regions of the rear suspension assembly which were photographed were chiefly those where there were welded joints, since it was for these regions that strain information was

basically required. In most cases, these were photographed such that the demagnification ratio was between 2 and 3 times. In order that regions of welding could be identified and examined on the specklegrams (in the subsequent analysis), care was taken in focussing the camera and in selecting exposure, and film processing times.

Figure 8.3.2 shows part of the rear suspension assembly and the arrangement for recording the specklegrams. In this case, the welded joint along one side of the flange was being photographed. An initial exposure was recorded with no applied load on the assembly section and then a double-exposure recording was made after a load producing an anticipated strain of about 500μ strain had been applied. (This value had been specified by B.L.T. vehicle testing section). Each of the exposures was of the same duration, namely 15 seconds. Similar recordings were made of other regions of the assembly and components using appropriate strain-producing loads specified for the particular section or part. Reference points and known surface lengths were used in each case so that strain magnitudes could subsequently be determined.

As shown in Figure 8.3.2. the 35mm S.L.R. recording camera was mounted on the optical bed and operated by a remote cable to avoid possible vibrations. The laser was mounted below the bed and passed by a series of mirrors to the beam expansion system. An air release remote control, which can be seen in the right-hand foreground

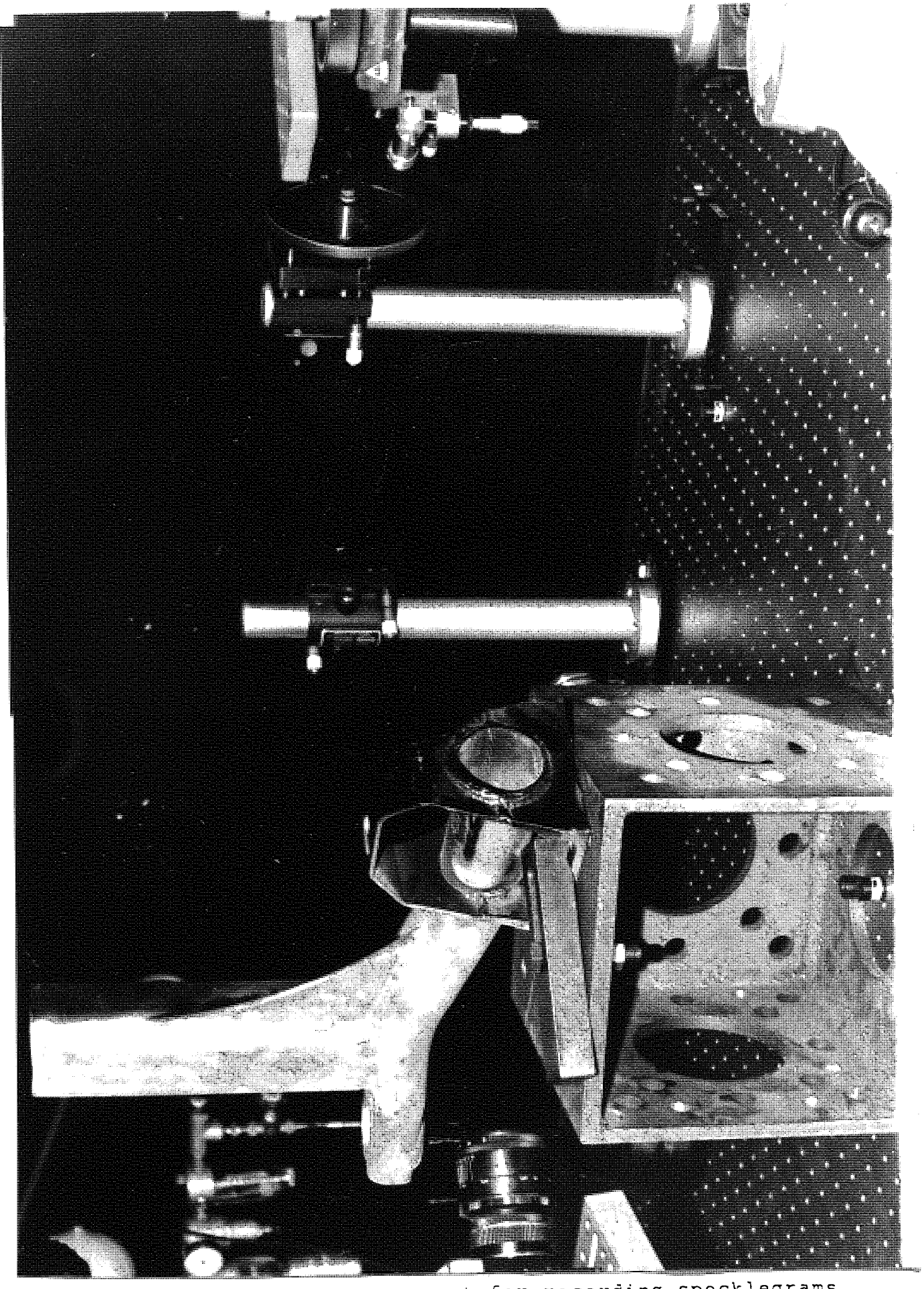

Fig.8.3.2. Arrangement for recording specklegrams of part of suspension unit

of Figure 8.3.2 operated a shutter which cut off the laser beam between exposures. A safelight was used when the strain-producing loads were being applied prior to double-exposure recordings. For identification purposes, a record was made of the specklegram number and the region of the assembly to which it corresponded. Film processing was undertaken according to the measures previously identified as producing doubly-exposed specklegrams which were of high contrast and definition.

These specklegrams were mounted in a coordinate slide unit which enabled precise movements of the specklegrams to be made with respect to the interrogating laser beam. Interference fringes obtained in this way were measured using the moiré pattern system as explained. Moreover, this system also enabled the orientation of the interference fringes to be measured with regard to the horizontal, so that differences in fringe angles could be identified along with the corresponding displacements. This was done by removing the reference grid and measuring the angles of the projected interference fringes on the system using the built-in protractor arrangement. A series of interference fringe spacings was obtained for each of the various regions of the assembly which were examined. The corresponding displacement values were then calculated, using the accurately known values of the 'throw' D of the projected fringes and the demagnification ratio, by employing a form of Equation 2.7.1, as before.

8.4. EXPERIMENTAL RESULTS.

(A) Monitoring of production machines.

After interrogating the doubly-exposed specklegrams initially recorded for each of the 4 automatically-controlled drilling units, it was found that only in the cases of units 2 and 4 were there significant interference fringes detectable in the region of section P (shown earlier in Figure 8.3.1.) Moreover, when the specklegrams that had been recorded after the machines had been operated for the equivalent of 1000 hours production use were interrogated, it was again found that only for units 2 and 4 were there detectable and measurable interference fringes. Similarly, for the specklegrams recorded after the machines had been operated for the equivalent of a further 1000 hours normal production use, only for units 2 and 4 were interference fringes detected and measured. The displacement results calculated for each successive monitoring in the case of these two units, were such that a small increase in displacement was identified after each period of use. For unit 2 the initial mean displacement increased from $0.040 \times 10^{-3}m \pm 1\%$ to $0.044 \times 10^{-3}m \pm 1\%$ and for unit 4 the displacement was initially $0.052 \times 10^{-3}m \pm 1\%$, this increased to $0.060 \times 10^{-3}m \pm 1\%$. There were no detectable fringes identified in the case of units 1 and 3 which had originally been almost new before the monitoring commenced. As pointed out, unit 2 had already been operated for the equivalent of several tens

of thousands of hours when the monitoring started and unit 4 had been modified to simulate the onset of deterioration.

A built-in electronic power level monitor failed to reveal any of the differences between the 4 units which were identified in this investigation. After units 2 and 4 had been stripped down the respective wear and deterioration in the components that were monitored was confirmed. This suggests that periodic monitoring using the speckle photography/moiré pattern system could be used in this context as a means of obtaining advance warning of deterioration or possible malfunction of this particular machine section.

There were no significant displacements observed for any of the sections of the new N.C. multiple-operation machine during the course of monitoring. Neverthless, displacements were detected in each case when the effects of significant wear or deterioration were simulated. Thus a 'profile' could be built up for each section so that any displacements or changes in displacement identified during periodic monitoring could be related to a particular cause and appropriate action taken. The frequency of monitoring could be adjusted as necessary, but, as this study has indicated, the process is so easy, cheap and reliable and does not disrupt manufacturing, that monitoring could be done with high frequency and a monitoring 'log' kept.

(B) Automobile structure and component analysis.

The interference fringes generated from the doubly-exposed specklegrams of the various sections of the rear suspension assembly were quite distinct, as can be seen from Figure 8.4.1. which shows interference fringes corresponding to strain produced by loading the mounting bush at the end of the vehicle rear suspension arm. Interrogation of the doubly-exposed specklegrams recorded of welded sections of the main assembly revealed significant differences in fringe spacing for regions on the welds compared to corresponding regions on the adjoining parent metal. Some differences in respective fringe orientation were also detected. This information could be linked to possible structural weaknesses.

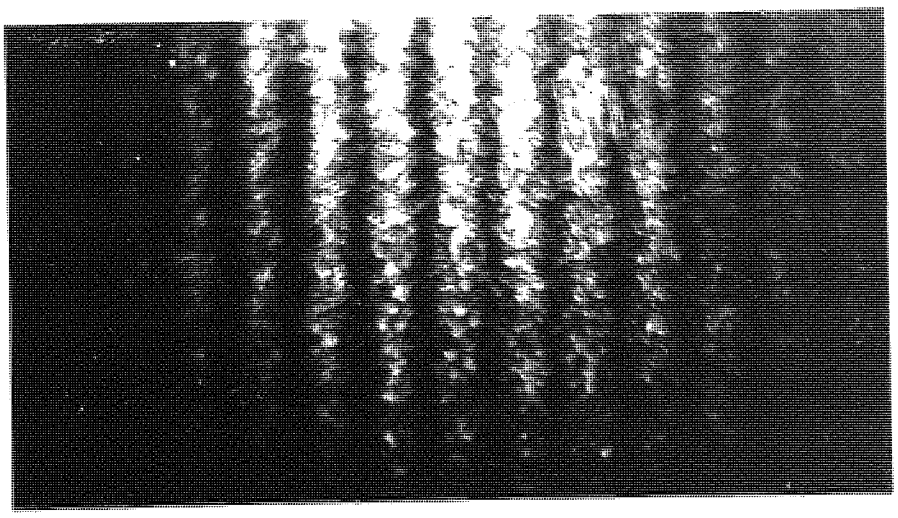

Fig.8.4.1. Interference fringes corresponding to strain-producing loading of part of rear suspension arm.

Having determined the interference fringe spacing for particular regions of the main structure subjected to specified strain producing loads, as outlined in

Section 8.3, the corresponding surface displacement magnitudes were calculated using the method previously outlined in Section 3.9. Differentiation of these results enabled the strain magnitudes to be obtained. Typically, the calculated strain values were between 400 and 500 μ strain. However, for some regions of the main assembly corresponding strains of around 650μ strain were determined (hence, the strain concentration factor for one such region would be: 650/500 = 1.3). This information is important because respective differences in strains of this magnitude indicate that there are stress concentrations in these regions. As a result of the detailed analysis of this information, a complete picture of the stress fields for the whole rear suspension assembly was built up.

8.5. CONCLUSIONS.

Although each of the two applied investigations which were undertaken using single illumination beam speckle photography and the moiré pattern fringe measurement system were different and the problems examined were different, they each demonstrated the applicability of this complete measurement scheme in industrial contexts. They also provided further evidence of the versatility, practicality and sensitivity of the moiré pattern fringe measurement system and showed that this simple, robust and portable system could be used in quite different environments.

The exploratory investigation of machine 'health monitoring' which was carried out in an actual factory production situation suggests that laser speckle photography, combined with the sensitive moiré pattern fringe measurement system, can be employed as a monitoring tool in situations where displacement and displacement changes can be linked to significant wear, premature failure or the development of faults in particular machine units. It could also be possible to employ the technique for assisting fault diagnosis of machines in cases where displacement identification can help to pinpoint or isolate faults .

It is clear that not all machine 'health monitoring' could be undertaken with this technique since not all machine units will produce displacements or displacement changes measurable in this way as a result of deterioration or malfunctioning. Nevertheless, in those cases where this is possible, the technique can enable reliable, low-cost routine monitoring to be undertaken. Once 'profiles' have been built up for particular machine units, all that would be required would be monitoring according to a time schedule so that changes are identified in good time.

Vikram and Vedham[95] have shown that it is possible to provide an increase in the lower measurement range of a dial gauge by measuring the displacement of the needle using speckle photography. A similar strategy could be

employed for monitoring certain machine control and adjustment units. This task would be simplified by using the moiré pattern fringe measurement system in conjunction with speckle photography.

Strain analysis and measurement using laser speckle photography has been described by investigators such as Archbold et al.[52] Gregory[21], Ennos and Virdee[96] and Luxmore[97]. The employment of single illumination beam speckle photography for the strain analysis of large structures has been reported by Martin[98]. He observes that a limitation of speckle photography in this context is that interference fringe analysis can be time-consuming. Nevertheless, as a result of the investigations undertaken using the moiré pattern fringe measurement system it is suggested that the time taken for this task is much reduced with the aid of this system. Ineichen et al.[99] have devised a Young's fringe processor which automatically measures fringe separation and they have employed this for the analysis of doubly-exposed specklegrams recorded for strain determination purposes. However, this system is fairly large and more complex than the moiré pattern system and is not quite so sensitive overall.

It is pointed out by Dändliker[100] that, although speckle photography may be less accurate and sensitive than holographic interferometry, for objects having fairly simple geometry, the former may be simpler to operate. Luxmore et al.[72] observe that speckle photography has

the advantage of being a non-contact method of strain measurement when compared to a strain gauge. Moreover, as explained in the introduction to a recent meeting of the Midland Region of the British Society for Strain Measurement, strain gauges cannot cheaply or easily provide full-field information. While it may be possible to employ brittle lacquers in some situations these must be allowed to 'cure' and their use generally requires that strains are fairly high. When speckle photography and the moiré pattern fringe measurement system is used it is possible to measure strains of quite small magnitude and no treatment of the surface may be necessary, providing it is non-specularly reflecting.

CHAPTER 9

CONCLUSIONS

CHAPTER 9.

9.1. SUMMARY OF INVESTIGATIONS.

Initial investigations were primarily concerned with the exploration and qualitative examination of laser speckle photography, with regard to identifying means of improving the technique and obtaining well-defined interference fringes. In particular, these investigations were concerned with single illumination beam, focused speckle photography (F.S.P.) and its application to lateral displacement analysis or measurement.

The research undertaken in this context was quite extensive and ranged from exploration of the effects of different surface illuminations, camera positions, surface finishes and camera aperture ratios to studies of different photographic emulsions, exposures, film processing conditions and treatment. This was carried out with a view to determining measures which would enable doubly-exposed specklegrams to be produced that were of high contrast and definition. These investigations resulted in a number of factors and measures being determined which proved to be significant in this respect.

Further studies were then undertaken with regard to devising means of producing interference fringes from these specklegrams that were of good definition and also

with determining basic ways of measuring the spacing of these fringes with good precision. Various techniques for improving the definition of these fringes were devised and explored and certain means of enhancing the precision of the fringe spacing measurement were determined.

Detailed investigations followed this with the aim of devising and developing methods and systems for the sensitive and accurate measurement of the interference fringes arising from speckle photography. Three distinct and novel systems were devised and subsequently explored. Their appraisal also provided useful comparative information.

Finally, the fringe measurement system which was found to be most practicable, appropriate and provided good accuracy of measurement, namely a method based upon a moiré pattern technique, was employed, in conjunction with speckle photography, for the investigation of certain applied, technical and engineering problems. These investigations not only provided significant information with regard to the problems explored but also enabled the applications of speckle photography to be demonstrated and, more importantly, provided evidence of the effectiveness and versatility of the moiré pattern fringe measurement system in applied contexts.

9.2. OVERALL CONCLUSIONS AND IMPLICATIONS ARISING FROM THE INVESTIGATIONS.

Specific conclusions and implications, both theoretical

and practical concerning the initial investigations, the fringe measurement systems and their properties, as well as the applied investigations, have been presented at appropriate stages in the preceding chapters. However, there are certain overall conclusions and general implications resulting from these integrated studies which will now be outlined. One such implication is that single illumination beam laser speckle photography, combined with a sensitive interference fringe measurement system, is not only a valuable method for measuring or examining such things as small in-plane translations in its own right, but can also be a useful complementary method in relation to other non-contact techniques. Briers[101] has stressed the importance of the equivalence and appropriateness of measurement techniques being accounted for. With respect to this particular method, it is sugg -ested that it is somewhat simpler, more adaptable and, if the moiré pattern fringe measurement system is employed, more robust and portable than certain holographic methods.

Regarding the single illumination beam method, the definition and contrast of the resulting interference fringes was not merely found to be improved by the use of measures related to the recording of the doubly-exposed specklegrams but also to the ways of generating and observing the fringes. Consequently, it is considered that attention is not isolated to the obtaining of the speckle-gram but to the composite factors which were identified

as influencing the clarity of the fringes subsequently measured. The exploitation of these factors can enable speckle photography to be a viable means of studying surface lateral displacement in situations, such as in a factory production environment, where the method may otherwise not provide satisfactory data.

Interference fringe measurement using a self-scanning linear photodiode array was shown to be feasible and, as Kaufmann et al.[68] later confirmed, it was indicated that automatic read-out of fringe spacings could be provided. If improvements in the electronic processing system are introduced so that the overall accuracy of measurement could be improved, as pointed out in Chapter 4, and the cost of such systems is somewhat reduced, then this method could be used to provide rapid analysis of fringes. This would be useful in cases of routine examination, such as in the context of 'quality control', where large numbers of specklegrams relating to large components require analysis.

Computer-controlled microdensitometers with digitized data output are beginning to be more common in industrial and research laboratories. As was demonstrated, it is possible to devise operating programmes for such systems and produce data analysis computer routines such that a photographic negative of interference fringes generated from a doubly-exposed specklegram can be analysed. Although such systems are very expensive they are fully

automatic and provide rapid but detailed analysis. Hence, if such a system is available and reasonable accuracy is acceptable, then it can be a valuable means of undertaking detailed analysis - such as when small changes in interference fringe spacings are being examined.

The interference fringe measurement systems based upon a moiré pattern technique were found to be particularly suitable in this context since the measurement of the fringe spatial frequency is actually made in angular terms. Consequently,the problem of speckle 'noise' and interference fringes being indistinct is less significant. Thus means of improving fringe definition, such as the use of a diffractometer system to produce the fringes, are not so necessary. Consequently, the systems are quite simple to set up, operate and transport. Moreover, the 'symmetrical' moiré pattern system provides good accuracy (±1%) and does not require great precision for its use. It is suggested that this system could, therefore, be employed by relatively unskilled persons and could mean that speckle photography could be used in applications such as 'reliability analysis' involving simple in-plane strain examination at a fairly low cost. In addition, the flexibility and high sensitivity of the symmetrical moiré pattern system for interference fringe spacing determination could help to make speckle photography more widely used than it currently appears to be. It is interesting to note that although moiré pattern

and laser speckle techniques are quite different in concept and practice, Luxmore[97] points out:

> "....both techniques depend on optical interferometry and diffraction, and conceptually they are similar".

A final overall implication arising from the applied investigations is that speckle photography combined with the moiré pattern fringe measurement system can be employed in all stages of manufacturing, that is, in research and prototype development, in production and machine monitoring and then in the non-destructive testing (N.D.T.)* and examination of the finished product.

9.3. SUGGESTIONS CONCERNING FURTHER RESEARCH.

In addition to the factors and possibilities mentioned in earlier chapters as meriting further exploration, there are a number of other theoretical and experimental aspects which require investigation. One such aspect is that, as reported in Chapter 4, hybrid charge coupled photosensors and photodiode arrays called charge coupled photodiode arrays are becoming available. An investigation could be undertaken to discover if such a device could be employed in place of a photodiode self-scanning linear array for measurement of interference fringe

---

*Shakher[102] has recently reported the use of a form of speckle photography for N.D.T.

spacing. It may be possible that a system incorporating a charge coupled photodiode array could be devised which would enable greater accuracy of measurement to be achieved along with improved control of sensitivity.

Although exploration of the measurement of small rotations and tilts was not undertaken using single illumination beam speckle photography in conjunction with the moiré pattern fringe measurement system, it is considered that such exploration would be valuable. The use of the moiré pattern system in this context could enable small tilts or rotations to be determined with good precision. A data analysis programme could be devised for this purpose so that the data from the moiré system could be simply fed in and the processed results read out.

The employment of speckle photography and the moiré pattern fringe analysis system in connection with the applied problems which were investigated enabled useful evidence and information to be gained but there is still further research that could be undertaken in each of the areas investigated. For instance, it is thought that a study of rail contaminant behaviour and thickness at low ambient temperatures (at and below the freezing point of water) could provide important information. Similarly, further investigations of complex machine 'health monitoring' could be undertaken to discover more regarding the uses of this system of monitoring. Furthermore, in view of the successful application of single illumination beam

speckle photography and the moiré pattern fringe analysis system with respect to applied and industrial problems, it is suggested that other problems could be investigated with the aid of this technique. Problems concerning strain measurement and the detection of small displacements in certain components or structures being developed for employment in nuclear power stations have been investigated by Martin[103] using speckle photography. However, there is further research which has yet to be undertaken in this sphere and it is believed that in this and other such investigations single illumination beam speckle photography, used in conjunction with the symmetrical moiré pattern fringe analysis system, could be profitably exploited.

9.4. SUMMARY CONCERNING THE APPLIED MOIRÉ PATTERN FRINGE MEASUREMENT TECHNIQUE

Focused speckle photography (F.S.P.) requires that lateral displacements of the object surface are greater than the imaged speckle diameter — in order that the interference fringes generated from the doubly-exposed specklegram do not fall outside the diffraction halo. Hence using the relation $\sigma = \underline{1.2\ M\lambda F,}$ derived in Chapter 2, for helium-neon laser illumination and an aperture ratio of f/4 the speckle diameter, for unit magnification, is 3μm. By employing very high demagnification, displacements of about 800μm could be measured but, due to optical and photographic limitations, it was found most satisfactory to employ F.S.P. and the moiré pattern technique for displacements chiefly in the range 15μm to around 300μm.

When using F.S.P to study surface movements due to deformation, strain and displacement the resulting interference fringes were sometimes indistinct - such that precise measurement of their spacing was difficult (e.g. for a recorded displacement of 150μm a displacement error of ±5% was typical). However, with a moiré pattern technique this problem is resolved since the fringe spacing is determined in terms of the moiré fringe angle.

Moreover, by using the 'symmetrical' moiré system both sensitivity and accuracy are improved (so that the above displacement could be measured with an error of ±1% overall.) This property, plus the adaptability, simplicity, robustness and portability of the system enabled a variety of applied industrial and technical problems, which had previously not been satisfactorily examined by other means, to be successfully investigated.

For example, concerning railway track contaminant layer thickness determination it had been found that eddy current probes were too fragile and sensitive to the target material and surrounding metal to be of practical use in this context. Both inductive and capacitive displacement probes were also found unsuitable because of difficulties in mounting the contacting probes and because of their sensitivity to temperature changes. A fibre optic system was unsatisfactory because it was sensitive to texture changes. Using moiré fringe gratings it was found difficult to count the fringes while the displacement at the wheel/rail interface was occurring.

The presence of oily matter, consisting of oils degraded

due to polymerization and oxidation plus oil additives (some of which are surface active), was also found to impare the viability of the latter two methods. Nevertheless, the F.S.P./moiré pattern method, with helium-neon monochromatic laser illumination, was not found to suffer in any such respect. Moreover, as it is a non-contact method the presence of extraneous matter does not pose problems of adhesion or contact of probes. Neither does the presence of water based contaminants (which are common on railway track) create difficulties for this method of measurement. In addition, small movements in the direction normal to the recording camera, such as those due to deformation of the wheel with increased loading, do not influence lateral displacement measurement using this system.

It was possible to record the complete wheel/rail 'contact' region, using a 2 to 3 times demagnification ratio, on a single specklegram and thus interrogate the whole region under the same conditions. This meant that variations in thickness along the contact could easily be detected. The sensitivity of the moiré system enabled differences between contaminant layer thicknesses (e.g. of 20μm)to be measured to an error of ±1%, which was required in this case, even under conditions of changing wheel loadings or sustained loadings of long duration..

The machine 'health' monitoring problem which was studied required an adaptable, reliable and portable monitoring system which could be used in a production environment. An electronic power level variation monitor, capable of detecting machine power and drive variations of ±10W (in levels between

0.2kW - 3.5kW) was not found to enable machine wear and deterioration to be detected in good time. It was also complex and did not give data which would allow wear or potential malfunctions to be pinpointed. What was required was a simple, easily set-up system which was sensitive enough to enable wear and the onset of failure to be isolated before this reached a specified level. The F.S.P/moiré pattern system not only satisfied these criteria but also provided permanent records which could readily be reproduced. Furthermore, it did not need the long exposures, comprehensive vibration isolation and peripheral equipment which some holographic and optical systems require.

In monitoring key machine units, of different shapes and sizes, double exposure recordings were made on a time-domain basis - so that the development of small displacements and displacement changes due to wear, aging and the onset of malfunction could be pinpointed. A 'profile' for each key unit was built up from data recorded in a monitoring 'log' and this enabled predetermined displacement magnitudes to be specified, so that the system could be used by relatively unskilled personnel for monitoring sophisticated machines. (For instance, displacement changes from 40 to 49μm, over 2×10^3 hours, were measured on the shop floor.) The same system could be employed to monitor a number of machines since it does not require mounting. However, it was noted that not all key units produced displacements or displacement changes that could be associated with wear or deterioration and so the method cannot always be used for all machine 'health' monitoring.

The motor vehicle structure and automobile component; strain analysis and measurement problems which were explored required a method capable of providing data for regions ranging from welds of a few millimetres to body sections of several hundreds of millimetres, or more, in area. Electric strain gauges did not adequately provide the required full-field data. Moreover, the units were generally of complex shape and difficulties had been experienced in interpreting data obtained using certain holographic methods. The magnitude of the displacements in some instances also meant that other techniques were not appropriate and, because of the time necessary to allow them to 'cure', brittle lacquers were not suitable for many of the necessary stress and strain analyses which were carried out in the manufacturing plant. These difficulties were not found to apply with regard to the F.S.P/moiré pattern method. However, in relation to checking the integrity of 'rectified' vehicle body shells it was difficult to specify a viable maximum figure for strain for some body sections (which was acceptable in both structural safety and economic commercial terms) because of the effects of 'flow' in the mild steel sections.

In the case of the automobile rear suspension units a method of strain measurement was also required that would enable routine, detailed examinations to be undertaken of strains ranging from about 400 to 750 μstrain (and higher at welds). These measurements were to be made to an accuracy of ±20 μstrain (maximum) for points 5mm apart. It was found that the F.S.P/moiré pattern method enabled all these requirements to be satisfied and also conveniently

provided data on the line of movement and its components, which the techniques outlined earlier failed to satisfactorily provide. All these and the previously enunciated properties of the relatively low-cost F.S.P/moiré pattern system, reinforce the applied viability of the system, which has potential applications ranging from aviation to shipbuilding and instrumentation.

APPENDIX 1

rface Texture
ef. British Standard 1134 : Part 1 and Part 2: 1172)
ithmetical mean deviation (R_a)
e arithmetical average value of the departure of the profile above
d below the reference line (centre or electrical mean line)
roughout the prescribed sampling length.
values are expressed as numbers of micrometers)
a

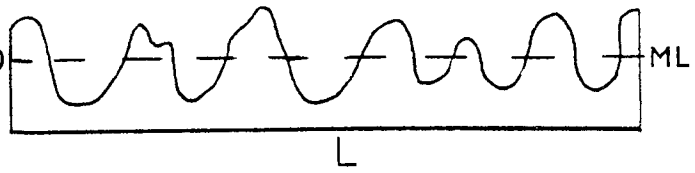

$$R_a = \frac{1}{L}\int_0^L y\,dL$$

L - roughness width cut-off of the measurement

= arithmetical average deviation from the mean line ML.

APPENDIX 2

tension tube: exposure correction.
ffective 'f' value $E_f = I_f \times \frac{\text{Focal length + Extension}}{\text{Focal length}}$

(I_f - Indicated 'f' value)

ence, for the recording camera used in the main studies the
llowing typical values apply:

Focal length	= 58mm
Extension tube length	= 20mm
I_f	= 2.8

$$E_f = 2.8 \times \frac{58 + 20}{58}$$

$$= \underline{3.76} \text{ (approx f/4)}$$

APPENDIX 3

asic Processing Scheme for Specklegrams
Carried out in total darkness)
. Wash: (pre-development wash) in running water was employed for 5 minutes(at 21°C).
. Development: (various developers were initially employed but Kodak D19 was used in the main studies).
D19 - full strength, continuous agitation for 4 to 5 minutes at 20°.
. Wash: 5 minutes in running water (at 21°C).
. Fixing: (Kodak fixer) continuous agitation for 5 minutes at 21°C.
. Wash: 15 minutes in running water at 21°C. (A wetting agent was initially employed).
. Drying: air drying (in dust-free atmosphere) at room temperature (20°C approx).

APPENDIX 4

inear photodiode array data: Reticon 'G' series (RL 256G).
onolithic self-scanning linear photodiode array
ample and hold circuit (motherboard): Reticon RC100B.
rovides an integrated sampled-and-held boxcar output.
lectro-optical data: (All at 25°C ambient temperature)
256 photodiodes on 25µm centres: diode aperture width 26µm.
hotodiode sensitivity 2.5 $pA^{-1}\ W^{-1}\ cm^2$: (non uniformity of sensitivity 4%).
ypical amplifier noise (r.m.s.) 0.1% of saturation level.
eak spectral response 800nm (limits:200-1100nm)
lectrical data: clock frequency 2 MHz (typical) to 7kHz.
ntegration time 30m sec (typical) to 0.5m sec

APPENDIX 5

icrodensitometer: Joyce-Loebl. Microdensitometer 6.
canning stage: max scan area 250mm x 250mm (step incr: 2.5µm or higher even multiples)

Cont/d over .....

APPENDIX 1

Surface Texture
(Ref. British Standard 1134 : Part 1 and Part 2: 1172)
Arithmetical mean deviation (R_a)
The arithmetical average value of the departure of the profile above and below the reference line (centre or electrical mean line) throughout the prescribed sampling length.
(R_a values are expressed as numbers of micrometers)

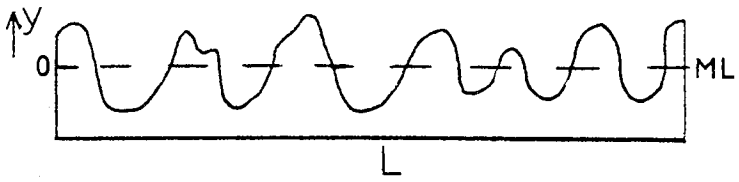

$$R_a = \frac{1}{L}\int_0^L y\,dL$$

L - roughness width cut-off of the measurement

R_a = arithmetical average deviation from the mean line ML.

APPENDIX 2

Extension tube: exposure correction.

$$\text{Effective 'f' value } E_f = I_f \times \frac{\text{Focal length + Extension}}{\text{Focal length}}$$

(I_f - Indicated 'f' value)

Hence, for the recording camera used in the main studies the following typical values apply:

Focal length	= 58mm
Extension tube length	= 20mm
I_f	= 2.8

$$E_f = 2.8 \times \frac{58 + 20}{58}$$

$$= 3.76 \text{ (approx f/4)}$$

APPENDIX 3

Basic Processing Scheme for Specklegrams
(Carried out in total darkness)

1. Wash: (pre-development wash) in running water was employed for 5 minutes(at 21°C).
2. Development: (various developers were initially employed but Kodak D19 was used in the main studies).
   D19 - full strength, continuous agitation for 4 to 5 minutes at 20°.
3. Wash: 5 minutes in running water (at 21°C).
4. Fixing: (Kodak fixer) continuous agitation for 5 minutes at 21°C.
5. Wash: 15 minutes in running water at 21°C. (A wetting agent was initially employed).
6. Drying: air drying (in dust-free atmosphere) at room temperature (20°C approx).

APPENDIX 4

Linear photodiode array data: Reticon 'G' series (RL 256G).
Monolithic self-scanning linear photodiode array
Sample and hold circuit (motherboard): Reticon RC100B.
Provides an integrated sampled-and-held boxcar output.
Electro-optical data: (All at 25°C ambient temperature)
256 photodiodes on 25μm centres: diode aperture width 26μm.
Photodiode sensitivity 2.5 $pA^{-1}\ W^{-1}\ cm^2$: (non uniformity of sensitivity 4%).
Typical amplifier noise (r.m.s.) 0.1% of saturation level.
Peak spectral response 800nm (limits:200-1100nm)
Electrical data: clock frequency 2 MHz (typical) to 7kHz.
Integration time 30m sec (typical) to 0.5m sec

APPENDIX 5

Microdensitometer: Joyce-Loebl. Microdensitometer 6.
Scanning stage: max scan area 250mm x 250mm (step incr: 2.5μm or higher even multiples)

Cont/d over .....

Illumination : 50W tungsten halogen lamp.
Scanning system : 2 silicon photodiodes (P.I.N) area 5mm^2.
Apertures from 0.4mm to 20mm.
Photometrics : 0-4D optical density or 0-100% transmittance.
Linearity 0.5-1.0% in range 0-4D.
Viewing/Illumination: influx object: 16x/0.3NA. efflux object: 16x/0.35N

Electronic Output control/data processing (Output : 10 bit binar
Microprocessor : Intel 8085, 4K memory: Controls microdensitomet
under instruction from the NOVA 3/12 (32K) mini computer.
Software : (Control) using Joyce-Loebl 'Wizard' software.
(Output) data analysis (Fortran) using 'Gens' program: I.B.M. 37
computer.

llumination : 50W tungsten halogen lamp.
canning system : 2 silicon photodiodes (P.I.N) area 5mm^2.
pertures from 0.4mm to 20mm.
notometrics : 0-4D optical density or 0-100% transmittance.
inearity 0.5-1.0% in range 0-4D.
iewing/Illumination: influx object: 16x/0.3NA. efflux object: 16x/0.35NA.
lectronic Output control/data processing (Output : 10 bit binary)
icroprocessor : Intel 8085, 4K memory: Controls microdensitometer, nder instruction from the NOVA 3/12 (32K) mini computer.
oftware : (Control) using Joyce-Loebl 'Wizard' software.
Output) data analysis (Fortran) using 'Gens' program: I.B.M. 370/16 omputer.

APPENDIX 6

COMPUTER DATA/SUBROUTINES FOR INTERFERENCE FRINGE ANALYSIS

CAU ENDS ...8 RECORDS ON DISK

INT 80.0 5.0 80.0 300.0 35.0 1.0
===

TRIP DEFINING POINTS X1= 80.0, Y1= 5.0 : X2= 80.0, Y2= 300.0

TRIP HALF WIDTH : 35.0

ORDERS OF STRIP BOX :
XP= 115.0, YP= 5.0 : XQ= 45.0, YQ= 300.0
XR= 45.0, YR= 5.0 : XS= 115.0, YS= 300.0

1	39.87	39.75	39.90	40.14	40.42	40.36	40.12	40.20	40.22
11	39.61	39.51	39.43	39.35	39.57	39.33	39.67	40.62	41.84
21	43.49	43.87	44.65	44.29	43.45	43.15	41.87	41.28	40.75
31	40.23	40.32	40.59	40.97	41.86	42.54	43.81	45.48	47.04
41	49.97	51.33	52.07	51.17	51.97	49.53	47.74	46.47	44.27
51	45.77	45.91	48.33	52.91	54.56	54.77	54.16	54.16	57.17
61	57.62	53.26	57.75	53.79	51.11	50.14	49.58	48.51	49.78
71	58.55	55.57	61.67	64.64	67.55	70.67	71.46	72.74	73.32
81	69.23	72.72	67.42	61.83	61.30	62.61	63.28	63.52	63.89
91	67.58	72.79	78.21	80.46	81.84	80.98	78.72	78.50	77.67
101	76.32	71.49	67.68	70.46	71.83	71.01	72.83	75.94	78.71
111	80.75	86.46	84.51	83.23	83.30	85.03	79.55	78.78	76.10
121	69.97	69.59	67.76	66.49	67.13	72.23	74.59	76.67	80.47
131	88.67	86.85	86.39	81.27	74.06	70.64	72.33	68.29	66.10
141	61.52	60.91	63.09	66.31	68.10	70.00	74.32	77.74	76.59
151	78.16	77.81	72.11	70.12	63.41	57.71	56.36	54.35	51.33
161	52.41	54.53	59.52	65.64	69.60	72.20	74.17	72.61	68.93
171	61.69	57.79	53.49	52.93	51.03	49.65	50.30	50.14	52.12
181	56.01	58.43	60.53	62.27	59.04	58.86	60.22	59.99	60.99
191	54.61	51.33	48.68	46.51	45.06	44.87	45.23	45.29	47.48
201	53.62	51.97	54.01	53.78	52.23	54.38	54.53	51.99	48.10
211	43.72	43.23	42.23	41.43	41.57	42.19	42.97	46.03	49.14
221	48.91	48.94	48.03	46.99	46.01	44.73	42.94	41.97	41.12
231	40.06	40.14	40.47	41.16	41.52	42.04	42.93	43.49	43.60
241	43.73	43.36	42.71	42.89	42.21	41.17	40.17	39.77	39.80
251	40.27	40.06	39.97	39.96	40.57	41.17	41.87	41.24	41.06
261	40.13	40.07	39.73	39.49	39.51	39.37	39.06	38.94	39.14
271	39.23	39.30	39.03	39.28	39.24	39.32	39.56	39.39	39.21
281	39.24	39.04	39.18	39.08	38.99	38.87	38.62	38.69	39.01
291	39.14	39.07	39.01	39.24	39.14				

END 6.0 12.0

CLN

APPENDIX 7

PUBLICATION: 'A moirĕ-pattern technique for measurement of fringe spacings'

Aston University

Content has been removed for copyright reasons

BL Technology Ltd.

Gaydon Proving Ground
Lighthorne Heath
Nr Leamington Spa
Warwickshire CV33 9UA

Telephone: 0926 641111
Telex: LEYCAR G 31331

NFIDENTIALITY UNDERTAKING

....Brian...R.Pickthorne..... having been allowed
cess to certain data, drawings, specifications, know how or other
chnical information in whatever form at Longbridge by BL Technology
mited ("BLT") of 35-38 Portman Square, London, W1H OHQ, hereby
ree to treat all such information and any other information in the
ssession of BLT which I may see or acquire, as confidential and
ll not use or disclose it directly or indirectly to any other
rty without the prior written consent of BLT.

further agree that I shall forthwith upon request by BLT and
thout retaining any copies, return any confidential material to
T.

less released earlier in writing therefrom by BLT, the above
ligations shall remain binding for five (5) years from the date
reof.

ch obligations shall not apply to:

Information already in the public domain or which enters the public domain other than by my default;

Information which we are able to prove was known to .....
.....at the time of the disclosure;

Information which is obtained from a third party who is lawfully in possession of such information and under no obligation of confidentiality to BLT.

thing in this undertaking shall be construed as granting me any
ghts in any of the information so disclosed.

ned by:...B. Pickthorne.....
e :.....4/2/82.....
ness :.....M. Lloyd.....

REFERENCES

REFERENCES

1. J.A.Leendertz, "Measurement of surface displacement by interference of speckle patterns." Proc.I.C.O, Reading 1969, Vol.8 (J.Home Dickson, ed.) Oriel Press: Newcastle-upon-Tyne, 1970.

2. J.A.Leendertz, "interferometric displacement measurement on scattering surfaces utilizing speckle effect." J.Phys.E. Sci.Instrum. 3, pp214-218, 1970.

3. E.Archbold, A.E.Ennos and P.A.Taylor "A laser interferometer for the detection of surface movements and vibration."'Optical Instruments and Techniques'. Ed.J.Home Dickson. Oriel Press: Newcastle-upon-Tyne, pp265-275, 1970.

4. J.M.Burch, "Interferometry with scattered light". 'Optical Instruments and Techniques'. Ed.J.Home Dickson. Oriel Press: Newcastle-upon-Tyne. pp213-229, 1970.

5. J.N.Butters and J.A.Leendertz, "A double exposure technique for speckle pattern interferometry". J.Phys.E: Sci.Instrum. 4, pp277-279, 1971.

6. K.A.Stetson, "New design for laser image-speckle interferometer". Opt.Laser Technol. 2, pp179-181, 1970.

7. A.E.Ennos, "Speckle Interferometry". In: 'Laser speckle and related phenomena' . Ed.J.C.Dainty. Springer-Verlag: Berlin, Heidelberg, 1975.

8. R.Jones and J.A.Leendertz, "Elastic constant and strain measurements using a three beam speckle pattern interferometer". J.Phys.E: Sci.Instrum. 7, pp253-57, 1974.

9. E.Archbold, J.M.Burch and A.E.Ennos, "Recording of in-plane surface displacement by double-exposure speckle photography". Opt.Acta 17, pp883-98, 1970.

10. J.N.Butters and J.A.Leendertz, "Holographic and video techniques applied to engineering measurement". J.Measurement and Control. 4, pp349-54, 1971.

11. G.Groh, "Engineering uses of laser produced speckle patterns". In: 'Engineering uses of holography'.Eds. E.R.Robertson and J.M.Harvey. Camb.Univ.Press: London and New York, 1970.

12. D.A.Gregory, "Speckle photography in engineering applications". In: 'Engineering uses of coherent optics'. Ed.E.R.Robertson. Camb. Univ.Press:London and New York, 1976.

13. J.C.Dainty, 'Laser Speckle and related phenomena'. Springer-Verlag: Berlin, Heidelberg, 1975.

14. K.Exner, Sitzungsber. Kaiserl.Akad.Wiss.(Wien)76. p522, 1877.

15. K.A.Stetson. "A review of speckle photography and interferometry". Opt.Eng.14, pp482-89, 1975.

16. A.E.Ennos, "Speckle Interferometry". (Proof Copy) North-Holland Pub.Co: Holland, 1977.

17. H.J.Tiziani, "Vibration analysis and deformation measurement". In: 'Speckle Metrology'. Ed.R.K.Erf. Academic Press: New York, 1978.

18. Y.Y.Hung, "Displacement and strain measurement" In: 'Speckle Metrology'. Ed.R.K.Erf.Academic Press, New York, 1978.

19. A.F.Harvey, 'Coherent Light'. Wiley: New York, pp720-1, 1970.

20. D.Gabor, "Laser speckle and its elimination".I.B.M.J. Res.Dev.14, p509, 1970.

21. D.A.Gregory, "Topological speckle and structures inspection". In: 'speckle metrology' Ed.R.K.Erf. Academic Press: New York, 1978.

22. J.D.Briers, "Speckle fluctuations as a screening test in the holographic measurement of plant motion and growth". J.Expt.Botany. 29, pp395-99, 1978.

23. M.Francon, 'Laser speckle and applications in Optics'. Academic Press: London, 1979.

24. D.C.O'Shea, W.R.Callen and W.T.Rhodes, 'An Introduction to lasers and their applications'. Addison-Wesley Pub.Co: Mass, 1977.

25. J.W.Goodman, "Statistical Properties of laser speckle patterns". In: 'Laser speckle and related phenomena'. Ed.J.C.Dainty. Springer-Verlag: Berlin, Heidelberg, 1975.

26. A.E.Ennos. Private Communication. 1979.

27. T.Asakura, "Surface roughness measurement". In: 'Speckle Metrology'. Ed.R.K.Erf.Academic Press: New York, 1978.

28. T.S.Mckechnie, "Statistics of coherent light speckle produced by stationary and moving apertures". Ph.D. Thesis: Univ.of London, 1974.

29. L.M.Tanner, "A study of fringe clarity in laser interferometry and holography". J.Phys.E: Sci.Instrum. 7, pp517-24, 1968.

30. L.I.Goldfischer, "Autocorrelation function and power spectral density of a laser produced speckle pattern". J.Opt.Soc.Amer. 55, p247, 1965.

31. C.M.Vest, 'Holographic Interferometry'. Wiley: New York, 1979.

32. G.Parry, "Speckle patterns in partially coherent light". In: 'Laser speckle and related phenomena'. Ed.J.C.Dainty. Springer-Verlag: Berlin, Heidelberg. 1975.

33. C.Wykes, "De-correlation effects in speckle -pattern interferometry. 1. Wavelength change dependent de-correlation with application to contouring and surface roughness measurement". Opt.Acta.24, pp517-32, 1977.

34. J.N.Butters and J.A.Leendertz, "Advances in electro-optical techniques and lasers for engineering metrology and N.D.T." Proc.Electro-Optics 72. Int.Conf. Brighton, England, pp139-45, 1972.

35. Y.Y.Hung and J.D.Hovanesian, "Full-field surface-strain and displacement analysis of three dimensional objects by speckle interferometry". Exp.Mech.12, pp454-60, 1972.

36. K.A.Stetson, "Analysis of double-exposure speckle photography with two-beam illumination". J.Opt.Soc. Amer.64, pp857-61, 1974.

37. E.Archbold and A.E.Ennos, "Displacement measurement from double-exposure laser photographs". Opt.Acta. 19, pp253-71, 1972.

38. H.J.Tiziani, "Application of speckling for in-plane vibration analysis". Opt.Acta.18, pp891-902, 1971.

39. U.Köpf, "A coherent optimal method for contactless measurements of local displacements and vibrations". Optic.35, p144, 1972.

40. D.E.Duffy, "Moiré gauging of in-plane displacement using double aperture imaging". Appl.Opt.11, pp1788-81, 1972.

41. R.P.Khetan and F.P.Chiang, "Strain analysis by one-beam laser speckle interferometry. 1. Single aperture method". App.Optics. 15, pp2205-15, 1976.

42. D.A.Gregory, "Basic physical principles of defocused speckle photography: a tilt topology inspection technique". Opt.Laser Technol. 8, pp201-13, 1976.

43. K.A.Stetson, "Problem of defocusing in speckle photography, its connection to hologram interferometry, and its solutions". J.Opt.Soc.Amer.66, pp1267-71, 1976.

44. F.D.Adams and W.I.Griffith, "Interference fit fastner displacement measurement by speckle photography". Proc.Army Symposium on solid mechanics. Cape Cod, Mass, U.S.A. 1974.

45. W.F.Fagan, "Novel Speckle Camera and Analyser". Lasers in meas.and testing. Laser 77 Conf. Munich I.P.C.Pub: Guildford, Surrey, U.K. pp456-61, 1977.

46. K.A.Stetson, "The vulnerability of speckle photography to lens aberrations". J.Opt.Soc.Amer.67, pp1587-90, 1977.

47. Agfa-Gevaert, Technical Information, 21.7271(581) Pub: Agfa-Gevaert N.V., Mortsel, Belgium, 1981.

48. E.Archbold and A.E.Ennos, "Two-dimensional vibrations analysed by speckle photography". Opt.Laser Technol. 7, pp17-21, 1975.

49. H.Tiziani, "A study of the use of laser speckle to measure small tilts of optically rough surfaces accurately". Opt.Commun.5, pp271-76, 1972.

50. G.B.Smith and K.A.Stetson, "Heterodyne readout of specklegram halo interference fringes". App.Optics. 19, pp3031-33, 1980.

51. E.Archbold and A.E.Ennos, "Measurement by laser photography". Proc.Electro-Optics 72 Int.Conf. Brighton, England. p65, 1972.

52. E.Archbold, A.E.Ennos and M.S.Virdee, "Speckle photography for strain measurement - a critical assessment". 1st. European Congr.on Optics. App. to Metrology: S.P.I.E, 136, pp258-63, 1977.

53. D.E.Duffy, "Measurement of surface displacement normal to the line of sight". Exp.Mech.14, pp378-84, 1974.

54. M.Francon, "Information processing using speckle patterns". In: 'Laser speckle and related phenomena'. Ed.J.C.Dainty. Springer-Verlag: Berlin, Heidelberg, 1975.

55. C.S.Vikram and K.Vedam, "Measurement of subspeckle - size changes by laser-speckle photography". Opt. Letters. 4, pp406-407, 1979.

56. G.L.Rogers, "A device for aligning a pinhole with a microscope objective". J.Sci.Instr. 43, pp763-4, 1966.

57. D.B.Coblitz and J.A.Carney, "Dye removal from holographic films". App.Optics. 13, p1994, 1974.

58. G.L.Rogers, "Safelight for Agfa 10E75 and 8E75 plates: a correction". App.Optics, p1125, 1979.

59. N.L.Roblin, G.Schalow, and B.Chourabi, "Interférométrie Diffiérentielle des Aberrations d'un système Optique par Photographie de Speckles". J.Opt. 8, pp149-158, 1977.

60. D.F.Malin, "Photography in Astronomy". Phys.Bull.33, pp207-210, 1982.

61. A.R.Luxmore, F.A.A.Amin and W.T.Evans, "In-plane strain measurement by speckle photography; a practical assessment of the use of Young's fringes". J.Strain Anal. 9, pp26-35, 1974.

62. P.W.Fry, "Silicon Photodiode Arrays", J.Phys.E: Sci.Instrum. 8, pp337-49, 1975.

63. P.Bartlam, "Electronic sight and its Application". Engineering, pp370-72, 1981.

64. P.J.W.Noble, "Light sense: Handbook of Integrated Opto-electronic devices and systems". Integrated Photomatrix: Dorchester, Dorset, 1967.

65. G.E.Maddux, S.L.Moorman and R.R.Corwin, "A programmable data-retrieval system for in-plane displacement from speckle photographs". AFFDL Report TM-78-109-FBE, Ohio, U.S.A, 1978.

66. B.I.Ineichen, P.Eglin and R.Dändliker. "Hybrid optical and electronical image processing for strain measurements by speckle photography". Proc.I.C.O. Conf. Madrid, Sept. 1978.(Graficas Tresde, Madrid) pp563-66, 1978.

67. B.I.Ineichen, P.Eglin and R.Dändliker,"Hybrid optical and electronic image processing for strain measurements by speckle photography". App.Optics. 19, pp2191-95, 1980.

68. G.H.Kaufmann, A.E.Ennos, B.Gale and D.J.Pugh, "An electro-optical read-out system for analysis of speckle photographs". J.Phys.E: Sci.Instrum. 13, pp579-84, 1980.

69. Reticon "G series solid state line scanners". Manuf. Data. Reticon Corp. U.S.A, 1976.

70. G.H.Kaufmann, A.E.Ennos, D.J.Pugh and B.Gale, "An electro-optical read-out system for the analysis of speckle photographs". N.P.L.England, (unpublished), 1980.

71. G.A.Costa, P.Ottonello and E.Piano, "Thermal expansion measurements by speckle interferometry". App. Optics. 19, pp1032-33, 1980.

72. A.R.Luxmore and F.A.A.Amin, "Measurement of crystal length changes". In: 'Speckle metrology'. Ed.R.K.Erf. Academic Press: New York, 1978.

73. A.R.Luxmore, "Measurement of displacements around crack tips". In:'Speckle metrology'. Ed.R.K.Erf. Academic Press: New York, 1978.

74. J.J.Snyder, "Algorithm for fast digital analysis of interference fringes". App.Optics. 19, pp1223-25, 1980.

75. M.Pickering, P.A.Machin and M.Elder, "GENS: An off-line Film processing program". S.R.C.Daresbury Lab., 1980.

76. J.C.Dainty and R.Shaw. 'Image Science'. Academic Press: London, 1974.

77. R.E.Swing, "The optics of microdensitometry". Opt. Engineering. 12, pp 185-98, 1973.

78. G.E.Maddux, S.L.Moorman, R.L.Corwin and R.E.Ramsey, "An automatic system for extracting in-plane displacements from speckle photographs". Project 2401 Rep. Air Force Wright Aero.Labs, U.S.A, 1982.

79. Lord Rayleigh, "On the manufacture and theory of diffraction gratings". Phil.Mag.S.4, 47, pp81-93, 1874.

80. L.A.Sayce, "Gratings in metrology". J.Phys.E.:Sci. Instrum.5, pp193-98, 1972.

81. B.Pickthorne and G.L.Rogers, "Moiré-pattern technique for measurement of fringe spacings" . Opt.Letters 7, pp474-76, 1982.

82. S.Yokozeki, "Moiré fringes". Opt. and Lasers in Engineering. 3, pp15-27, 1982.

83. J.Guild, 'The interference systems of crossed diffraction gratings'. Oxford Univ.Press. 1956.

84. G.L.Rogers, "A simple method of calculating moiré patterns". Proc.Phys.Soc.London. 73,pp142-43, 1959.

85. G.L.Rogers, "A geometrical approach to moiré pattern calculations". Opt.Acta.24, pp1-13, 1977.

86. J.J.Kalker, "Simplified theory of rolling contact". Mech. and Aero.Eng and Shipbuilding. 1, pp1-10, 1973.

87. S.P.Timoshenko and J.N.Goodier, 'Theory of elasticity'. 3rd.Ed. Mc.Graw-Hill: New York, 1970.

88. D.A.Smith, "A basic study of wheel/rail adhesion". British Railways Res.Dept: Report CR46, 1970.

89. K.L.Johnson and A.D.Roberts, "Observations of visco-elastic behaviour of an elastohydrodynamic lubricant film". Proc.Roy.Soc.A, 337, pp217-247, 1974.

90. A.Cameron, 'Principles of Lubrication'. Longmans: London 1966.

91. R.A.Collacott, 'Mechanical fault diagnosis and condition monitoring'. Chapman and Hall: London,1977.

92. R.A.Collacott, "Why condition monitoring (an over-view)". Condit.Monit.Proc.2nd.Nat.Conf.London, Session 1, pp1-11, 1979.

93. P.Williams, "Sophisticated techniques-design audit and condition monitoring". Condit.Monit.Proc. 2nd. Nat.Conf. London, Session 4a, 6pp, 1979.

94. R.K.Erf,"Application of laser speckle to measurement". In: 'Laser Applications'. Eds.J.W.Goodman and M.Ross. Academic Press: London, 1980.

95. C.S.Vikram and K.Vedam, "Laser speckle photography for supersentivie dial gauge". Opt.Letters. 5, pp441-42, 1980.

96. A.E.Ennos and M.S.Virdee "Laser speckle photography as a practical alternative to holographic interferometry for measuring plate deformation". Opt.Engineering. 21, pp478-82, 1982.

97. A.R.Luxmore, "Developments in moiré and laser methods of stress analysis". In:'Developments in stress analysis - 1'. Ed.G.S.Holister. App.Science Pubs, London, England, 1979.

98. D.J.V.Martin, "Laser speckle photography measurements of movement and strain in steel structures at temperatures of 20-520°C. "Materials Eval., 36, pp53-56, 1978.

99. B.Ineichen, P.Eglin and R.Dändliker, "Hybrid optical and electronical image processing for strain measurements by speckle photography". Paper submitted to Brown Boveri Res.Cent., Baden, Switzerland, 1978.

100. R.Dändliker, "Holographic interferometry and speckle photography for strain measurement: a comparison". Opt. and Lasers in Engineering. 1, pp3-19, 1980.

101. J.D.Briers, "The interpretation of holographic interferograms". Opt.Quant.Electron. 8, pp469-501, 1976.

102. C.Shakher, "Laser speckle photography used for N.D.T. of diaphragms". App.Optics. 21, pp367-69, 1982.

103. D.J.V.Martin, "Laser holographic and speckle photography methods for defect detection and strain evaluation in pressure vessels." Nuc.Eng. and Design..43, pp227-36, 1977.